research report

Sheathing Braced Design of Wall Studs

RESEARCH REPORT RP13-1

2013

American Iron and Steel Institute

Steel Framing Alliance™

Steel. The Better Builder.

DISCLAIMER

The material contained herein has been developed by researchers based on their research findings and is for general information only. The information in it should not be used without first securing competent advice with respect to its suitability for any given application. The publication of the information is not intended as a representation or warranty on the part of the American Iron and Steel Institute, Steel Framing Alliance, or of any other person named herein, that the information is suitable for any general or particular use or of freedom from infringement of any patent or patents. Anyone making use of the information assumes all liability arising from such use.

FINAL REPORT
Sheathing Braced Design of Wall Studs

February 2013

B.W. Schafer
Johns Hopkins University

This report was prepared as part of the American Iron and Steel Institute sponsored project: Sheathing Braced Design of Wall Studs. The project also received supplementary support and funding from the Steel Stud Manufacturers Association. Additional project information and documentation is available at www.ce.jhu.edu/bschafer/sheathedwalls. Any opinions, findings, and conclusions or recommendations expressed in this publication are those of the author and do not necessarily reflect the views of the American Iron and Steel Institute, nor the Steel Stud Manufacturers Association.

Table of Contents

Introduction

This report provides a summary document and final report for the multi-year project on Sheathing Braced Design of Wall Studs conducted at Johns Hopkins University. This project examined the axial behavior and axial + bending behavior of cold-formed steel stud walls braced solely by sheathing connected to the stud and track flanges. This report is a practical summary of the work: the history of sheathing braced design, derivations of new analytical methods, testing on components and full sheathing-braced walls, modeling of sheathing-braced members, and the development of the proposed design method are all provided in accompanying documents. Here the focus is on the proposed design method and its application.

The research resulted in an extensive series of publications that are summarized in the next section. Comprehensive summaries of the work are available in the Ph.D. thesis of Dr. Vieira and the M.S. essay of Ms. Peterman. These documents provide a complete recording of the conducted work. Two journal publications: Vieira and Schafer (2013) and Peterman and Schafer (2013) provide the most concise summaries of the total work, and are thus included as appendices to this report.

An important step in the translation of the work from research to practice is the creation of draft Specification language, i.e., draft ballots. The existing publications provide recommendations, but not in Specification language, and in some cases not all details are provided. This final report provides a complete set of draft ballots encompassing all of the work conducted. The effort is significant and thirteen different draft ballots are provided. The ballots may be broken into four groups:

- Ballots 1-5 address the determination of the stiffness supplied by the fastener-sheathing restraint to the stud wall. Both analytical and test methods are addressed.
- Ballots 6-9 determine the elastic buckling load and/or moment when a stud has additional sheathing-based restraint. This is best summarized in a commentary on elastic buckling determination written to accompany the Appendix 1 Direct Strength Method.
- Ballots 11-12 determine fastener demands and capacity (in bearing and pull-through).
- Ballots 10,13 make a clear path for sheathing-braced design from COS to COFS standards and simplify the design in COFS standards with proposed strength tables.

An expanded design example follows the ballots. The design example illustrates the basic methodology and demonstrates how the sheathing-braced design check would work in compression and bending. The example is provided in Mathcad and provides a basis for the creation of the strength tables addressed in Ballot 13.

The first appendix provides an exchange between the project PI and the project monitoring task group on certain key aspects of implementing the research. The exchange is included as a reference for the Specification committee as the ballots go forward. Finally, the two key manuscripts for the research: Vieira and Schafer (2013) and Peterman and Schafer (2013) are included.

Publications

As of this writing, the following publications are derived wholly or in part from research associated with this project. Most publications are available at the website www.ce.jhu.edu/bschafer/sheathedwalls for the project. In some cases, due to copyright the articles cannot be posted directly. Please contact the author of this report for a personal copy if needed.

Dissertations

Vieira Jr., L.C.M. (2011) Behavior and design of cold-formed steel stud walls under axial compression, Department of Civil Engineering, Ph.D. Dissertation, Johns Hopkins University.

Peterman, K.D.P. (2012) Experiments on the stability of sheathed cold-formed steel stud under axial load and bending, M.S. Essay, Department of Civil Engineering, Johns Hopkins University.

Journal Articles

Submitted

***Peterman, K.D., Schafer, B.W. "Sheathed Cold-Formed Steel Studs Under Axial and Lateral Load." Submitted to *Journal of Structural Engineering* (Submitted 2 January 2013).

Published/In Press

***Vieira Jr., L.C.M., Schafer, B.W. (2013). "Behavior and Design of Sheathed Cold-Formed Steel Stud Walls under Compression." ASCE, *Journal of Structural Engineering* (DOI: 10.1061/(ASCE)ST.1943-541X.0000731). *In Press*

Vieira Jr., L.C.M., Schafer, B.W. (2012). "On the design methods of cold-formed steel wall studs by the AISI specification." Revista da Estrutura de Aço. 1 (2) 79-94.

Vieira Jr., L. C. M., Schafer, B.W. (2012). "Lateral Stiffness and Strength of Sheathing Braced Cold-Formed Steel Stud Walls." Elsevier, *Engineering Structures.* 37, 205 - 213 (doi:10.1016/j.engstruct.2011.12.029)

Vieira Jr., L. C. M., Shifferaw, Y., Schafer, B.W. (2011) "Experiments on Sheathed Cold-Formed Steel Studs in Compression." Elsevier, *Journal of Constructional Steel Research.* 67 (10) 1554-1566 (doi:10.1016/j.jcsr.2011.03.029).

Conference Proceedings

Vieira Jr., L.C.M., Schafer, B.W. (2010) "Behavior and Design of Axially Compressed Sheathed Wall Studs." *Proceedings of the 20th Int'l. Spec. Conf. on Cold-Formed Steel Structures*, St. Louis, MO. November, 2010. 475-492.

Vieira Jr. , L.C.M., Schafer, B.W. (2010). "Bracing Stiffness and Strength in Sheathed Cold-Formed Steel Stud Walls." *Proceedings SDSS'Rio 2010 STABILITY AND DUCTILITY OF STEEL STRUCTURES*, E. Batista, P. Vellasco, L. de Lima (Eds.), Rio de Janeiro, Brazil, September 8 - 10, 2010. 1069-1076.

Shifferaw, Y., Vieira† Jr., L.C.M., Schafer, B.W. (2010). "Compression testing of cold-formed steel columns with different sheathing configurations." *Proceedings of the Structural Stability Research Council - Annual Stability Conference*, Orlando, FL. 593-612.

Vieira Jr., L.C.M., Schafer, B.W. (2010). "Full-scale testing of sheathed cold-formed steel wall stud systems in axial compression." *Proceedings of the Structural Stability Research Council - Annual Stability Conference*, Orlando, FL. 533-552.

Miscellaneous Reports

The following reports are unpublished works derived by students during the course of the project. The work is available in report form and was presented to the AISI COFS Design Methods committee or the Project Monitoring Task Group during the course of the research.

Iuorio, O., Schafer, B.W. (2008). "FE Modeling of Elastic Buckling of Stud Walls." Supplemental report to AISI-COFS Design Methods Subcommittee, September 2008

Blum et al. (2011). "A few thoughs on bracing and accumulation." Supplemental report to AISI-COFS Design Methods Subcommittee, February 2011

Post, B. (2012). “Fastener Spacing Study of Cold-Formed Steel Wall Studs Using Finite Strip and Finite Element Methods.” Research Report, December 2012.

*** These two papers are provided in the Appendices of this report.

Basic Design Formulation

The basic design formulation for determining the available strength of a sheathed wall is as follows.

1. Determine the stiffness of the fastener-sheathing systems that provide bracing restraint to the studs. This may be completed by testing (preferred) or from closed-form design expressions that are generally geared to providing a lowerbound estimate to the stiffness. In general, the stiffness to be determined include k_x, k_y, and k_ϕ springs at every fastener location.

2. Determine the elastic stability (P_{cr} and/or M_{cr}) of the studs with the bracing restraint included. This includes local ($P_{cr\ell}$ and/or $M_{cr\ell}$), distortional (P_{crd} and/or M_{crd}), and global buckling (P_{cre} and/or M_{cre}). This may be completed by finite strip analysis (preferred) or shell finite element analysis or from closed-form design expressions. The closed-form expressions can be lengthy and are only provided in the commentary. A closed-formed expression for global buckling (i.e., LTB) in bending with the bracing restraint in place is not currently available.

3. Assess the member limit states utilizing the appropriate increased elastic stability load or moment.

> 3a. For the Direct Strength Method (AISI-S100 Appendix 1) the local, distortional, and global buckling loads and moments are used in the existing formulas directly, and no further change is needed.
>
> 3b. For conventional, Effective Width Method (AISI-S100 Main Body) design, the global buckling load or moment replaces F_e in the main Specification (for columns and for beams as appropriate) in determining F_n. Local buckling A_e and S_e is determined at the appropriate F_n. Distortional buckling utilizes the existing provisions.

4. Assess the fastener demands and limit states. For bending, torsional bracing dominates and fastener demand is based on the applied torsion created by having loads that are not applied at the shear center. For axial, stability bracing dominates and the fastener demand is based on a simplification of the forces that develop in a second order analysis. For both bending and axial load the demands are converted into fastener demands in bearing and pull-through. These demands are compared against capacities in these two limit states to assess the adequacy of the fasteners for the applied load and/or moment.

The following sections provide the first draft of specification language for completion of steps 1 through 4. In many cases the method can be formulated in tables or other derivative presentations to simplify its design use, see ballot 13 for a specific presentation of such a derivative presentation, here the fundamental formulas are provided.

Basic Illustration for Definition of Sheathed Wall Variables

All variables are defined in the draft ballots that follow. The illustrations provided here attempt to summarize key variables with respect to the larger design problem.

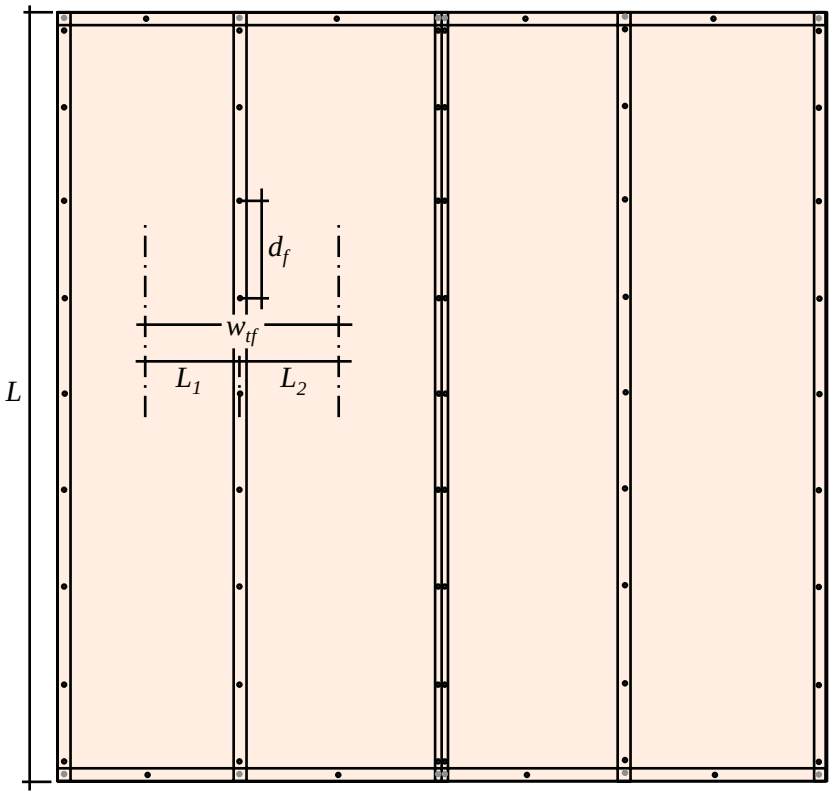

Basic illustration of a sheathed stud wall. Example wall has two full sheets as would be typical in an 8’ x 8’ wall with studs spaced 24 in. o.c. Basic variables for a fastener attached to one of the field studs is illustrated.

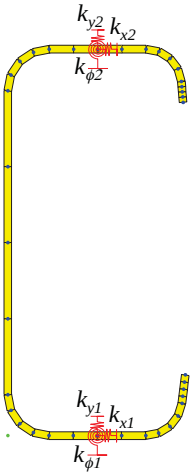

Illustration of the springs that are developed at the fastener locations on the two faces of the stud. These springs provide bracing for the stud and determination of their stiffness is the first major step of the design method.

Draft Ballot 1: Lateral Restraint Provided by Fastener-Sheathing System (k_x)

X.1 Sheathing Braced Member - Available Lateral Stiffness at Fastener (k_x)

The available lateral stiffness provided at a fastener location from a fastener-sheathing combination providing bracing restraint to a member shall be determined as follows.

$$k_x = \frac{1}{\frac{1}{k_{x\ell}} + \frac{1}{k_{xd}}} \tag{X.1.1}$$

where:

k_{xd} = Lateral stiffness supplied to the fastener by the sheathing under diaphragm action

$$k_{xd} = \frac{\pi^2 G_b t_b d_f w_{tf}}{L^2} \tag{X.1.2}$$

d_f = distance between fasteners
w_{tf} = width of sheathing tributary to the fastener
G_b = shear modulus of the sheathing, and shall be determined via testing (ASTM-D2719-89 or utilizing tabulated values from NDS (NDS 2005) or APA Panel Design Specification.
t_b = thickness of the sheathing board
L = sheathing height

and

$k_{x\ell}$ = localized lateral stiffness developed at the fastener during tilting and bearing, $k_{x\ell}$ may be determined through testing per AISI S990-13, or as follows:

$$k_{x\ell} = \frac{3\pi E d^4 t^3}{4t_b^2\left(9\pi d^4 + 16 t_b t^3\right)} \tag{X.1.3}$$

E = Young's modulus of the CFS member (stud, joist, girt, etc.)
t = thickness of the flange of the CFS member
d = diameter of the fastener
t_b = thickness of the sheathing board

Commentary: Resistance of a stud to lateral movement (as developed from weak-axis buckling, torsion, etc.) is developed from two distinct mechanisms, in series, in a sheathed wall: local and diaphragm. The diaphragm stiffness develops as the sheathing undergoes shear. The local stiffness develops as the fastener bears against the sheathing and tilts at its attachment point. The expressions and guidance provided here are detailed in Vieira and Schafer (2012). The method may be extended to purlins, girts, joists, or any member in which restraint is provided, in part, by the lateral stiffness that develops at the connection between a cold-formed steel member and sheathing.

Vieira Jr., L. C. M., Schafer, B.W. (2012). "Lateral Stiffness and Strength of Sheathing Braced Cold-Formed Steel Stud Walls." Elsevier, *Engineering Structures.* 37, 205–213.

Draft Ballot 2: Testing for Local Lateral Restraint of Sheathed Members ($k_{x\ell}$)

AISI S990-13
TEST STANDARD FOR DETERMINATION OF LOCAL LATERAL STIFFNESS OF FASTENER-SHEATHING RESTRAINT

1. Scope

This Standard shall apply for the determination of the local lateral stiffness ($k_{x\ell}$) supplied by sheathing, fastened to cold-formed steel members.

This Standard shall include Sections 1 though 10 inclusive.

Commentary: Wall studs braced solely by sheathing primarily rely on the lateral bracing restraint that is experimentally determined in this test standard. The use of this simple test for determining lateral restraint began with Winter (1960) and an updated treatment and discussion is available in Vieira and Schafer (2012). The test method may be extended to purlins, girts, joists, or any member in which restraint is provided, in part, by the localized lateral stiffness that develops at the connection between a cold-formed steel member and sheathing.

Winter, G. (1960). "Lateral Bracing of Beams and Columns." ASCE, *J. of the Structural Division*.
Vieira Jr., L. C. M., Schafer, B.W. (2012). "Lateral Stiffness and Strength of Sheathing Braced Cold-Formed Steel Stud Walls." Elsevier, *Engineering Structures*. 37, 205–213.

2. Referenced Documents

The following documents or portions thereof are referenced within this Standard and shall be considered as part of the requirements of this document.

a. American Iron and Steel Institute (AISI), Washington, DC:
   S100-12, North American Specification for the Design of Cold Formed Steel Structural Members, 2012 Edition.
   S200-12, North American Standard for Cold-Formed Steel Framing – General Provisions, 2012 Edition.

b. ASTM International (ASTM), West Conshohoken, PA:
   A370-<latest edition>, Standard Test Methods and Definitions for Mechanical Testing of Steel Products
   ASTM E6-<latest edition>, Standard Terminology Relating to Methods of Mechanical Testing
   IEEE/ASTM-SI-10-<latest edition>, American National Standard for Use of the International System of Units (SI): The Modern Metric System

3. Terminology

Where the following terms appear in this standard they shall have the meaning as defined in AISI S100, AISI S200, or as defined herein. Terms not defined in Section 3 of this standard, or AISI S100, or AISI S200 shall have the ordinary accepted meaning for the context for which they

are intended.

4 Symbols

P_{test} = lateral force at peak load for complete test specimen
P_i = lateral force at an individual fastener
$\Delta_{0.4}$ = lateral displacement at 0.4Ptest as measured in test
Δ_i = lateral displacement at an individual fastener
$k_{x\ell}$ = local lateral stiffness of fastener-sheathing system

5 Precision

5.1 Loads shall be recorded to a precision of 1 percent of the ultimate load during application of test loads.

5.2 Deflections shall be recorded to a precision of 0.001 in. (0.025 mm).

6 Test Fixture

6.1 The test may be conducted in a Universal Testing Machine or similar.

6.2 The test consists of two horizontal studs connected by sheathing fastened to the flanges (4 fasteners on a side) where the studs are pulled apart (perpendicular to the long axis of the stud). An example test setup is provided in Figure 1.

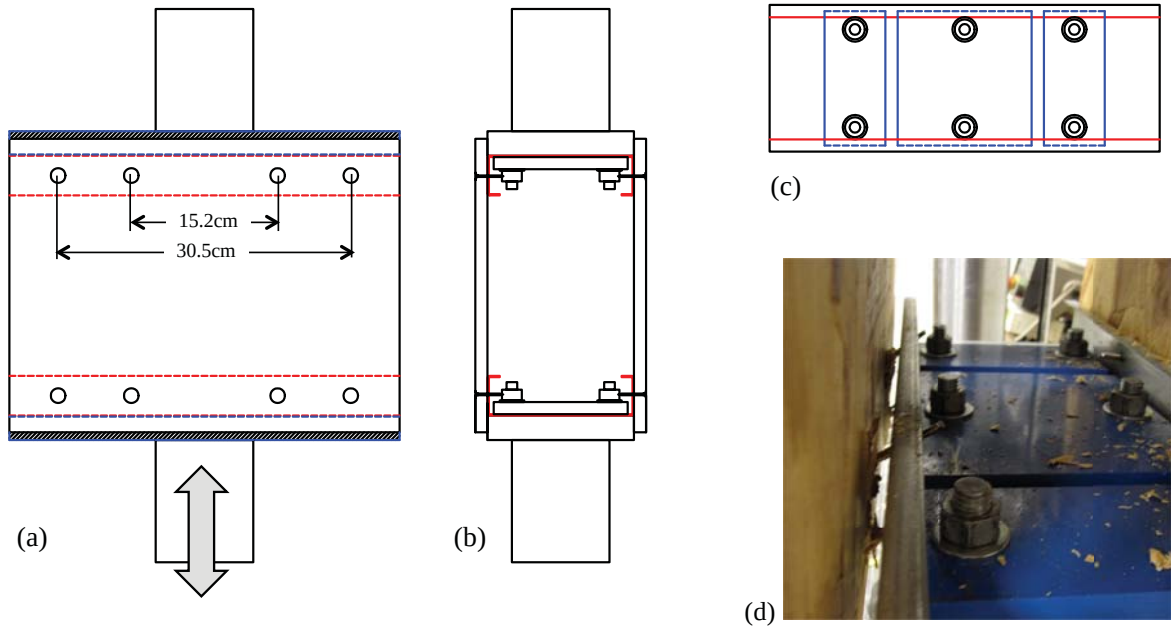

Figure 1 (a) Front view of rig and specimen, dashed lines indicate hidden stud, arrow indicates location and direction of loading (note circles indicate potential fastening locations not actual holes in sheathing) (b) Side view of specimen in rig (c) Inside view of stud clamping system (d) photograph of clamping system

6.3 Bending in the web of the studs shall be minimized by use of clamping plates or other

means.

6.4 Fasteners shall be free to tilt.

7 Test Specimen

The test specimen consists of the studs, fasteners, and sheathing.

7.1 The stud should be representative of intended end use. However, the stud web depth does not have to match intended end use, as web deformation is minimized by the test fixture. The stud thickness shall not be greater than 20% above the design value. The stud length should be at least twice the fastener spacing.

7.2 The fasteners should be representative of intended end use. Fastener diameter shall not be greater than 20% above the design value. All fasteners should be driven to flush using the same installation methods as intended end use. Fasteners are not allowed to have their tips bear against the flange web as they tilt, if this condition occurs the fasteners should be shortened and the test redone.

7.3 The sheathing should be representative of intended end use. The sheathing material should be environmentally conditioned to a cited standard. The sheathing thickness shall not be greater than 20% above the design value. The sheathing width shall match the stud length. The sheathing length shall be at least equal to the fastener spacing, but not greater than the stud spacing in intended end use.

Commentary: The basic premise of the test specimen is the construction of a small segment of the wall consistent with final application. However, this analogy is incomplete and the test standard recognizes that the primary variables are the stud thickness, the fastener diameter (and local details of the fastener and the fastener head), and the sheathing thickness and material properties of the sheathing. Fastener spacing and stud spacing are not typically critical variables. Note, as discussed in Section 1, the stud may be replaced by a purlin, girt, joist, or any member in which restraint is provided, in part, by the localized lateral stiffness that develops at the connection between a cold-formed steel member and sheathing.

8 Test Procedure

8.1 The test should be conducted under pseudo-static monotonic load until a peak (failure) load is reached. A specific loading rate is not prescribed, but the test shall not reach peak load in less than 5 minutes.

8.2 Displacement shall be measured across the test specimen. Machine displacements (from the internal LVDT that drives the actuator of the Universal Testing Machine) may be used as the specimen displacement.

8.3 The test procedure shall be consistent with AISI S100, that is "Evaluation of the test results shall be made on the basis of the average value of test data resulting from tests of not fewer than three identical specimens, provided the deviation of any individual test result from the average value obtained from all tests does not exceed ±15 percent. If such deviation from the average value exceeds 15 percent, more tests of the same kind shall be made until the deviation of any individual test result from the average value obtained from all tests does not exceed ±15 percent, or until at least three additional tests have been made. No test result shall be eliminated unless a rationale for its exclusion can be given." For this criteria, the evaluation of consistency is made on the stiffness $k_{x\ell}$.

9 Data Evaluation

9.1 The local lateral stiffness of the fastener-sheathing system ($k_{x\ell}$) is determined at 40% of the ultimate strength (i.e., peak load or P_{test}) of the specimen. Specifically:

$$P_{0.4} = 0.4P_{test} \quad (1)$$

$$P_i = P_{0.4} / 4 \quad (2)$$

$$\Delta_{0.4} = \Delta\left(0.4P_{test}\right) \quad (3)$$

$$\Delta_i = \Delta_{0.4} / 2 \quad (4)$$

$$k_{x\ell} = P_i / \Delta_i \quad (5)$$

where

P_{test} = lateral force at peak load for complete test specimen

P_i = lateral force at an individual fastener

$\Delta_{0.4}$ = lateral displacement at $0.4P_{test}$ as measured in test

Δ_i = lateral displacement at an individual fastener

$k_{x\ell}$ = local lateral stiffness of fastener-sheathing system

9.2 No test result shall be eliminated unless a rationale for its exclusion can be given.

Commentary: Free body diagrams for the conversion from the specimen to the individual fastener values are provided in Figure 2 and 3 below. Additional discussion of the determination of the stiffness may be found in Vieira and Schafer (2012).

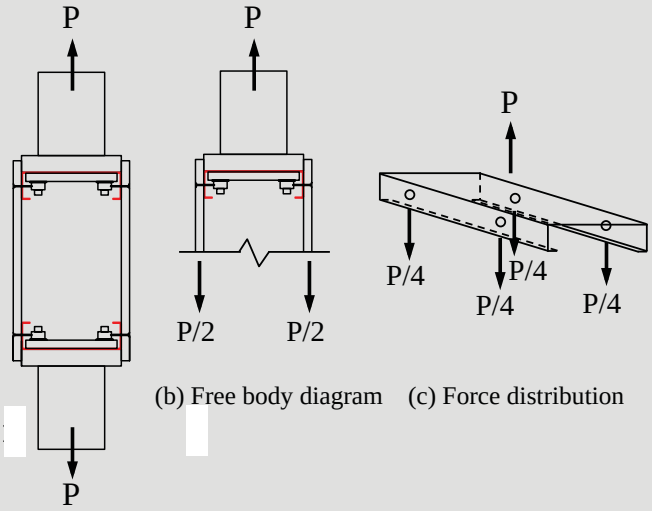

(b) Free body diagram (c) Force distribution

(a) Applied Force, P

Figure 2 Free-body diagrams for determination of individual fastener forces, P_i

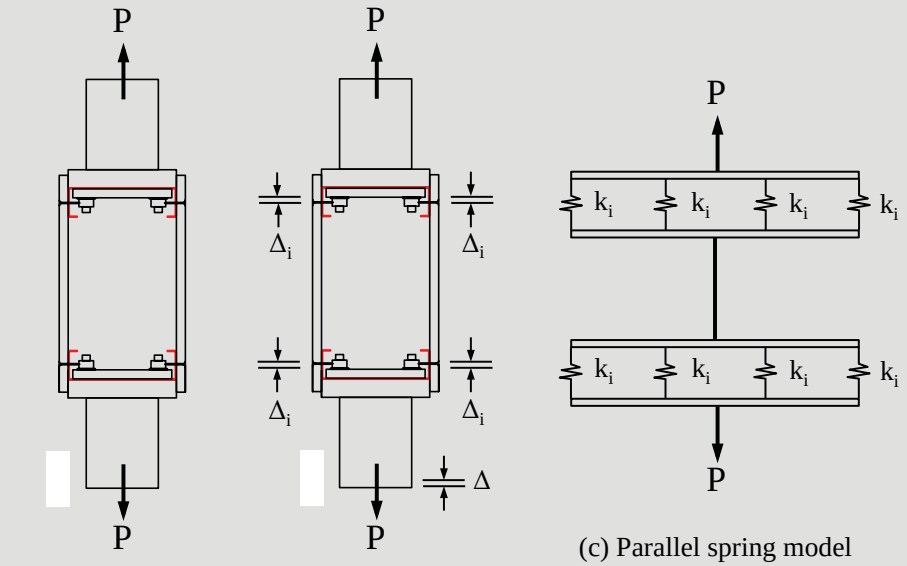

(a) Applied Force, P (b) Deformed shape (c) Parallel spring model

Figure 3 Free-body diagram for determination of individual fastener stiffness, $k_i = k_{x\ell}$

10 Report

10.1 The test report shall include a description of the tested specimens, including a drawing detailing all pertinent dimensions.

10.2 The test report shall include the measured physical properties consistent with the limitations outlined in Section 7.

10.3 The test report shall include a detailed drawing of the test setup, depicting location and direction of load application, location of displacement instrumentation and their point of reference, and details of any deviations from the test requirements. Additionally, photographs shall supplement the detailed drawings of the test setup.

10.4 The test report shall include individual and average load-versus-deformation values and curves, as plotted directly, or as reprinted from data acquisition systems.

10.5 The stiffness determined at 40% of the peak load ($k_{x\ell}$) shall also be drawn on the load-versus-deformation curves. Values of $k_{x\ell}$ shall be provided for all tested specimens.

10.5 The test report shall include individual and average maximum test load values observed (i.e., P_{test}). Description of the nature, type and location of failure exhibited by each specimen tested, and a description of the general behavior of the test fixture during load application. Additionally, photographs shall supplement the description of the failure mode(s).

10.6 The test report shall include a description of the test method and loading procedure used, rate of loading or rate of motion of the crosshead movement, and time to maximum load.

Draft Ballot 3: Vertical Restraint Provided by Fastener-Sheathing System (k_y)

Y.1 Sheathing Braced Member - Available Vertical Stiffness at Fastener (k_y)

The available vertical stiffness provided at a fastener location from a fastener-sheathing combination providing bracing restraint to a member shall be determined as follows.

$$k_y = \frac{(EI)_w \pi^4 d_f}{L^4} \tag{Y.1.1}$$

where:

d_f = distance between fasteners
L = sheathing height
$(EI)_w$ = additional bending rigidity contributed by the sheathing

if composite action between the member and sheathing *is ignored*:

$(EI)_w$ = bending sheathing rigidity per APA-D510C for OSB and plywood sheathing, and GA-235-10 for gypsum sheathing

if composite action between the member and sheathing *is included*, then the additional bending rigidity shall be determined from a composite wall system test using the same test configuration as ASTM-E72:

$$(EI)_w = \tfrac{1}{2}\left[(EI)_{system} - (EI)_{stud}\right] \tag{Y.1.2}$$

where:

$(EI)_{stud}$ = major-axis bending rigidity of the stud
$(EI)_{system}$ = major-axis bending rigidity of the tested, sheathed, wall

Depending on the test configuration employed

$$(EI)_{system} = \frac{11HL^3}{384\delta} \text{ (two point loads)} \tag{Y.1.3}$$

$$(EI)_{system} = \frac{5wL^4}{384\delta} \text{ (uniform distributed load)} \tag{Y.1.4}$$

where
H = concentrated load applied perpendicular to the wall,
L = height of the wall,
w = uniform load perpendicular to the wall, and
d = maximum measured displacement for the respective loading case (H or w)

Commentary: In the method developed here the vertical spring, k_y, does not represent the pull-out stiffness of the fastener, but rather the additional stiffness that the sheathing adds to the major-axis bending rigidity of the stud. This stiffness can be an important restriction in flexural-torsional buckling of the stud. The composite action of the sheathing is only utilized to develop the bracing restraint, the maximum member strength is still limited to the stud properties alone.

See Vieira and Schafer (2012, 2013) for further discussion included expressions for $(EI)_w$ if full composite action is included (this provides an upper bound solution that can be useful in some instances).

Vieira Jr., L. C. M., Schafer, B.W. (2012). "Lateral Stiffness and Strength of Sheathing Braced Cold-Formed Steel Stud Walls." Elsevier, *Engineering Structures.* 37, 205–213.

Vieira Jr., L.C.M., Schafer, B.W. (2013). "Behavior and Design of Sheathed Cold-Formed Steel Stud Walls under Compression." ASCE, *Journal of Structural Engineering* (DOI: 10.1061/(ASCE)ST.1943-541X.0000731). *In Press*

Draft Ballot 4: Rotational Restraint Provided by Fastener-Sheathing System (k_ϕ)

Note: Determination of rotational restraint is already provided in AISI-COFS standards. However, it likely makes the most sense to move that material to be parallel with the k_x and k_y springs – to that end a draft ballot is provide here that provides this information. The ballot is a modified form of that already available in AISI COFS standards.

In addition, some care must be taken with the current use of k_ϕ and whether this quantity is a spring stiffness or a foundation stiffness (i.e. the spring stiffness divided by a tributary length). Existing provisions for distortional buckling in the main Specification of AISI-S100 require a foundation stiffness, but k_x and k_y are spring stiffness values. The notation developed in Vieira and Schafer (2013) is extended here: k_x, k_y, k_ϕ refer to spring stiffness and $\underline{k}_x, \underline{k}_y, \underline{k}_\phi$ refers to foundation stiffness, i.e., the spring stiffness divided by the fastener spacing. Foundation stiffness $\underline{k}_x, \underline{k}_y, \underline{k}_\phi$ is also what is utilized in an FSM analysis.

Vieira Jr., L.C.M., Schafer, B.W. (2013). "Behavior and Design of Sheathed Cold-Formed Steel Stud Walls under Compression." ASCE, *Journal of Structural Engineering* (DOI: 10.1061/(ASCE)ST.1943-541X.0000731). *In Press*

Z.1 Sheathing Braced Member - Available Rotational Stiffness at Fastener (k_ϕ)

The available vertical stiffness provided at a fastener location from a fastener-sheathing combination providing bracing restraint to a member shall be determined as follows.

The rotational stiffness k_ϕ shall be determined per test using AISI-S991, or as follows:

$$k_\phi = \underline{k}_\phi d_f \qquad \text{(Eq. Z.1-1)}$$

where

d_f = fastener spacing

$$\underline{k}_\phi = (1/\underline{k}_{\phi w} + 1/\underline{k}_{\phi c})^{-1} \qquad \text{(Eq. Z.1-2)}$$

where

$\underline{k}_{\phi w}$ = Sheathing rotational restraint

= $EI_w/L_1 + EI_w/L_2$ for interior members (joists or rafters) with *structural sheathing* fastened on both sides (Eq. Z.1-3)

= EI_w/L_1 for exterior members (joists or rafters) with *structural sheathing* fastened on one side (Eq. Z.1-4)

where

EI_w = Sheathing bending rigidity

= Values as given in Table Z.1-1(a) for plywood and OSB
Values as given in Table Z.1-1(b) for gypsum board.

L_1, L_2 = One half joist spacing to the first and second sides respectively, as illustrated in Figure Z.1-1

$\underline{k}_{\phi c}$ = Connection rotational restraint

= Values as given in Table Z.1-2 for fasteners spaced 12 in. o.c. or closer (*Eq.* Z.1-5)

Table Z.1-1 (a)[1,2]
Plywood and OSB Sheathing Bending Rigidity, EI_w (lbf-in^2/ft)

Span Rating	Strength Parallel to Strength Axis				Stress Perpendicular to Strength Axis			
	Plywood			OSB	Plywood			OSB
	3-ply	4-ply	5-ply		3-ply	4-ply	5-ply	
24/0	66,000	66,000	66,000	60,000	3,600	7,900	11,000	11,000
24/16	86,000	86,000	86,000	86,000	5,200	11,500	16,000	16,000
32/16	125,000	125,000	125,000	125,000	8,100	18,000	25,000	25,000
40/20	250,000	250,000	250,000	250,000	18,000	39,500	56,000	56,000
48/24	440,000	440,000	440,000	440,000	29,500	65,000	91,500	91,500
16oc	165,000	165,000	165,000	165,000	11,000	24,000	34,000	34,000
20oc	230,000	230,000	230,000	230,000	13,000	28,500	40,500	40,500
24oc	330,000	330,000	330,000	330,000	26,000	57,000	80,500	80,500
32oc	715,000	715,000	715,000	715,000	75,000	615,000	235,000	235,000
48oc	1,265,000	1,265,000	1,265,000	1,265,000	160,000	350,000	495,000	495,000

Note:
1. To convert to lbf-in^2/in., divide table values by 12.
   To convert to N-mm^2/m, multiply the table values by 9415.
   To convert to N-mm^2/mm, multiply the table values by 9.415.
2. Above Plywood and OSB bending rigidity is obtained in accordance APA, Panel Design Specification (2004).

Table Z.1-1 (b)[1]
Gypsum Board Bending Rigidity
Effective Stiffness (Typical Range), EI_w

Board Thickness (in.) (mm)	EI (Lb-in^2/in) of width (N-mm^2/mm)
0.5 (12.7)	1500 to 4000 (220,000 to 580,000)
0.625 (15.9)	3000 to 8000 (440,000 to 1,160,000)

Note:
1. Above Gypsum board bending rigidity is obtained from Gypsum Association, GA-235-01 (2001). See commentary for further information.

Table Z.1-2[1]
Connection Rotational Restraint

t (mils)	t (in.)	k_{rc} (lbf-in./in./rad)	k_{rc} (N-mm/mm/rad)
18	0.018	78	348
27	0.027	83	367
30	0.03	84	375
33	0.033	86	384
43	0.043	94	419
54	0.054	105	468
68	0.068	123	546
97	0.097	172	766

Note:
1. Fasteners spaced 12 in. (25.4 mm) o.c. or less.

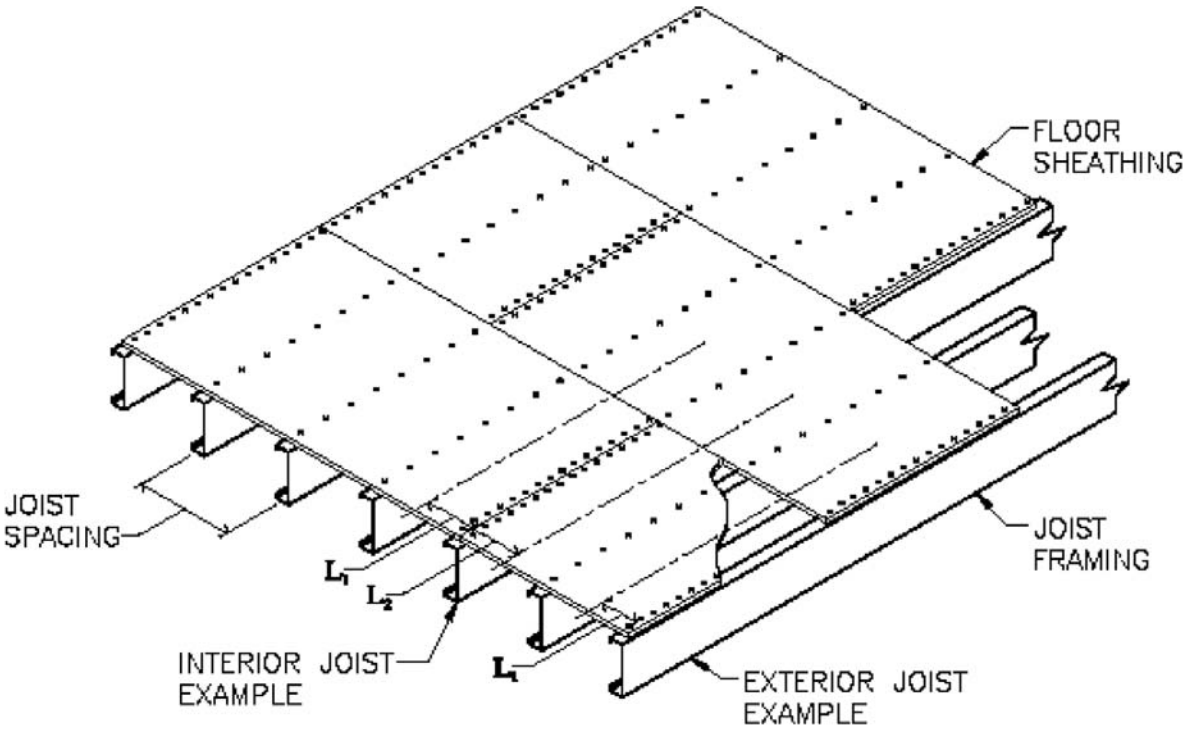

Figure Z.1-1, Illustration of L_1 and L_2 for Sheathing Rotational Restraint

Draft Ballot 5: New Test Standard, Similar to AISI S901, for Rotational Restraint (k_ϕ)

Note: AISI S901 provides several test methods for determining rotational restraint. This standard was used as the experimental basis for finding k_ϕ, the rotational restraint against distortional buckling, but the test standard was never updated. This same rotational restraint is also used in the sheathing braced design of wall studs. S901 is a relative complex test standard, it is proposed that the simplest method is to create a new standard, a draft of that new standard is provided here.

AISI S991-13
TEST STANDARD FOR DETERMINATION OF FASTENER-SHEATHING ROTATIONAL RESTRAINT

1. Scope

This Standard shall apply for the determination of the rotational restraint (k_ϕ) supplied by sheathing, fastened to cold-formed steel members.

This Standard shall include Sections 1 though 10 inclusive.

Commentary: This test standard is conceptually related to AISI S901; however, the specifics of the test and instrumentation are modified for the use intended here. When a cold-formed steel member is connected to sheathing the sheathing can provide beneficial rotational restraint of the member (stud, joist, etc.). One direct mechanism for developing such rotational restraint is a combination of bearing between the flange and sheathing, and pull-through resistance at a fastener location, as the member rotates. This mechanical combination may be idealized as a rotational restraint at the fastener location. This rotational restraint provides the primary bracing restraint against distortional buckling. See Schafer et al. (2010) for a complete discussion.

Schafer, B. W. Vieira Jr., L. C. M., Sangree, R. H., Guan, Y. (2010) "Rotational Restraint and Distortional Buckling in Cold-Formed Steel Framing Systems." Revista Sul-Americana de Engenharia Estrutural (South American Journal of Structural Engineering), Special issue on cold-formed steel structures, 7 (1) 71-90.

2. Referenced Documents

The following documents or portions thereof are referenced within this Standard and shall be considered as part of the requirements of this document.

a. American Iron and Steel Institute (AISI), Washington, DC:

S100-12, North American Specification for the Design of Cold Formed Steel Structural Members, 2012 Edition.

S200-12, North American Standard for Cold-Formed Steel Framing – General Provisions, 2012 Edition.

b. ASTM International (ASTM), West Conshohoken, PA:

A370-<latest edition>, Standard Test Methods and Definitions for Mechanical Testing of Steel Products

ASTM E6-<latest edition>, Standard Terminology Relating to Methods of Mechanical Testing

IEEE/ASTM-SI-10-<latest edition>, American National Standard for Use of the International System of Units (SI): The Modern Metric System

3. Terminology

Where the following terms appear in this standard they shall have the meaning as defined in AISI S100, AISI S200, or as defined herein. Terms not defined in Section 3 of this standard, or AISI S100, or AISI S200 shall have the ordinary accepted meaning for the context for which they are intended.

4 Symbols

d_f = distance between fasteners

P = vertical force applied a distance ho from member-sheathing connection

h_o = out-to-out distance of the web of member

w = width of the test specimen

Δ_v = vertical displacement at face of flange where load P is applied

Δ_h = horizontal displacement of sheathing at connector location

L = length (height) of the sheathing from fixed end to connector location

5 Precision

5.1 Loads shall be recorded to a precision of 1 percent of the ultimate load during application of test loads.

5.2 Deflections shall be recorded to a precision of 0.001 in. (0.025 mm).

6 Test Fixture

6.1 The test consists of a cantilevered piece of sheathing fastened to a horizontally oriented member (i.e., joist, stud, etc.). An example test setup is provided in Figure 1.

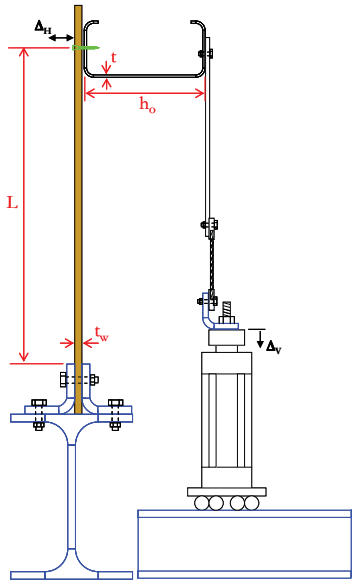

Figure 1 Side view of cantilever specimen.

6.2 The actuator that supplies the force to the end of the member must be free to translate.

7 Test Specimen

The test specimen consists of the sheathing, fasteners, and CFS member (joist, stud, etc.).

7.1 The sheathing should be representative of intended end use. The sheathing material should be environmentally conditioned to a cited standard. The sheathing thickness shall not be greater than 20% above the design value. The sheathing width shall match the member length. The sheathing length shall be at least equal to ½ the spacing between CFS members, but not less than 12 in. [305mm].

7.2 The fasteners should be representative of intended end use. Fastener diameter shall not be greater than 20% above the design value. All fasteners should be driven to flush using the same installation methods as intended end use. At least three fasteners shall be used per test. Fastener spacing shall match intended end use.

7.3 The CFS member should be representative of intended end use. The stud thickness shall not be greater than 20% above the design value. The stud length should be at least four times the fastener spacing.

8 Test Procedure

8.1 The test should be conducted under pseudo-static monotonic load until a peak (failure) load is reached. A specific loading rate is not prescribed, but the test shall not reach peak load in less than 5 minutes.

8.2 Displacement shall be measured in the test specimen. Actuator displacements (from the internal LVDT of the actuator) may be used as the vertical displacement, Δ_v. If the rotational stiffness is to be separated into connector and sheathing components (as utilized in AISI-COFS standards) then the horizontal displacement, Δ_h, must also be recorded.

8.3 The test procedure shall be consistent with AISI S100, that is "Evaluation of the test

results shall be made on the basis of the average value of test data resulting from tests of not fewer than three identical specimens, provided the deviation of any individual test result from the average value obtained from all tests does not exceed ±15 percent. If such deviation from the average value exceeds 15 percent, more tests of the same kind shall be made until the deviation of any individual test result from the average value obtained from all tests does not exceed ±15 percent, or until at least three additional tests have been made. No test result shall be eliminated unless a rationale for its exclusion can be given." For this criteria, the evaluation is made on the stiffness $\underline{k}_{\phi}$, or $\underline{k}_{\phi c}$, or $\underline{k}_{\phi w}$.

9 Data Evaluation

9.1 The rotational stiffness of the fastener-sheathing system is determined at 40% of the ultimate strength (i.e., peak load or P_{test}) of the specimen. Specifically, $P = 0.4P_{test}$ and Δ_v and Δ_h are determined at $0.4P_{test}$:

Rotational stiffness if separation between connector and sheathing is not needed:

$$k_{\phi} = \underline{k}_{\phi} d_f \tag{1}$$

$$\underline{k}_{\phi} = \underline{M} / \theta \tag{2}$$

$$\underline{M} = (P / w) h_o \tag{3}$$

$$\theta = \tan^{-1}\left(\Delta_v / h_o\right) \tag{4}$$

where

d_f = distance between fasteners

P = vertical force applied a distance ho from member-sheathing connection

h_o = out-to-out distance of the web of member

w = width of the test specimen

Δ_v = vertical displacement at face of flange where load P is applied

Rotational stiffness if separation between connector and sheathing is desired:

connector:

$$k_{\phi c} = \underline{k}_{\phi c} d_f \tag{5}$$

$$\underline{k}_{\phi c} = \underline{M} / \theta_c = \underline{M} / (\theta - \theta_w) \tag{6}$$

$$\theta_w = 2\Delta_h / L$$

where

Δ_h = horizontal displacement of sheathing at connector location

L = length (height) of the sheathing from fixed end to connector location

sheathing:

$$k_{\phi w} = \underline{k}_{\phi w} d_f \tag{7}$$

$$\underline{k}_{\phi w} = \underline{M} / \theta_w = \underline{M} / (2\Delta_h / L) \tag{8}$$

total:

$$k_\phi = \underline{k}_\phi d_f \tag{9}$$

$$\underline{k}_\phi = 1/[(1/\underline{k}_{\phi c}) + (1/\underline{k}_{\phi w})] \tag{10}$$

9.2 No test result shall be eliminated unless a rationale for its exclusion can be given.

Commentary: Separation of the rotational restraint into connector and sheathing restraint is conceptually summarized in Figure 2. In existing testing (Schafer et al. 2010) the total rotational restraint was found to be highly variable due principally to large variations in sheathing properties; however, connector rotational stiffness was found to be more repeatable. Both connector and sheathing rotational restraint are utilized in AISI COFS standards, and may be replaced by the experimental values developed here.

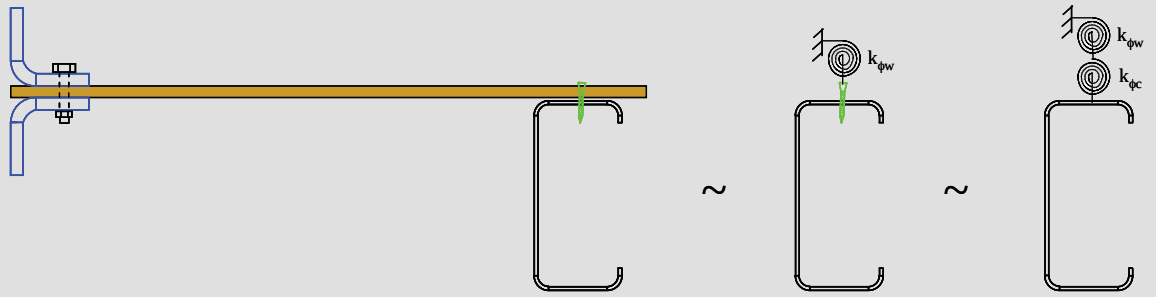

Figure 2 Separation of rotational resistance into connector and sheathing components

10 Report

10.1 The test report shall include a description of the tested specimens, including a drawing detailing all pertinent dimensions.

10.2 The test report shall include the measured physical properties consistent with the limitations outlined in Section 7.

10.3 The test report shall include a detailed drawing of the test setup, depicting location and direction of load application, location of displacement instrumentation and their point of reference, and details of any deviations from the test requirements. Additionally, photographs shall supplement the detailed drawings of the test setup.

10.4 The test report shall include individual and average load-versus-deformation values and curves, as plotted directly, or as reprinted from data acquisition systems.

10.5 The test report shall include individual and average moment-versus-rotation values and curves, as plotted directly, or as reprinted from data acquisition systems.

10.6 The stiffness determined at 40% of the peak load ($\underline{k}_\phi$) shall also be drawn on the moment-versus-rotation curves. Values of $\underline{k}_\phi$ shall be provided for all tested specimens.

10.7 The test report shall include individual and average maximum test load values observed (i.e., P_{test}). Description of the nature, type and location of failure exhibited by each specimen tested, and a description of the general behavior of the test fixture during load application. Additionally, photographs shall supplement the description of the failure

mode(s).

10.8 The test report shall include a description of the test method and loading procedure used, rate of loading or rate of motion of the crosshead movement, and time to maximum load.

Draft Ballot 6: Commentary Addition to Appendix 1 Direct Strength Method for Elastic Stability of Sheathed Walls with emphasis on using the Finite Strip Method

1.1.2 Elastic Buckling

Members with Sheathing
In addition to finding the stability of bare cold-formed steel members it is also possible to model, and determine the elastic buckling loads of members which have semi-rigid restraints developed through attachments to panels, sheathing, or discrete braces. Such restraint can greatly increase the elastic stability loads and moments of a cross-section and even alter the observed buckling modes.

For the specific case of light steel framing, e.g. a cold-formed steel stud wall braced by sheathing, research has been conducted to determine (a) how to characterize the semi-rigid restraints developed at the fastener-sheathing connection to the cold-formed steel member, and (b) how to model the elastic stability of the resulting section (Vieira and Schafer 2013, Peterman and Schafer 2013). AISI-COFS standards provide guidance in terms of design expressions and test standards to determine the key springs: k_x, k_y, k_ϕ that are developed in a sheathing braced member, Figure C-1.1.2-3 summarizes.

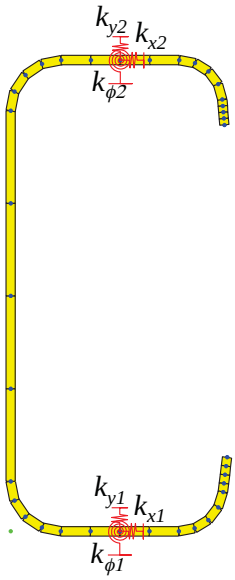

k_x, k_y, k_ϕ springs are included at fastener locations and reflect the stiffness developed through deformations at in the flange-fastener-sheathing system. The stiffness may be different for the two sides (1 and 2) of the member if the sheathing or fastening details vary across the two sides.

k_x is the lateral restraint developed through bearing and tilting of the fastener against the sheathing acting in series with shearing of the sheathing as a diaphragm, see AISI-COFS X.1 and AISI S990 for further information on this restraint.

k_y is the vertical restraint developed as composite action of the member and sheathing occurs in major-axis bending, see AISI-COFS Y.1 for further information on this restraint.

k_ϕ is the rotational restraint developed as the flange attempts to rotate against the face of the sheathing, see AISI-COFS Z.1 and AISI S991 for further information on this restraint.

Figure C-1.1.2-3 Cold-formed steel cross-section partially restrained by sheathing, introduced as springs

Peterman, K.D., Schafer, B.W. “Sheathed Cold-Formed Steel Studs Under Axial and Lateral Load.” Submitted to *Journal of Structural Engineering* (Submitted 2 January 2013). [to be updated after final publication, see Peterman M.S. thesis or research report in the interim]

Vieira Jr., L.C.M., Schafer, B.W. (2013). “Behavior and Design of Sheathed Cold-Formed Steel Stud Walls under Compression.” ASCE, *Journal of Structural Engineering* (DOI: 10.1061/(ASCE)ST.1943-541X.0000731). *In Press*

1.1.2.1 Elastic Buckling Numerical Solutions

Members with Sheathing
It is possible to construct full shell finite element models of members, fasteners, and sheathing and use these models to determine the elastic buckling loads and moments. However, since much of the

deformations are developed locally at the fastener locations (often through damage in the sheathing material) it is difficult to properly capture the stiffness and interactions between the components (Vieira and Schafer 2012). Modeling and experimentation has shown that the complex member-fastener-sheathing interaction can be simplified to a series of springs at the fastener locations as indicated in Figure C-1.1.2-3.

Shell finite element models of the member with springs added at the fastener locations can provide an accurate prediction of the elastic critical loads and moments, see Vieira (2011) or Post (2013). In addition, such models readily allow for a mixture of discrete bracing (springs) and sheathing-based springs. In that sense, this approach is the most general. However, startup time for developing and analyzing such models is relatively significant. Further, identification of the individual local, distortional, and global buckling modes must be done visually, and can be time consuming. As a result, the finite strip method is generally preferred.

Finite strip models of members with springs may be completed in CUFSM. However, it is important to note that the springs in CUFSM are foundation springs, i.e. continuous along the length of the member, not discrete at the fastener locations. Conversion of discrete k_x, k_y, k_ϕ springs to foundation $\underline{k}_x, \underline{k}_y, \underline{k}_\phi$ springs only requires dividing the discrete springs by the fastener spacing. The accuracy of this smeared spring stiffness or (foundation) stiffness approximation is addressed in sections 1.1.2.1.1 - .3 for local, distortional, and global buckling respectively. For practical dimensions it is found to work well.

Vieira Jr., L. C. M., Schafer, B.W. (2012). "Lateral Stiffness and Strength of Sheathing Braced Cold-Formed Steel Stud Walls." Elsevier, *Engineering Structures*. 37, 205 - 213 (doi:10.1016/j.engstruct.2011.12.029)

Vieira Jr., L.C.M. (2011) Behavior and design of cold-formed steel stud walls under axial compression, Department of Civil Engineering, Ph.D. Dissertation, Johns Hopkins University.

Post, B. (2012). "Fastener Spacing Study of Cold-Formed Steel Wall Studs Using Finite Strip and Finite Element Methods." Research Report, December 2012.

1.1.2.1.1 Local Buckling via Finite Strip ($P_{cr\ell}$, $M_{cr\ell}$)

Members with Sheathing

Due to its short wavelength sheathing has little impact on local buckling and it is recommended to ignore the any bracing restraint. Theoretically, $\underline{k}_x$ and $\underline{k}_*$ (if located at the exact mid-width of the flange) have no influence on local buckling, only $\underline{k}_y$. The out-of-plane stiffness, $\underline{k}_y$, is derived consistent with global bending resistance and not localized resistance. Due to the short wavelength of the buckling mode, end conditions also have little influence on local buckling. Thus, a conventional finite strip signature curve result completed on the bare stud (or similar shell finite element model) is adequate for finding the local elastic buckling load or moment. For industry standard studs local elastic buckling loads and moments have been tabled (Li and Schafer 2011).

Li, Z., Schafer, B.W. (2011). "Local and Distortional Elastic Buckling Loads and Moments for SSMA Stud Sections." Cold-Formed Steel Engineers Institute, Tech Note G103-11, 5pp.

1.1.2.1.2 Distortional Buckling via Finite Strip (P_{crd}, M_{crd})

Members with Sheathing

Sheathing provides beneficial rotational restraint against distortional buckling, and $\underline{k}_\phi$ should be included when determining the elastic distortional buckling load or moment. For studs with deep webs (and narrow flanges) the additional restraint supplied by $\underline{k}_x$ may also be influential – its inclusion is optional, but if included requires the use of computational stability solutions (finite strip, finite element, etc.). Stiffness $\underline{k}_y$ should not be included when determining distortional buckling. In distortional buckling $\underline{k}_y$ would be engaged, but as derived, $\underline{k}_y$'s deformations are consistent with strong-axis stud flexure, not rotation of the flange. Further, $\underline{k}_\phi$ already accounts for the moment couple that develops between $\underline{k}_y$ at the fastener and bearing between the flange and sheathing.

End conditions have influence on distortional buckling at practical lengths. General end conditions may be treated in the (CUFSM) finite strip solution directly (Li and Schafer 2010), in shell finite element models, or by using a correction factor (D_{boost} in Moen 2008) for fixed-fixed end conditions on a simply-supported model, i.e. a correction to the conventional signature curve FSM. In some cases the distortional buckling mode can be difficult to identify in a finite strip model, in such cases the constrained FSM is recommended (Li and Schafer 2010b). For industry standard studs, tables are provided to aid in the determination of $\underline{k}_\phi$ and P_{crd} and M_{crd} along with full design examples of the available analytical hand solutions (Li and Schafer 2011, Schafer 2008) including the P_{crd} and M_{crd} solutions adopted in the main Specification of AISI-S100.

The use of the smeared foundation stiffness ($\underline{k}_\phi$ as opposed to k_ϕ, see the discussion in Section 1.1.2.1) in the prediction of distortional buckling has been shown to be adequate for a large variety of members with fastener spacing of 12 in. [305mm]. In general the fastener spacing (d_f) should be less than the distortional buckling half-wavelength (L_{crd}) and it is generally recommended that $d_f/L_{crd} \leq 0.5$ for the use of the smeared foundation stiffness. Otherwise the bracing should be ignored, or a model capable of accounting for the discrete spacing (e.g., shell finite element model) should be employed.

Li, Z., Schafer, B.W. (2010b). "Application of the finite strip method in cold-formed steel member design." Elsevier, *Journal of Constructional Steel Research.* 66 (8-9) 971-980. (doi:10.1016/j.jcsr.2010.04.001)

Li, Z., Schafer, B.W. (2010) "Buckling analysis of cold-formed steel members with general boundary conditions using CUFSM: conventional and constrained finite strip methods." *Proceedings of the 20th Int'l. Spec. Conf. on Cold-Formed Steel Structures,* St. Louis, MO. November, 2010. 17-32.

Moen, C. D. (2008). "Direct strength design for cold-formed steel members with perforations." Ph.D., Johns Hopkins University, Baltimore, MD USA.

Li, Z., Schafer, B.W. (2011). "Local and Distortional Elastic Buckling Loads and Moments for SSMA Stud Sections." Cold-Formed Steel Engineers Institute, Tech Note G103-11, 5pp.

Schafer, B.W. (2008) "Design Aids and Examples for Distortional Buckling" Cold-Formed Steel Engineers Institute, Tech Note G100-08, 22 pp.

1.1.2.1.3 Global (Euler) Buckling via Finite Strip (P_{cre}, M_{cre})

Members with Sheathing

Sheathing greatly influences the global buckling load or moment. For determining P_{cre} or M_{cre} inclusion of all available fastener-sheathing springs ($\underline{k}_x$, $\underline{k}_y$, $\underline{k}_\phi$) is recommended, but $\underline{k}_x$ is critical as it provides the primary fastener-sheathing restraint for both weak-axis flexure and torsion (when present on both flanges).

It is generally beneficial to account for end conditions. To include the impact of fixed end conditions the finite strip model for general end conditions (Li and Schafer 2010, CUFSM v4 or higher) or shell finite element models may be utilized. Alternatively, classical analytical solutions with appropriate effective length factors may be employed as discussed in Section 1.1.2.2 below.

The use of smeared foundation stiffness as opposed to discrete springs (see the discussion in Section 1.1.2.1) in the elastic buckling prediction has been shown to be adequate when the fastener spacing (d_f) is less than the global buckling half-wavelength (L_{cre}). Specifically it is recommended that $d_f/L_{cre} \leq 0.25$ in Post (2012). Otherwise the bracing should be ignored, or a model capable of accounting for the discrete spacing (e.g., shell finite element model, or beam model with discrete springs) should be employed.

Post, B. (2012). "Fastener Spacing Study of Cold-Formed Steel Wall Studs Using Finite Strip and Finite Element Methods." Research Report, December 2012.

1.1.2.2 Elastic Buckling – Manual Solutions

Members with Sheathing

Local buckling: As discussed in Section 1.1.2.1.1 the sheathing is ignored, and solutions based on the bare section as previously described should be employed.

Distortional buckling: If $\underline{k}_x$ and $\underline{k}_\phi$ are included (Figure C-1.1.2-3, also see discussion in Section 1.1.2.1.2) no readily available manual solution exists and computational stability solutions should be pursued. If only $\underline{k}_\phi$ is included the previously provided discussion on distortional buckling is to be followed – namely see AISI S100 C3.1.4 and C4.2.

Global buckling: For axial load an analytical solution that follows the general treatment of Timoshenko and Gere (1961) for the buckling of an unsymmetric section with multiple foundation springs has recently been made available (Vieira and Schafer 2013). The solution does not model each individual bracing spring, but rather uses the same foundation stiffness approximation as used in the FSM analysis. Buckling load determination still requires solution of a 3x3 eigenvalue problem or the related cubic equation. However, the solution is analytical and may be solved in Mathcad, Excel, etc. Application and validation of the solution are provided in Vieira and Schafer (2013). Further details are discussed in the commentary to Section C4.1.6.

For major-axis bending a purely analytical solution to lateral-torsional buckling, including the influence of bracing springs is not generally available. Numerical solutions such as the finite strip method discussed in Section 1.1.2.1.3 are recommended.

Vieira Jr., L.C.M., Schafer, B.W. (2013). "Behavior and Design of Sheathed Cold-Formed Steel Stud Walls under Compression." ASCE, *Journal of Structural Engineering* (DOI: 10.1061/(ASCE)ST.1943-541X.0000731). *In Press*

Timoshenko, S. P., Gere, James M. (1961). *Theory of Elastic Stability*, McGraw-Hill, New York.

Draft Ballot 7: Clean up Distortional buckling notation in AISI-S100 C3.1.4 and C4.2

Note: Cleanup notation and make reference to new provisions for $\underline{k}_\phi$

C3.1.4 Distortional Buckling Strength [Resistance]

Modified definition of k_ϕ: change to $\underline{k}_\phi$ and modestly amend definition.

$\underline{k}_\phi$ = Rotational foundation (i.e., per unit length) stiffness provided by an ~~restraining~~ element (brace, panel, sheathing) ~~to~~ that restrains rotation about the *flange/web* juncture of a member. ~~(z~~Zero if the compression *flange* is unrestrained~~).~~ Also, may be taken as zero if this restraint is conservatively ignored. For sheathing-based restraint, see AISI-S200 Z.1 for determining $\underline{k}_\phi$ analytically, or AISI S991 for determining $\underline{k}_\phi$ by testing.

Also, update notation in Eq. C3.1.4-6.

$$F_d = \beta \frac{\underline{k}_{\phi fe} + \underline{k}_{\phi we} + \underline{k}_\phi}{\tilde{k}_{\phi fg} + \tilde{k}_{\phi wg}} \qquad (Eq.\ \text{C3.1.4-6})$$

Also, update definitions and expressions for $\underline{k}_{\phi fe}$ and $\underline{k}_{\phi we}$ in C3.1.4 (notation change only).

C4.2 Distortional Buckling Strength [Resistance]

Modified definition of k_ϕ: change to $\underline{k}_\phi$ and modestly amend definition.

$\underline{k}_\phi$ = Rotational foundation (i.e., per unit length) stiffness provided by an ~~restraining~~ element (brace, panel, sheathing) ~~to~~ that restrains rotation about the *flange/web* juncture of a member. ~~(z~~Zero if the *flange* is unrestrained~~).~~ Also, may be taken as zero if this restraint is conservatively ignored. If rotational stiffness provided to the two flanges is dissimilar, the smaller rotational stiffness is used. For sheathing-based restraint, see AISI-S200 Z.1 for determining $\underline{k}_\phi$ analytically, or AISI S991 for determining $\underline{k}_\phi$ by testing.

Also, update notation in Eq. C4.2-6.

$$F_d = \beta \frac{\underline{k}_{\phi fe} + \underline{k}_{\phi we} + \underline{k}_\phi}{\tilde{k}_{\phi fg} + \tilde{k}_{\phi wg}} \qquad (Eq.\ \text{C4.2-6})$$

Also, update definitions and expressions for $\underline{k}_{\phi fe}$ and $\underline{k}_{\phi we}$ in C4.2 (notation change only).

Draft Ballot 8: Add new section to C4.1 for Flexural-Torsional Buckling with Sheathing

Note: AISI S100 covers global buckling strength of concentrically loaded compression members. A new section should be added, proposed as C4.1.6, to cover sheathed compression members. Alternatively these provisions could be added to Chapter D under assemblies, but since it is all about calculating F_e, it may make more sense to have it with the other F_e expressions. Given the complexity of F_e, a preference is for computational solutions, so the analytical solution is in the commentary only.

C4 Concentrically Loaded Compression Members

..

C4.1 Nominal Strength for Yielding, Flexural, Flexural-torsional, and Torsional Buckling

..

[The following section is entirely new]

C4.1.6 Sections with sheathing attached to the flanges

The elastic buckling stress F_e, for a section with sheathing attached to the member shall be determined by rational elastic buckling analysis.

Commentary: The elastic buckling stress of a member with sheathing attached is often significantly greater than the bare section. The fastener-sheathing restraint may be modeled as a series of springs, see AISI COFS X.1, Y.1, Z.1 and AISI S990, and 991 for further details. Numerical methods for rational elastic buckling analysis of a section with sheathing attached to the flanges are covered in detail in the Commentary to Appendix 1, Section 1.1.2. See Section 1.1.2.1.3 for specific guidance on finite strip modeling. An analytical rational elastic buckling analysis is provided here.

For axial load an analytical solution that follows the general treatment of Timoshenko and Gere (1961) for the buckling of an unsymmetric section with multiple foundation springs has recently been made available (Vieira and Schafer 2013) and is provided here. Consider a cross-section which at any location "i" in its section has springs $\underline{k}_x, \underline{k}_y$, and $\underline{k}_\phi$. These springs are foundation stiffness values, i.e. per unit length. Each set of springs at location i are distance h_x, h_y from the centroid and h_{xs}, h_{ys} from the shear center, as illustrated in Figure C-4.1.6-1.

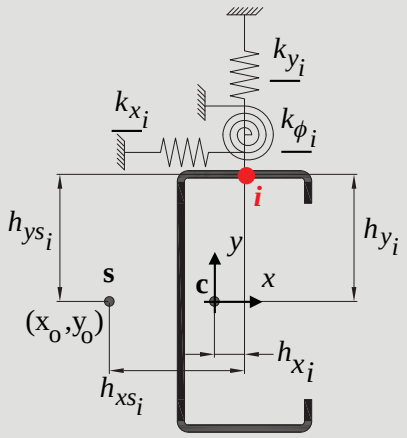

Figure C-4.1.6-1 Definition of variables for a member with foundation springs at i

The stability of this section loaded at its centroid is an eigenvalue problem, where:

$$([K_e] - \lambda[K_g])\Phi = 0$$

the elastic stiffness matrix is:

$$[K_e] = \begin{bmatrix} P_{cry} + \frac{(K_{y,sp}L)^2}{m^2\pi^2}\sum_{i=1}^{n}\underline{k}_{xi} & 0 & \frac{(K_{y,sp}L)^2}{m^2\pi^2}\sum_{i=1}^{n}\underline{k}_{xi}h_{ysi} \\ & P_{crx} + \frac{(K_{x,sp}L)^2}{m^2\pi^2}\sum_{i=1}^{n}\underline{k}_{yi} & -\frac{(K_{x,sp}L)^2}{m^2\pi^2}\sum_{i=1}^{n}\underline{k}_{yi}h_{xsi} \\ sym & & \frac{I_0}{A}P_{cr\phi} + \frac{(K_{t,sp}L)^2}{m^2\pi^2}\sum_{i=1}^{n}\underline{k}_{xi}(h_{ysi})^2 + \frac{(K_{t,sp}L)^2}{m^2\pi^2}\sum_{i=1}^{n}\underline{k}_{yi}(h_{xsi})^2 + \frac{(K_{t,sp}L)^2}{m^2\pi^2}\sum_{i=1}^{n}\underline{k}_{\phi i} \end{bmatrix}$$

where

$$P_{crx} = \frac{m^2\pi^2 E I_x}{(K_x L)^2}$$

$$P_{cry} = \frac{m^2\pi^2 E I_y}{(K_y L)^2}$$

$$P_{cr\phi} = \frac{A}{I_o}\left(GJ + \frac{m^2\pi^2 E C_w}{(K_t L)^2}\right)$$

and the geometric stiffness matrix is:

$$[K_g] = P\begin{bmatrix} 1 & 0 & y_o \\ & 1 & -x_o \\ sym & & \frac{I_o}{A} \end{bmatrix}$$

Solving the eigen problem results in three eigenvalues (roots to the characteristic equation), the minimum of which is the critical eigenvalue:

$$\lambda_{cr} = \min(\lambda_1, \lambda_2, \lambda_3)$$

which allows the elastic buckling load and stress to be determined:

$P_{cr} = \lambda_{cr} P$

$F_e = P_{cr} / A$

where:

A = cross-sectional area of the stud

C_w = Warping constant of stud

E = Young's modulus of steel

h_{xi} = x-distance from centroid to spring i

h_{xs} = x-distanced from shear center to spring i

h_{yi} = y-distance from centroid to spring i

h_{ysi} = y-distance from shear center to spring i

I_o = polar moment of inertia of stud ($I_0=I_0+I_y+A(x_o^2+y_o^2)$)

I_x = Moment of inertia about x-axis of stud

I_y = Moment of inertia about y-axis of stud

J = St. Venant Torsional Constant of stud
K_x = effective length about x-axis (for fixed-fixed, m=1 K_x=0.5, m=2 K_x=0.7)
K_y = effective length about y-axis (for fixed-fixed, m=1 K_y=0.5, m=2 K_y=0.7)
K_t = effective length in torsion about shear center (for fixed-fixed, m=1 K_t=0.5, m=2 K_t=0.7)
$K_{x,sp}$ = effective length for the spring foundation about x-axis (for fixed-fixed $K_{x,sp}= \sqrt{3} / 2 = 0.866$)
$K_{y,sp}$ = effective length for the spring foundation about y-axis (for fixed-fixed $K_{y,sp}= \sqrt{3} / 2 = 0.866$)
$K_{t,sp}$ = effective length for the spring foundation about shear center (for fixed-fixed $K_{t,sp}= \sqrt{3} / 2 = 0.866$)
$\underline{k}_x$ = foundation lateral fastener-sheathing stiffness in x
$\underline{k}_y$ = foundation lateral fastener-sheathing stiffness in y
$\underline{k}_\nu$ = foundation rotational fastener-sheathing stiffness in the x-y plane
L = stud length
m = number of buckling half-waves along the length
P = axial reference load in buckling analysis
x_o = x distance from centroid to shear center
y_o = y distance from centroid to shear center
λ_j = eigenvalues for the buckling modes (j=1, 2, 3)
Φ = eigenvector of the buckling mode

Draft Ballot 9: Add new section to C3.1.2.3 for Lateral-Torsional Buckling with Sheathing

Note: Similar to columns, beams also need a trigger for sheathing-braced members in AISI S100. Note, no analytical solution is currently readily available, so computational solutions must be employed for finding F_e.

C3.1 Bending

..

C3.1.2 Lateral-Torsional Buckling Strength [Resistance]

..

[The following section is entirely new]

C3.1.2.3 Sections with sheathing attached to the flanges

The elastic buckling stress F_e, for a section with sheathing attached to the member shall be determined by rational elastic buckling analysis.

Commentary: The lateral-torsional buckling stress of a member with sheathing attached is often significantly greater than the bare section. The fastener-sheathing restraint may be modeled as a series of springs, see AISI COFS X.1, Y.1, Z.1 and AISI S990, and 991 for further details. Numerical methods for rational elastic buckling analysis of a section with sheathing attached to the flanges are covered in detail in the Commentary to Appendix 1, Section 1.1.2. See Section 1.1.2.1.3 for specific guidance on finite strip modeling. An analytical rational elastic buckling analysis for lateral-torsional buckling similar to that provided in the commentary of Section C4.1.6 is mechanically possible, but expressions have not been formally derived at this time.

Draft Ballot 10: Clean up Sheathing-Braced Design Charging Language in S100

Note: Modifications to D4 in AISI S100 are needed to make it clear how sheathing braced design can now work. It is not clear where the best place to state this language is, this ballot provides a placeholder to remind the committee that at some point D4 will need to be cleaned up, in some fashion, to make sheathing-braced design parallel to all-steel design in AISI S100.

D4 Cold-Formed Steel Light-Frame Construction

The design and installation of *structural members* utilized in cold-formed steel repetitive framing applications where the specified minimum base steel *thickness* is not greater than 0.1180 in. (2.997 mm) shall be in accordance with the AISI S200 and the following, as applicable:

(a) Framing for floor and roof systems in buildings shall be designed in accordance with AISI S210 or solely in accordance with this *Specification.*

(b) Wall studs shall be designed in accordance with AISI S211, or solely in accordance with this *Specification* either on the basis of an all-steel system in accordance with Section D4.1 or on the basis of a sheathing-braced system in accordance with Section D4.2~~on the basis of sheathing braced design in accordance with an appropriate theory, tests, or *rational engineering analysis*.~~ Both solid and perforated *webs* are permitted. Both ends of the stud shall be connected to restrain rotation about the longitudinal stud axis and horizontal displacement perpendicular to the stud axis.

(c) Headers, shall be designed in accordance with AISI S212 or solely in accordance with this *Specification*.

(d) Light-framed *shear walls*, diagonal strap bracing (that is part of a structural wall) and *diaphragms* to resist wind, seismic and other in-plane lateral *loads* shall be designed in accordance with AISI S213.

(e) Trusses shall be designed in accordance with AISI S214.

D4.1 All-Steel Design of Wall Stud Assemblies

Wall stud assemblies using an all-steel design shall be designed neglecting the structural contribution of the attached sheathings and shall comply with the requirements of Chapter C. For compression members with circular or non-circular *web* perforations, the effective section properties shall be determined in accordance with Section B2.2.

D4.2 Sheathing Braced Design of Wall Stud Assemblies

Wall stud assemblies using a sheathing braced design philosophy shall be designed per this Specification, including Appendix 1, with the contribution from the sheathing bracing accounted for in distortional buckling (k_ϕ in C3.1.4 and C4.2, or P_{crd} and M_{crd} in Appendix 1) and in global buckling (C4.1.6 for axial, C3.1.2.3 for major-axis bending, or P_{cre} and M_{cre} in Appendix 1).

Draft Ballot 11: Fastener (Bearing and Pull-through) Demands [Required Loads]

Note: Once member limit states are checked, fastener limit states need to be considered. In axial only testing of studs member limit states controlled. In axial + bending tests fastener limit states controlled for gypsum or partially sheathed with gypsum cases. This ballot deals with the demand side, i.e., what are the required forces on the fastener-sheathing system.

F.D.1 Bearing and Pull-Through Demands at Connections in Sheathing-Braced Members

The required demand in *bearing* ($F_{r\text{-}br}$) for a connection supplying sheathing bracing is the sum of the required demands from direct torsional bracing in bending and axial stability bracing, as provided in this section.

The required demand in *pull-through* ($F_{r\text{-}pt}$) for a connection supplying sheathing bracing is the sum of the required demands from direct torsional bracing in bending and axial stability bracing as provided in this section.

Commentary: The two dominant connection failure modes observed in testing on sheathing-braced members are bearing and pull-through (Peterman and Schafer 2013). These failure modes are triggered in response to the fastener-sheathing system resisting lateral and torsional deformations. Demands from axial stability bracing (Vieira and Schafer 2013) are typically less than those developed in resisting the direct torsion that develops in bending. However, total demand on the connection should be checked, and is the summation of the axial and bending requirements.

Peterman, K.D., Schafer, B.W. "Sheathed Cold-Formed Steel Studs Under Axial and Lateral Load." Submitted to *Journal of Structural Engineering* (Submitted 2 January 2013).

Vieira Jr., L.C.M., Schafer, B.W. (2013). "Behavior and Design of Sheathed Cold-Formed Steel Stud Walls under Compression." ASCE, *Journal of Structural Engineering* (DOI: 10.1061/(ASCE)ST.1943-541X.0000731). *In Press*

F.D.1.1 Required Demands to Resist Direct Torsion in Bending in Sheathing-Braced Members

The required torsion (T_r) at a fastener location that develops due to transverse loads on a sheathing-braced stud (member) shall be determined as follows:

T_r = Summation of demands from point and distributed loads:

Point load:

$T_r = 0.4 H_r e$ for fastener closest to point load (*Eq*. F.D.1-1)

$T_r = 0.3 H_r e$ for the two fasteners adjacent to the fastener closest to point load (*Eq*. F.D.1-2)

Distributed load:

$T_r = w_r d_f e$ for each fastener (*Eq*. F.D.1-3)

where:
H_r = transverse point load
w_r = transverse distributed load
d_f = fastener spacing
e = distance from the shear center to the termination of the flange flat

Commentary: In bending the connection demands developed to provide torsional bracing generally exceed those developed to provide stability bracing; therefore, only torsional bracing demands are considered in bending. The forces developed at the connection are a function of the torsional stiffness of the member and the torsional stiffness of the fastener-sheathing system. A stiffness analysis may be employed to precisely determine the torsion carried in the member vs. that carried by the fastener-sheathing system. The distributions assumed in the *Specification* represent typical values for a member sheathed on both sides, as provided in Peterman and Schafer (2013). Demands from point loads and transverse loads should be summed.

The pull-through and bearing demands that develop at the fastener-sheathing connections shall be determined as follows:

(a) Similar Sheathing on both flanges

Pull-through

$$F_{r-pt} = \frac{T_r}{(b/2)} \frac{k_\phi}{2k_\phi + 2k_x(h^2/4)} \quad \text{(Eq. F.D.1-4)}$$

Bearing

$$F_{r-br} = T_r(h/2) \frac{k_x}{2k_\phi + 2k_x(h^2/4)} \quad \text{(Eq. F.D.1-5)}$$

(b) Dis-similar sheathing on the two flanges

$$\theta_r = T_r / [k_{\phi 1} + k_{x1}(h^2/4) + k_{\phi 2} + k_{x2}(h^2/4)] \quad \text{(Eq. F.D.1-6)}$$

Side 1/Flange 1

Pull-through

$$F_{r-pt1} = k_{\phi 1}\theta_r / (b/2) \quad \text{(Eq. F.D.1-7)}$$

Bearing

$$F_{r-br1} = k_{x1}(h/2)\theta_r \quad \text{(Eq. F.D.1-8)}$$

Side 2/Flange 2

Pull-through

$$F_{r-pt2} = k_{\phi 2}\theta_r / (b/2) \quad \text{(Eq. F.D.1-9)}$$

Bearing

$$F_{r-br2} = k_{x2}(h/2)\theta_r \quad \text{(Eq. F.D.1-10)}$$

where:
h = out-to-out depth of the stud (member)
b = out-to-out width of the stud (member) flange
k_x = lateral stiffness of the fastener-sheathing assembly per AISI COFS X.1, subscript refers to flange 1 or 2 in members with dis-similar sheathing.
k_ϕ = rotational stiffness of the fastener-sheathing assembly per AISI COFS Z.1, subscript refers to flange 1 or 2 in members with dis-similar sheathing

Commentary: The expressions assume that bearing and pull-through mechanisms both combine to provide torsional resistance for the fastener-sheathing system as shown in Figure C-F.D.1.1-1 and developed in Peterman and Schafer (2013). The relative stiffness of the mechanisms is utilize to determine how the demands distribute.

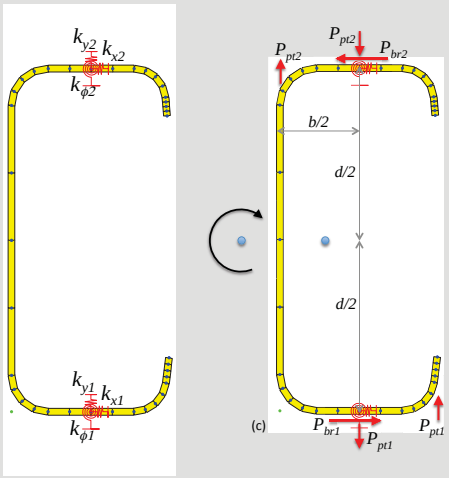

Figure C-F.D.1.1-1 Sheathing-based springs and torsion free-body diagram

The Specification assumes the member is singly symmetric with depth *h*, and the fasteners are placed at mid-width of the flange (*b*/2). For the more general case, of two fasteners connected at arbitrary locations similar to the AISI-S100 C4.1.6 Commentary, then the following more general expressions may be employed:

$$\theta_r = T_r / [k_{\phi 1} + k_{x1} h_{ys1}^2 + k_{\phi 2} + k_{x2} h_{ys2}^2] \quad \text{(Eq. C-F.D.1-1)}$$

$$F_{r-pt1} = k_{\phi 1} \theta_r / h_{xs1} \quad \text{(Eq. C-F.D.1-2)}$$

$$F_{r-br1} = k_{x1} h_{ys1} \theta_r \quad \text{(Eq. C-F.D.1-3)}$$

$$F_{r-pt2} = k_{\phi 2} \theta_r / h_{xs2} \quad \text{(Eq. C-F.D.1-4)}$$

$$F_{r-br2} = k_{x2} h_{ys2} \theta_r \quad \text{(Eq. C-F.D.1-5)}$$

F.D.1.2 Required Demands for Axial Stability Bracing in Sheathing-Braced Members

(a) Similar Sheathing on both flanges

Pull-through

$$F_{r-pt} = \frac{0.02 P_r}{L / d_f} \frac{(h/b)}{(1+n)} \quad \text{(Eq. F.D.1-11)}$$

$$n = \frac{k_x (h^2/4)}{k_\phi} \quad \text{(Eq. F.D.1-12)}$$

Bearing

$$F_{r-br} = \frac{0.02 P_r}{L / d_f} \quad \text{(Eq. F.D.1-13)}$$

(b) Dis-similar sheathing on the two flanges

Side 1/Flange 1

Pull-through

$$F_{r-pt1} = \frac{0.04P_r}{L/d_f}\frac{k_{\phi 1}(h/b)}{(1+n)[k_{\phi 1}+k_{\phi 2}]} \quad \text{(Eq. F.D.1-14)}$$

$$n = \frac{k_{x1}(h^2/4)+k_{x2}(h^2/4)}{k_{\phi 1}+k_{\phi 2}} \quad \text{(Eq. F.D.1-15)}$$

Bearing

$$F_{r-br1} = \frac{0.04P_r}{L/d_f}\frac{k_{x1}}{k_{x1}+k_{x2}} \quad \text{(Eq. F.D.1-16)}$$

Side 2/Flange 2

Pull-through

$$F_{r-pt2} = \frac{0.04P_r}{L/d_f}\frac{k_{\phi 2}(h/b)}{(1+n)[k_{\phi 1}+k_{\phi 2}]} \quad \text{(Eq. F.D.1-17)}$$

Bearing

$$F_{r-br2} = \frac{0.04P_r}{L/d_f}\frac{k_{x2}}{k_{x1}+k_{x2}} \quad \text{(Eq. F.D.1-18)}$$

where:

P_r = Required axial force in the stud (member)
L = Length of the stud (member)
d_f = Distance (spacing) between fasteners along the stud length
k_x = lateral stiffness of the fastener-sheathing assembly per AISI COFS X.1, subscript refers to flange 1 or 2 in members with dis-similar sheathing.
k_ϕ = rotational stiffness of the fastener-sheathing assembly per AISI COFS Z.1, subscript refers to flange 1 or 2 in members with dis-similar sheathing

Commentary: For stability bracing, in general, if the stiffness of the bracing system is known and an initial imperfection in the member to be braced is assumed the forces that develop in the bracing system may be determined. However the situation becomes complicated when multiple buckling modes are involved, e.g., in a sheathing-braced stud wall, the sheathing supplies bracing resistance against local, distortional, and global (weak-axis flexure, and strong-axis flexural-torsional buckling). Vieira and Schafer (2013) provide an explicit method for determining the bracing force in combined global modes (flexure and flexural-torsional) and demonstrate how to integrate knowledge of the exact buckling mode shape and imperfections to predict forces developed at fasteners in a sheathing-braced design. The method is an extension of the stability solution provided in the Commentary to C-4.1.6, see Vieira (2011) for a design example. Although the method is verified against detailed shell finite element analysis, the expressions and final methodology are complicated. Explicitly determining the bracing demands as a function of imperfection and initial stiffness in every mode is not amenable to design.

Examination of the total force developed in sheathing-braced studs under axial load in Vieira (2011) demonstrates that even when considering the additional forces that develop due to the full combination of possible buckling modes the total force at peak load remains less than 4% of the applied force. Further, the force distribution across the stud is approximately regular, therefore a simple approach for the fastener

forces was considered. For weak-axis flexural buckling the expressions are straightforward, the lateral stiffness of the two flanges resists the applied bracing demand:

$$F_r = 0.04P_r / (L / d_f) = (k_{x1} + k_{x2})\Delta_r \qquad \text{(Eq. C-F.D.1-6)}$$

for one fastener (e.g. on side 1):

$$F_{r-br1} = k_{x1}\Delta_r \qquad \text{(Eq. C-F.D.1-7)}$$

after substitution this results in:

$$F_{r-br1} = \frac{0.04P_r}{L / d_f}\frac{k_{x1}}{k_{x1} + k_{x2}}, \qquad \text{(Eq. C-F.D.1-8)}$$

and, for the case of similar sheathing (on the two flanges):

$$F_{r-br1} = \frac{0.02P_r}{L / d_f} \qquad \text{(Eq. C-F.D.1-9)}$$

The situation is decidedly more complex when torsion is involved in the buckling mode being resisted. In the absence of an exact mode shape, consider pure torsion as a worst case demand for torsional buckling, in this case the basic method explained in the commentary to C-F.D.1.1 applies. It is assumed that 2%P developed in both flanges is adequate, therefore:

$$T_r = 0.02P_r h / (L / d_f) \qquad \text{(Eq. C-F.D.1-10)}$$

this may be substituted into Eq. F.D.1.1-6 and 7 to provide the pull-through demand for side 1:

$$F_{r-pt1} = \frac{0.04P_r}{L / d_f}\frac{k_{\phi 1}(h / b)}{k_{\phi 1} + k_{x1}(h^2 / 4) + k_{\phi 2} + k_{x2}(h^2 / 4)}, \qquad \text{(Eq. C-F.D.1-11)}$$

and Eq. F.D.1.1-6 and 8 to provide the bearing demand for side 1:

$$F_{r-br1} = \frac{0.04P_r}{L / d_f}\frac{k_{x1}(h^2 / 4)}{k_{\phi 1} + k_{x1}(h^2 / 4) + k_{\phi 2} + k_{x2}(h^2 / 4)}. \qquad \text{(Eq. C-F.D.1-12)}$$

If we recognize that the dominant mechanism for the resistance is the lateral stiffness we may further simplify, specifically, define:

$$n[k_{\phi 1} + k_{\phi 2}] = k_{x1}(h^2 / 4) + k_{x2}(h^2 / 4), \qquad \text{(Eq. C-F.D.1-13)}$$

where n is typically much greater than 1. Therefore, pull-through and bearing simplify to:

$$F_{r-pt1} = \frac{0.04P_r}{L / d_f}\frac{k_{\phi 1}(h / b)}{(1+n)[k_{\phi 1} + k_{\phi 2}]} \qquad \text{(Eq. C-F.D.1-14)}$$

$$F_{r-br1} = \frac{0.04P_r}{L / d_f}\frac{k_{x1}}{(1+1/n)[k_{x1} + k_{x2}]} \qquad \text{(Eq. C-F.D.1-15)}$$

As n increases the bearing expression may be conservatively simplified to:

$$F_{r-br1} = \frac{0.04P_r}{L / d_f}\frac{k_{x1}}{k_{x1} + k_{x2}}. \qquad \text{(Eq. C-F.D.1-16)}$$

Thus, with these simplifications resisting flexure and torsion are similar enough to warrant a simple approach to the bracing demands that is independent of the buckling mode shape.

Draft Ballot 12: Fastener (Bearing and Pull-through) Capacity [Available Loads]

Note: The demands of F.D.1 must be compared against capacities. However, currently analytical expressions do not exist, and even manufacturer data can be difficult to come by.

F.C.1 Available Strength of Member-Fastener-Sheathing in Bearing

Except where otherwise indicated, the following *safety factor* or *resistance factor* shall be used to determine the *allowable strength* or *design strength* [*factored resistance*] in accordance with the applicable design method in Section A4, A5, or A6.

Ω = 3.00 (*ASD*)
ϕ = 0.50 (*LRFD*)
= 0.40 (*LSD*)

Alternatively, design values for a particular application are permitted to be based on tests, with the *safety factor*, Ω, and the *resistance factor*, ϕ, determined according to Chapter F.

$P_{n\text{-}br}$ = *Nominal bearing strength* [*resistance*] of member-fastener-sheathing combination as reported by manufacturer or determined by independent laboratory testing.

Note: The proposed lateral stiffness test method (Draft Ballot 2, AISI S990) could be extended to failure capacities as a means to determine the bearing capacity. Average experimental bearing strength (P_{br}) from lateral stiffness tests reported in Vieira and Schafer (2012) are 2570 N [578 lbf] for a #8 connecting a nominal 68 mil stud to 11mm [7/16 in.] OSB (24/16 rated, exposure 1), and 380 N [86 lbf] for a #6 connecting a nominal 68 mils stud to in 12.7 mm [1/2in.] gypsum.

It is possible that NDS or APA has a rational method for determining bearing strength. Dowel bearing strength in Chapter 11 of NDS appears potentially applicable. Such a method, with appropriate modification, would be beneficial for rational application without testing.

To the authors knowledge manufacturers do not currently provide this $P_{n\text{-}br}$ data.

F.C.1 Available Strength of Member-Fastener-Sheathing in Pull-through

Except where otherwise indicated, the following *safety factor* or *resistance factor* shall be used to determine the *allowable strength* or *design strength* [*factored resistance*] in accordance with the applicable design method in Section A4, A5, or A6.

Ω = 3.00 (*ASD*)
ϕ = 0.50 (*LRFD*)
= 0.40 (*LSD*)

Alternatively, design values for a particular application are permitted to be based on tests, with the *safety factor*, Ω, and the *resistance factor*, ϕ, determined according to Chapter F.

$P_{n\text{-}pt}$ = *Nominal pull-through strength* [*resistance*] of member-fastener-sheathing combination as reported by manufacturer or determined by independent laboratory testing.

Note: The proposed rotational stiffness test method (Draft Ballot 5, AISI S991) could be extended

to failure capacities as a means to determine the pull-through capacity. Average experimental pull-through strength (P_{pt}) from rotational stiffness tests reported in Vieira (2011) and summarized for failure capacitities in Peterman and Schafer (2013) are 1944 N [437 lbf] for a #8 connecting a nominal 68 mil stud to 11mm [7/16 in.] OSB (24/16 rated, exposure 1), and 178 N [40 lbf] for a #6 connecting a nominal 68 mils stud to in 12.7 mm [1/2in.] gypsum.

It is possible that NDS or APA has a rational method for determining pull-through strength. The author did not find such a method under a cursory review of NDS. Withdrawal is discussed in Chapter 11 of NDS, but the pull-through mechanism seems specific to cold-formed steel in that the fastener anchors in the steel so completely that pulling the head through the sheathing is actually a weaker mode. If a large washer or other modifications were made to the head of the fastener, eventually the withdrawal from the steel would limit strength, but in testing to date pull-through has been the observed limit state. An analysis based method for pull-through would be beneficial for rational application without testing.

To the authors knowledge manufacturers do not currently provide this $P_{n\text{-}pt}$ data.

In 2012 preliminary efforts were made by the author to generate isolated pull-through data using a simple testing rig, this information can be shared with the committee and manufacturers interested in supplying this data.

Draft Ballot 13: Strength Table (Mock Up) for COFS or Design Manual

Note: It is recognized that the complete method, while blissfully general, is complex. Therefore it is important that derivative products exist for use. It is possible to provide tables for the fastener-sheathing restraint springs, but the real burden to use is the computational buckling analysis. To that end, once the general method is voted upon, it is proposed to create strength tables in a form similar to what is shown here to expedite use of the method. These tables are simply derivative products of the method and could be in COFS standards, AISI Design Manual, CFSEI Aids, or Manufacturer Technical Guides.

sheathing side 1: 7/16" OSB with #8 screws														
sheathing side 2: 1/2" Gypsum with #6 screws														
		AXIAL CAPACITY (Pn) [kips]						BENDING CAPACITY (Mn) [kip-in.]						
stud	stud	8		9		10		8		9		10		<-- sheathing height [ft]
designation*	spacing [in.]	6	12	6	12	6	12	6	12	6	12	6	12	<-- fastener spacing [in.]
362S162-33 [33 ksi]	16													
	24													
362S162-43 [33 ksi]	16													
	24													
362S162-54 [33 ksi]	16													
	24													
362S162-68 [33 ksi]	16	[axial capacities here, possibly with limit state						[bending capacities listed here]						
	24	designated in some form, note, some thickness												
362S162-97 [33 ksi]	16	and fastener combinations not possible, so												
	24	some cells may be blank in the end, or stud												
362S162-54 [50 ksi]	16	list decreased]												
	24													
362S162-68 [50 ksi]	16													
	24													
362S162-97 [50 ksi]	16													
	24													
[continued]														

sheathing side 1: 5/32" Structural 1 with #8 screws														
sheathing side 2: 1/2" Gypsum with #6 screws														
		AXIAL CAPACITY (Pn) [kips]						BENDING CAPACITY (Mn) [kip-in.]						
stud	stud	8		9		10		8		9		10		<-- sheathing height [ft]
designation*	spacing [in.]	6	12	6	12	6	12	6	12	6	12	6	12	<-- fastener spacing [in.]
362S162-33 [33 ksi]	16													
	24													
362S162-43 [33 ksi]	16													
	24													
362S162-54 [33 ksi]	16													
	24													
362S162-68 [33 ksi]	16	[axial capacities here, possibly with limit state						[bending capacities listed here]						
	24	designated in some form, note, some thickness												
362S162-97 [33 ksi]	16	and fastener combinations not possible, so												
	24	some cells may be blank in the end, or stud												
362S162-54 [50 ksi]	16	list decreased]												
	24													
362S162-68 [50 ksi]	16													
	24													
362S162-97 [50 ksi]	16													
	24													
[continued]														

*track matches stud thickness

Appendix: Design Example

Design Example: Sheathing Braced Design of a Wall Stud

BWS, 27 January 2013

Objective: Determine the nominal axial and bending capacity (under a unifrom distribtued load) of an 8' x 8' stud wall with OSB on one face and gypsum board on the other face employing a sheathing-braced design philosophy.

Given:
wall: 8' x 8' wall, studs spaced 24 in. o.c.
studs: 362S162-68 [50ksi]
track: 362T125-68 [50ksi]
face 1 sheathing: 7/16 in. OSB (24/16 rated, exposure 1)
face 1 fasteners: #8 at 12 in. o.c.
face 2 sheathing: 1/2 in. Gypsum Board
face 2 fasteners: #6 at 12 in. o.c.

Basic illustration of sheathing braced wall

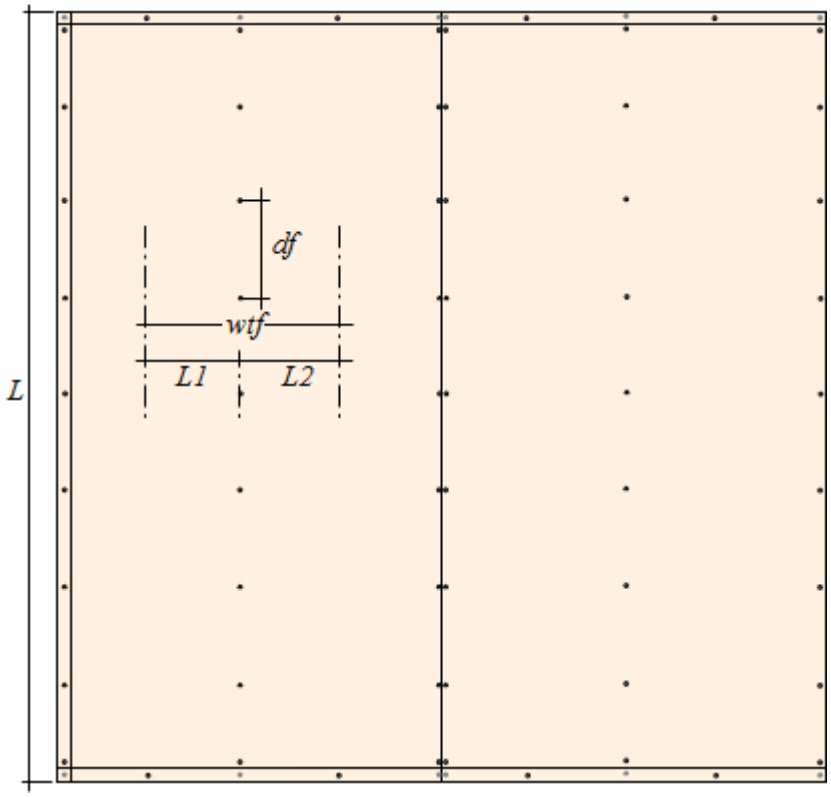

Basic variables:

$L := 96 \cdot in$

$d_f := 12 \cdot in$

$w_{tf} := 24 \cdot in$

$L_1 := 12 \cdot in$

$L_2 := 12 \cdot in$

other variables and dimensioans are defined as needed in the problem below.

ASSUME the field stud controls the capacity, in full design all studs would have to be checked, here only the field stud dimensioned above is checked.

Method:
1. Find stiffness of fastener-sheahting bracing springs
2. Find elastic buckling of stud with bracing
3. Calculate member capacities
4. Check fasteners (in bearing and pull-through)

k_x Lateral Restraint Provided by the Fastener Sheathing System

Face 1: 7/16 in. OSB (24/16 rated, exposure 1)

$$k_x := \frac{1}{\frac{1}{k_{xl}} + \frac{1}{k_{xd}}}$$ (Eq. X.1.1 of draft ballot 1)

$$k_{xd} := \frac{\pi^2 G_b \cdot t_b \cdot d_f \cdot w_{tf}}{L^2}$$ (Eq. X.1.2 of draft ballot 1)

$t_b := 0.437 \cdot in$ (APA panel design Spec. 2004, Table 5)

$G_b := \frac{83500 \cdot \frac{lbf}{in}}{t_b}$ $G_b = 191.076 \cdot ksi$ (APA panel design Spec. 2004, Table 4a) (NDS 2005, SDPWS-2005, Table C4.2.2A)

$d_f = 12 \cdot in$ $w_{tf} = 24 \cdot in$ $L = 96 \cdot in$ as defined previously

$k_{xd} := \frac{\pi^2 G_b \cdot t_b \cdot d_f \cdot w_{tf}}{L^2}$ $k_{xd} = 25.753 \cdot \frac{kip}{in}$

k_{xl} may be determined by test or by formula provided. First consider the provided (conservative formula) to demonstrate how the terms work, etc.

$$k_{xl} := \frac{3 \cdot \pi \cdot E \cdot d^4 \cdot t^3}{4 \cdot t_b^2 \cdot \left(9 \cdot \pi \cdot d^4 + 16 \cdot t_b \cdot t^3\right)}$$ (Eq. X.1.3 of draft ballot 1)

$E := 29500 \cdot ksi$ (per AISI S100)

$t := 0.0713 \cdot in$ (design stud thickness per AISI S200, or SSMA or SFIA...)

$d := 0.164 \cdot in$ (per CFSEI TN-F701-12 or manufacturer)

$t_b = 0.437 \cdot in$ (as defined previously)

$k_{xl} := \frac{3 \cdot \pi \cdot E \cdot d^4 \cdot t^3}{4 \cdot t_b^2 \cdot \left(9 \cdot \pi \cdot d^4 + 16 \cdot t_b \cdot t^3\right)}$ $k_{xl} = 4.152 \cdot \frac{kip}{in}$

For these details lateral stiffness tests were also conducted to determine the stiffness. These tests were conducted as proposed in draft ballot 2 and are fully detailed in Vieira and Schafer (2012) "Lateral stiffness and strength of sheathing braced cold-formed steel stud walls." from this work we have

$k_{xl} := 7.08 \cdot \frac{kip}{in}$ here one can see the advantage of conducting the testing, for this example we will use this experimental value going forward.

k_x Lateral Restraint Provided by the Fastener Sheathing System

Face 1: 7/16 in. OSB (24/16 rated, exposure 1) **(CONTINUED)**

$$k_{x1} := \frac{1}{\frac{1}{k_{xl}} + \frac{1}{k_{xd}}} \qquad k_{x1} = 5.553 \cdot \frac{kip}{in}$$

Note for FSM or other analysis we use a foundation stiffness not a spring stiffness. In publications and proposed codes this is designated with an underbar. Here, since such notation is not available in Mathcad it is denoted with the subscript "fnd"

$$k_{x1\_fnd} := \frac{k_{x1}}{d_f} \qquad k_{x1\_fnd} = 0.463 \cdot \frac{\frac{kip}{in}}{in}$$

k_x Lateral Restraint Provided by the Fastener Sheathing System

Face 2: 1/2 in. Gypsum Board

$$k_{xd} := \frac{\pi^2 G_b \cdot t_b \cdot d_f \cdot w_{tf}}{L^2}$$ (Eq. X.1.2 of draft ballot 1)

$t_b := 0.5 \cdot in$ (cite to other nominal thickness, not known, use specified thickness)

$G_b := \frac{40000 \cdot \frac{lbf}{in}}{t_b}$ $G_b = 80 \cdot ksi$ (NDS 2005, SDPWS-2005, Table C4.2.2B)

$d_f = 12 \cdot in$ $w_{tf} = 24 \cdot in$ $L = 96 \cdot in$ as defined previously

$k_{xd} := \frac{\pi^2 G_b \cdot t_b \cdot d_f \cdot w_{tf}}{L^2}$ $k_{xd} = 12.337 \cdot \frac{kip}{in}$

$$k_{xl} := \frac{3 \cdot \pi \cdot E \cdot d^4 \cdot t^3}{4 \cdot t_b^2 \cdot \left(9 \cdot \pi \cdot d^4 + 16 \cdot t_b \cdot t^3\right)}$$ (Eq X.1.3 of draft ballot 1)

$E := 29500 \cdot ksi$ $t := 0.0713 \cdot in$ $t_b = 0.5 \cdot in$ (as defined previously)

$d := 0.138 \cdot in$ (#6, per CFSEI TN-F701-12 or manufacturer)

$k_{xl} := \frac{3 \cdot \pi \cdot E \cdot d^4 \cdot t^3}{4 \cdot t_b^2 \cdot \left(9 \cdot \pi \cdot d^4 + 16 \cdot t_b \cdot t^3\right)}$ $k_{xl} = 2.779 \cdot \frac{kip}{in}$

Tests conducted in Vieira and Schafer (2012) provided an average

$k_{xl} := 2.43 \cdot \frac{kip}{in}$ similar to the design formula. again, the test data is preferred and is thus used here going forward. (Note, variability is high in test data for Gypsum based values.)

$k_{x2} := \frac{1}{\frac{1}{k_{xl}} + \frac{1}{k_{xd}}}$ $k_{x2} = 2.03 \cdot \frac{kip}{in}$

Note for FSM or other analysis we use a foundation stiffness not a spring stiffness in publications and proposed codes this is designated with an underbar. Here, since such notation is not available in Mathcad it is denoted with the subscript "fnd"

$k_{x2\_fnd} := \frac{k_{x2}}{d_f}$ $k_{x2\_fnd} = 0.169 \cdot \frac{\frac{kip}{in}}{in}$

k_y Vertical Restraint Provided by the Fastener Sheathing System

Face 1: 7/16 in. OSB (24/16 rated, exposure 1)

$$k_{y1} := \frac{EI_w \cdot \pi^4 \cdot d_f}{L^4}$$ (Eq. Y.1.1 of draft ballot 3)

$d_f = 12 \cdot in$ $L = 96 \cdot in$ (as previously defined)

$EI_w := 78000 \cdot \frac{lbf \cdot in^2}{ft} \cdot w_{tf}$ $EI_w = 156 \cdot kip \cdot in^2$ (per APA panel design spec. 2004, Table 4a, stress paralell to strength axis)

$k_{y1} := \frac{EI_w \cdot \pi^4 \cdot d_f}{L^4}$ $k_{y1} = 2.147 \times 10^{-3} \cdot \frac{kip}{in}$ $d_f = 12 \cdot in$

$k_{y1\_fnd} := \frac{k_{y1}}{d_f}$ $k_{y1\_fnd} = 1.789 \times 10^{-4} \cdot \frac{\frac{kip}{in}}{in}$

(note, this is a lower bound value for non-composite action. additional guidance is provided in draft ballot 3 if partially composite action is accounted for in the bracing resistance. Often, even the non-composite action may be enough to restrict the strong-axis flexural portion of flexural-torsional buckling adequately.)

Face 2: 1/2 in. Gypsum Boaard

$$k_{y2} := \frac{EI_w \cdot \pi^4 \cdot d_f}{L^4}$$ (Eq. Y.1.1 of draft ballot 3)

$d_f = 12 \cdot in$ $L = 96 \cdot in$ (as previously defined)

$EI_w := 1500 \cdot \frac{lbf \cdot in^2}{in} \cdot w_{tf}$ $EI_w = 36 \cdot kip \cdot in^2$ (per GA-235-10, minimum effective stiffness provided)

$k_{y2} := \frac{EI_w \cdot \pi^4 \cdot d_f}{L^4}$ $k_{y2} = 4.954 \times 10^{-4} \cdot \frac{kip}{in}$ $d_f = 12 \cdot in$

$k_{y2\_fnd} := \frac{k_{y2}}{d_f}$ $k_{y2\_fnd} = 4.129 \times 10^{-5} \cdot \frac{\frac{kip}{in}}{in}$

k_ϕ Rotational Restraint Provided by the Fastener Sheathing System

Face 1: 7/16 in. OSB (24/16 rated, exposure 1)

$k_\phi := k_{\phi\_fnd} \cdot d_f$ (Eq. Z.1-1 of draft ballot 4)

$k_{\phi\_fnd} := \dfrac{1}{\dfrac{1}{k_{\phi w\_fnd}} + \dfrac{1}{k_{\phi c\_fnd}}}$ (Eq. Z.1-2 of draft ballot 4)

$k_{\phi w\_fnd} := \dfrac{EI_w}{L_1} + \dfrac{EI_w}{L_2}$ (Eq. Z.1-3 of draft ballot 4)

$EI_w := 16000 \cdot \dfrac{lbf \cdot in^2}{ft}$ (stress perp. to strength axis, per Table Z.1-1 of draft ballot 4, or per APA panel design spec.)

$L_1 := \dfrac{w_{tf}}{2}$ $L_1 = 12 \cdot in$ $L_2 := \dfrac{w_{tf}}{2}$ $L_2 = 12 \cdot in$

$k_{\phi w\_fnd} := \dfrac{EI_w}{L_1} + \dfrac{EI_w}{L_2}$ $k_{\phi w\_fnd} = 0.222 \cdot \dfrac{\frac{kip \cdot in}{rad}}{in}$

$k_{\phi c\_fnd} := 123 \cdot \dfrac{\frac{lbf \cdot in}{rad}}{in}$ (per Table Z.1-2 of draft ballot 4)

$k_{\phi 1\_fnd} := \dfrac{1}{\dfrac{1}{k_{\phi w\_fnd}} + \dfrac{1}{k_{\phi c\_fnd}}}$ $k_{\phi 1\_fnd} = 0.079 \cdot \dfrac{\frac{kip \cdot in}{rad}}{in}$

$k_{\phi 1} := k_{\phi 1\_fnd} \cdot d_f$ $k_{\phi 1} = 0.95 \cdot \dfrac{kip \cdot in}{rad}$

Alternatively the rotational stiffness may be determined by test using the method of draft ballot 5. Test results on this configuration are reported in Vieira and Schafer (2012) and Vieira's thesis (2011) in Table 3.1.

$k_{\phi 1\_fnd} := 70.3 \cdot \dfrac{\frac{lbf \cdot in}{rad}}{in}$ $k_{\phi 1\_fnd} = 0.07 \cdot \dfrac{\frac{kip \cdot in}{rad}}{in}$ (average tested value)

$k_{\phi 1} := k_{\phi 1\_fnd} \cdot d_f$ $k_{\phi 1} = 0.844 \cdot \dfrac{kip \cdot in}{rad}$ (slightly less than the value predicted by equations, but considered more accurate, so employed herein).

k_ϕ Rotational Restraint Provided by the Fastener Sheathing System

Face 2: 1/2 in. Gypsum Board

$$k_\phi := k_{\phi\_fnd} \cdot d_f$$ (Eq. Z.1-1 of draft ballot 4)

$$k_{\phi\_fnd} := \frac{1}{\frac{1}{k_{\phi w\_fnd}} + \frac{1}{k_{\phi c\_fnd}}}$$ (Eq. Z.1-2 of draft ballot 4)

$$k_{\phi w\_fnd} := \frac{EI_w}{L_1} + \frac{EI_w}{L_2}$$ (Eq. Z.1-3 of draft ballot 4)

$EI_w := 1500 \cdot \frac{lbf \cdot in^2}{in}$ (per Table Z.1-1 of draft ballot 4, or per GA-235-10)

$L_1 := \frac{w_{tf}}{2}$ $L_1 = 12 \cdot in$ $L_2 := \frac{w_{tf}}{2}$ $L_2 = 12 \cdot in$

$k_{\phi w\_fnd} := \frac{EI_w}{L_1} + \frac{EI_w}{L_2}$ $k_{\phi w\_fnd} = 0.25 \cdot \frac{\frac{kip \cdot in}{rad}}{in}$

$k_{\phi c\_fnd} := 123 \cdot \frac{\frac{lbf \cdot in}{rad}}{in}$ (per Table Z.1-2 of draft ballot 4)

$k_{\phi 2\_fnd} := \frac{1}{\frac{1}{k_{\phi w\_fnd}} + \frac{1}{k_{\phi c\_fnd}}}$ $k_{\phi 2\_fnd} = 0.082 \cdot \frac{\frac{kip \cdot in}{rad}}{in}$

$k_{\phi 2} := k_{\phi 2\_fnd} \cdot d_f$ $k_{\phi 2} = 0.989 \cdot \frac{kip \cdot in}{rad}$

Alternatively the rotational stiffness may be determined by test using the method of draft ballot 5. Test results on this configuration are reported in Vieira and Schafer (2012) and Vieira's thesis (2011) in Table 3.1.

$k_{\phi 2\_fnd} := 70.8 \cdot \frac{\frac{lbf \cdot in}{rad}}{in}$ $k_{\phi 2\_fnd} = 0.071 \cdot \frac{\frac{kip \cdot in}{rad}}{in}$ (average tested value)

$k_{\phi 2} := k_{\phi 2\_fnd} \cdot d_f$ $k_{\phi 2} = 0.85 \cdot \frac{kip \cdot in}{rad}$ (slightly less than the value predicted by equations, but considered more accurate, so employed herein).

Note, elasic kϕ for gypsum and OSB are essentially the same. As detailed in draft ballot 4 and the related research, the thickness of the stud (in which the fastener is anchored into) is the most influential variable in determining kϕ.

Summary of Sheathing-Braced Stiffness

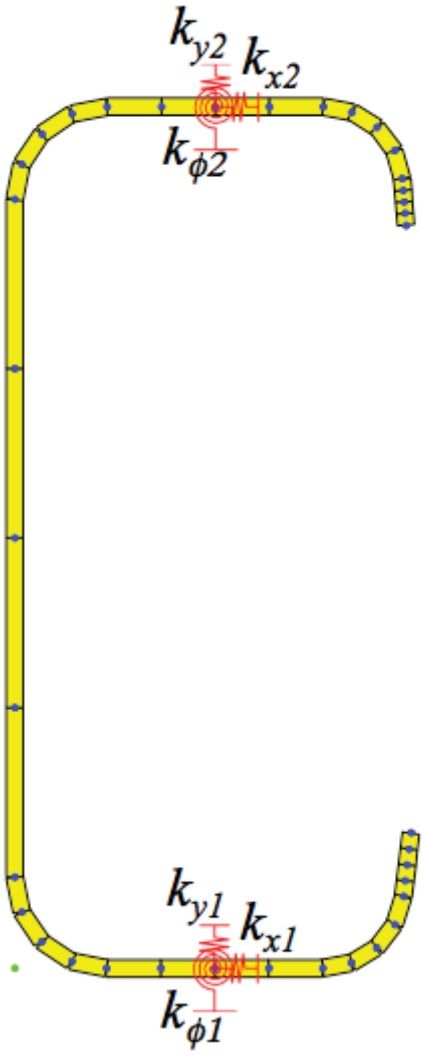

Face 2: 1/2 in. Gypsum Board

$k_{x2} = 2.03 \cdot \frac{kip}{in}$ $\quad k_{x2\_fnd} = 0.169 \cdot \frac{\frac{kip}{in}}{in}$

$k_{y2} = 4.954 \times 10^{-4} \cdot \frac{kip}{in}$ $\quad k_{y2\_fnd} = 4.129 \times 10^{-5} \cdot \frac{\frac{kip}{in}}{in}$

$k_{\phi 2} = 0.85 \cdot \frac{kip \cdot in}{rad}$ $\quad k_{\phi 2\_fnd} = 0.071 \cdot \frac{\frac{kip \cdot in}{rad}}{in}$

Face 1: 7/16 in. OSB

$k_{x1} = 5.553 \cdot \frac{kip}{in}$ $\quad k_{x1\_fnd} = 0.463 \cdot \frac{\frac{kip}{in}}{in}$

$k_{y1} = 2.147 \times 10^{-3} \cdot \frac{kip}{in}$ $\quad k_{y1\_fnd} = 1.789 \times 10^{-4} \cdot \frac{\frac{kip}{in}}{in}$

$k_{\phi 1} = 0.844 \cdot \frac{kip \cdot in}{rad}$ $\quad k_{\phi 1\_fnd} = 0.07 \cdot \frac{\frac{kip \cdot in}{rad}}{in}$

Summary of Elastic Buckling Analysis

Elastic buckling analysis of the 362S162-68 [50ksi] with the sheathing-based springs is completed in CUFSM version 4. **Complete details of the analysis are available in an Appendix to this report.** The results from the analysis are summarized here:

AXIAL RESULTS

$A_g := 0.524 \cdot in^2$

$F_y := 50 \cdot ksi$

$P_y := A_g \cdot F_y \qquad P_y = 26.2 \cdot kip$

$P_{crl} := 1.207 \cdot P_y \qquad P_{crl} = 31.623 \cdot kip$ (local)

$P_{crd} := 1.579 \cdot P_y \qquad P_{crd} = 41.37 \cdot kip$ (distortional)

$P_{cre} := 2.88 \cdot P_y \qquad P_{cre} = 75.456 \cdot kip$ (global)

MAJOR-AXIS BENDING RESULTS

$S_g := 0.590 \cdot in^3$

$F_y = 50 \cdot ksi$

$M_y := S_g \cdot F_y \qquad M_y = 29.5 \cdot kip \cdot in$ (local)

$M_{crl} := 5.08 \cdot M_y \qquad M_{crl} = 3.806\,m \cdot kip$ (distortional)

$M_{crd} := 2.84 \cdot M_y \qquad M_{crd} = 2.128\,m \cdot kip$ (global)

note, Mcrd is reported for constant moment, we can increase slightly to account for moment gradient following C3.1.4 β expression, but the boost is quite small and ignored here.

$M_{cre} := 5.26 \cdot M_y \qquad M_{cre} = 3.941\,m \cdot kip$

note Mcre is reported for constant moment, to account for a uniform load we can introduce Cb, it is clear in this case that the elastic buckling moment is already so high that Cb is not necessary; however, since Cb is so commonly used, for completeness.

$C_b := 1.32$ for a uniform load on a simply supported span

$M_{cre} := C_b \cdot M_{cre} \qquad M_{cre} = 204.824 \cdot kip \cdot in \qquad \frac{M_{cre}}{M_y} = 6.943$

Axial member capacity per Direct Strength Method (AISI-S100 App 1)

Global buckling check per DSM 1.2.1.1

$\lambda_c := \sqrt{\frac{P_y}{P_{cre}}}$ $\lambda_c = 0.589$ note $P_y = 26.2 \cdot kip$ $P_{cre} = 75.456 \cdot kip$ (Eq. 1.2.1-3)

$$P_{ne} := \begin{cases} 0.658^{\lambda_c^2} \cdot P_y & \text{if } \lambda_c \le 1.5 \quad \text{(Eq. 1.2.1-1)} \\ \frac{0.877}{\lambda_c^2} \cdot P_y & \text{if } \lambda_c > 1.5 \quad \text{(Eq. 1.2.1-2)} \end{cases}$$

$P_{ne} = 22.7 \cdot kip$

Local buckling check per DSM 1.2.1.2

$\lambda_l := \sqrt{\frac{P_{ne}}{P_{crl}}}$ $\lambda_l = 0.846$ (Eq. 1.2.1-7)

$$P_{nl} := \begin{cases} P_{ne} & \text{if } \lambda_l \le 0.776 \quad \text{(Eq. 1.2.1-5)} \\ \left[1 - 0.15 \cdot \left(\frac{P_{crl}}{P_{ne}}\right)^{0.4}\right]\left(\frac{P_{crl}}{P_{ne}}\right)^{0.4} \cdot P_{ne} & \text{if } \lambda_l > 0.776 \quad \text{(Eq. 1.2.1-6)} \end{cases}$$

$P_{nl} = 21.5 \cdot kip$

Distortional buckling check per DSM 1.2.1.3

$\lambda_d := \sqrt{\frac{P_y}{P_{crd}}}$ $\lambda_d = 0.796$ (Eq. 1.2.1-10)

$$P_{nd} := \begin{cases} P_y & \text{if } \lambda_d \le 0.561 \quad \text{(Eq. 1.2.1-8)} \\ \left[1 - 0.25 \cdot \left(\frac{P_{crd}}{P_y}\right)^{0.6}\right]\left(\frac{P_{crd}}{P_y}\right)^{0.6} \cdot P_y & \text{if } \lambda_d > 0.561 \quad \text{(Eq. 1.2.1-9)} \end{cases}$$

$P_{nd} = 23.1 \cdot kip$

Predicted nominal compressive strength per DSM 1.2

$P_n := \min((P_{ne} \; P_{nl} \; P_{nd}))$ $P_n = 21.5 \cdot kip$

Available axial capacity $\Omega_c := 1.80$ $\phi_c := 0.85$ note, section is prequalified.

$\frac{P_n}{\Omega_c} = 11.917 \cdot kip$ $\phi_c \cdot P_n = 18.234 \cdot kip$

Axial member capacity per main Specification (AISI-S100)

(NEW) C4.1.6 Sections with sheathing attached to flanges (draft ballot 8)

The elastic buckling stress Fe is to be determiend by rational elastic buckling analysis, per the earlier provided CUFSM results this is known:

$$F_e := \frac{P_{cre}}{A_g} \qquad F_e = 144\cdot ksi$$

C4.1 Nominal compressive strength

$$\lambda_c := \sqrt{\frac{F_y}{F_e}} \qquad \lambda_c = 0.589 \qquad \text{note } F_y = 50\cdot ksi \qquad F_e = 144\cdot ksi \qquad \text{(Eq. C4.1-4)}$$

$$F_n := \begin{cases} 0.658^{\lambda_c^2}\cdot F_y & \text{if } \lambda_c \le 1.5 \quad \text{(Eq. C4.1-2)} \\ \frac{0.877}{\lambda_c^2}\cdot F_y & \text{if } \lambda_c > 1.5 \quad \text{(Eq. C4.1-3)} \end{cases}$$

$F_n = 43.2\cdot ksi$

Determine effective area per Chapter B at Fn. This step is not detailed here in the interest of space.

$A_e := 0.482\cdot in^2$ calculated in CFS v7, by chaging Fy to Fn=43.2 ksi.

$P_{nC4.1} := A_e\cdot F_n \qquad P_{nC4.1} = 20.84\cdot kip$

C4.2 Nominal distortional buckling strength

$F_d := \frac{P_{crd}}{A_g} = 78.95\cdot ksi$ using provisions of C4.2(b), or equations in C4.2(a) may be utilized. Also, see AISI Design Manual, or CFSEI Tech Notes for tabulated values.

returning back to the main part of C4.2

$P_{crd} := A_g\cdot F_d \qquad P_{crd} = 41.37\cdot kip$ (Eq. C4.2-5)

$$\lambda_d := \sqrt{\frac{P_y}{P_{crd}}} \qquad \lambda_d = 0.796 \qquad \text{(Eq. C4.2-3)}$$

$$P_{ndC4.2} := \begin{cases} P_y & \text{if } \lambda_d \le 0.561 \quad \text{(Eq. C4.2-1)} \\ \left[1 - 0.25\cdot\left(\frac{P_{crd}}{P_y}\right)^{0.6}\right]\left(\frac{P_{crd}}{P_y}\right)^{0.6}\cdot P_y & \text{if } \lambda_d > 0.561 \quad \text{(Eq. C4.2-2)} \end{cases}$$

$P_{ndC4.2} = 23.1\cdot kip$ (identical provisions to DSM)

Predicted nominal compressive strength per C4

$P_{nC4} := \min\left(\left(P_{nC4.1} \quad P_{ndC4.2}\right)\right) \qquad P_{nC4} = 20.8\cdot kip \qquad \Omega_c := 1.80 \qquad \phi_c := 0.85$

Available axial capacity $\frac{P_{nC4}}{\Omega_c} = 11.578\cdot kip \qquad \phi_c\cdot P_{nC4} = 17.714\cdot kip$

Major-axis member bending capacity per Direct Strength Method

Lateral-torsional buckling check per DSM 1.2.2.1.1

$\frac{M_{cre}}{M_y} = 6.943$ per Eq. 1.2.2-3 $M_{ne} := M_y$ $M_{ne} = 29.5 \cdot kip \cdot in$

because Mcre/My is > 2.78 inelastic LTB could also be considered per 1.2.2.1.1.1.2. here it is not included, but certainly some capacity is available through inelastic reserve.

Local buckling check per DSM 1.2.2.1.2

$\lambda_l := \sqrt{\frac{M_{ne}}{M_{crl}}}$ $\lambda_l = 0.444$ section will see no reduction.. (Eq. 1.2.2-9)

$$M_{nl} := \begin{cases} M_{ne} & \text{if } \lambda_l \le 0.776 \\ \left[\left[1 - 0.15 \cdot \left(\frac{M_{crl}}{M_{ne}}\right)^{0.4}\right]\left(\frac{M_{crl}}{M_{ne}}\right)^{0.4} \cdot M_{ne}\right] & \text{if } \lambda_l > 0.776 \end{cases}$$ (Eq. 1.2.2-7) (Eq. 1.2.2-8)

$M_{nl} = 29.5 \cdot kip \cdot in$

Distortional buckling check per DSM 1.2.2.1.3

$\lambda_d := \sqrt{\frac{M_y}{M_{crd}}}$ $\lambda_d = 0.593$ section will see no reduction.. (Eq. 1.2.2-19)

$$M_{nd} := \begin{cases} M_y & \text{if } \lambda_d \le 0.673 \\ \left[\left[1 - 0.22 \cdot \left(\frac{M_{crd}}{M_y}\right)^{0.5}\right]\left(\frac{M_{crd}}{M_y}\right)^{0.5} \cdot M_y\right] & \text{if } \lambda_d > 0.673 \end{cases}$$ (Eq. 1.2.2-17) (Eq. 1.2.1-18)

$M_{nd} = 29.5 \cdot kip \cdot in$

Predicted nominal compressive strength per DSM 1.2.2

$M_n := \min\left(\left(M_{ne} \;\; M_{nl} \;\; M_{nd}\right)\right)$ $M_n = 29.5 \cdot kip \cdot in$ i.e. sheathing creates a fully braced beam behavior.

Available bending capacity $\Omega_b := 1.67$ $\phi_b := 0.90$ note, section is prequalified

$\frac{M_n}{\Omega_b} = 17.665 \cdot kip \cdot in$ $\phi_b \cdot M_n = 26.55 \cdot kip \cdot in$

Major-axis member bending capacity per main Spec. (AISI-S100)

C3.1.2 Lateral-torsional buckling strength

(NEW) C3.1.2.3 Sections with sheathing attached to the flanges

Fe is to be determined by rational elastic buckling analysis. In this case the previously conducted CUFSM analysis provides the results

$F_e := \frac{M_{cre}}{S_g}$ $F_e = 347.16 \cdot ksi$

returning to the body of C3.1.2..

$\frac{F_e}{F_y} = 6.943$ per C3.1.2.1 no LTB $F_n := F_y$ $F_n = 50 \cdot ksi$

the effective modulus shall be determined at Fn, in this case from SSMA or SFIA tables.. (Fn=Fy)

$S_e := 0.579 \cdot in^3$

$M_{nC3.1.2} := S_e \cdot F_y$ $M_{nC3.1.2} = 28.95 \cdot kip \cdot in$ (Eq. C3.1.1-1)

C3.1.4 Distortional buckling strength

The elastic distortional buckling stress may be found using the expresions of C3.1.4(a) or elastic buckling analysis of C3.1.4(b). Since elastic buckling analysis is available this is used here. Thus, in the end the DSM and main Spec. provisions for distortional buckling are the same.

$\lambda_d := \sqrt{\frac{M_y}{M_{crd}}}$ $\lambda_d = 0.593$ (Eq. 1.2.2-19)

$M_{ndC3.1.4} := \begin{cases} M_y & \text{if } \lambda_d \le 0.673 \\ \left[1 - 0.22 \cdot \left(\frac{M_{crd}}{M_y}\right)^{0.5}\right]\left(\frac{M_{crd}}{M_y}\right)^{0.5} \cdot M_y & \text{if } \lambda_d > 0.673 \end{cases}$ (Eq. 1.2.2-17) (Eq. 1.2.1-18)

$M_{ndC3.1.4} = 29.5 \cdot kip \cdot in$

Predicted nominal compressive strength per DSM 1.2

$M_{nC3.1} := \min\left(\left(M_{nC3.1.2} \quad M_{ndC3.1.4}\right)\right)$ $M_{nC3.1} = 28.9 \cdot kip \cdot in$

Available bending capacity $\Omega_b := 1.67$ $\phi_b := 0.90$

$\frac{M_{nC3.1}}{\Omega_b} = 17.335 \cdot kip \cdot in$ $\phi_b \cdot M_{nC3.1} = 26.055 \cdot kip \cdot in$

Summary of predicted member capacity

Main Specification

$P_{nC4} = 20.84 \cdot kip$

$\phi_c \cdot P_{nC4} = 17.714 \cdot kip$

$M_{nC3.1} = 28.95 \cdot kip \cdot in$

$\phi_b \cdot M_{nC3.1} = 26.055 \cdot kip \cdot in$

stud distributed load

$w_{nC3.1} := \frac{M_{nC3.1} \cdot 8}{L^2}$

$w_{nC3.1} = 301.563 \cdot \frac{lbf}{ft}$

$\phi_b \cdot w_{nC3.1} = 271.406 \cdot \frac{lbf}{ft}$

wall pressure

$p_{nC3.1} := \frac{w_{nC3.1}}{w_{tf}}$

$p_{nC3.1} = 150.781 \cdot psf$

$\phi_b \cdot p_{nC3.1} = 135.703 \cdot psf$

DSM Appendix 1 of Specification

$P_n = 21.451 \cdot kip$

$\phi_c \cdot P_n = 18.234 \cdot kip$

$M_n = 29.5 \cdot kip \cdot in$

$\phi_b \cdot M_n = 26.55 \cdot kip \cdot in$

stud distributed load

$w_n := \frac{M_n \cdot 8}{L^2}$

$w_n = 307.292 \cdot \frac{lbf}{ft}$

$\phi_b \cdot w_n = 276.563 \cdot \frac{lbf}{ft}$

wall pressure

$p_n := \frac{w_n}{w_{tf}}$

$p_n = 153.646 \cdot psf$

$\phi_b \cdot p_n = 138.281 \cdot psf$

$\phi M := \begin{pmatrix} 0 \\ \phi_b \cdot M_{nC3.1} \end{pmatrix} \quad \phi P := \begin{pmatrix} \phi_c \cdot P_{nC4} \\ 0 \end{pmatrix}$

$\phi M_{dsm} := \begin{pmatrix} 0 \\ \phi_b \cdot M_n \end{pmatrix} \quad \phi P_{dsm} := \begin{pmatrix} \phi_c \cdot P_n \\ 0 \end{pmatrix}$

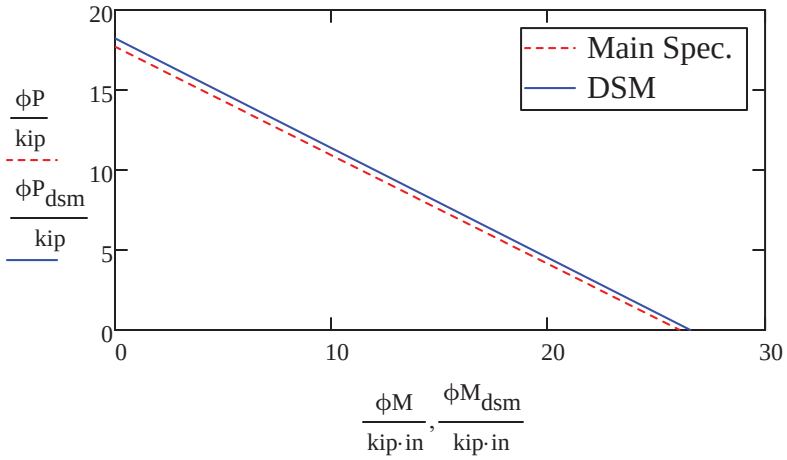

Check Fasteners - Fastener Demands in Bending

Fastener demands in pull-through (pt) and bearing (br) are a function of the required axial force (Pr) and moment (Mr). First, consider the case of bending only, and consider the maximum possible Mr, i.e. Mr = full available capacity.

$M_r := \phi_b \cdot M_n \qquad M_r = 26.55 \cdot kip \cdot in$

$w_r := \frac{8 \cdot M_r}{L^2} \qquad w_r = 0.023 \cdot \frac{kip}{in}$

F.D.1.1 Required Forces to Resist Direct Torsion in Bending (per draft ballot 11)

first find the eccentricity, i.e., distance from the shear center (s.c) to the end of the flange flat.

$m := 0.765 \cdot in$ per SSMA or SFIA table, dist. from s.c. to centerline of web

$r_{inner} := 0.1070 \cdot in$ again per SSMA or SFIA table. $t = 0.071 \cdot in$

$r_{outer} := r_{inner} + t$

$e := m - \frac{t}{2} + r_{outer} \qquad e = 0.908 \cdot in$

now the torsion demand, tributary to a fastener, that must be resisted

$T_r := w_r \cdot d_f \cdot e \qquad T_r = 0.251 \cdot kip \cdot in$ (Eq. F.D.1-3)

$h := 3.62 \cdot in$ (out-to-out depth of the stud) $b := 1.62 \cdot in$ (flange width)

$\theta_r := T_r \cdot \left(k_{\phi 1} + k_{x1} \cdot \frac{h^2}{4} + k_{\phi 2} + k_{x2} \cdot \frac{h^2}{4} \right)^{-1}$ (Eq. F.D.1-6)

Side 1 / Flange 1 (#8 in 7/16 in. OSB)

pull-through:

$F_{rM\_pt1} := \frac{k_{\phi 1} \cdot \theta_r}{\frac{b}{2}} \qquad F_{rM\_pt1} = 9.852 \cdot lbf$ (Eq. F.D.1-7)

bearing:

$F_{rM\_br1} := k_{x1} \cdot \frac{h}{2} \cdot \theta_r \qquad F_{rM\_br1} = 95.079 \cdot lbf$ (Eq. F.D.1-8)

Side 2 / Flange 2 (#6 in 1/2in. Gypsum)

pull-through:

$F_{rM\_pt2} := \frac{k_{\phi 2} \cdot \theta_r}{\frac{b}{2}} \qquad F_{rM\_pt2} = 9.922 \cdot lbf$ (Eq. F.D.1-9)

bearing:

$F_{rM\_br2} := k_{x2} \cdot \frac{h}{2} \cdot \theta_r \qquad F_{rM\_br2} = 34.758 \cdot lbf$ (Eq. F.D.1-10)

Fastener Demands under Axial Load

Consider axial load only at its maximum posible required force.

$P_r := \phi_c \cdot P_n \qquad P_r = 18.234 \cdot kip$

F.D.1.2 Required Demands for Axial Stability Bracing (per draft ballot 11)

per F.D.1.2(b) for dissimilar sheathing

Side 1 / Flange 1 (#8 in 7/16 in. OSB)

pull-through

$$n := \frac{k_{x1} \cdot \left(\frac{h^2}{4}\right) + k_{x2} \cdot \left(\frac{h^2}{4}\right)}{k_{\phi 1} + k_{\phi 2}} \qquad n = 14.673 \qquad \text{(Eq. F.D.1-15)}$$

note, n is a measure of what modes resist twisting of the stud, the higher the n the more that the bearing mode resists the twist of the stud, only the rotational springs directly engage the pull-through mechanism.

$$F_{rP\_pt1} := \frac{0.04 \cdot P_r}{\frac{L}{d_f}} \cdot \frac{k_{\phi 1} \cdot \frac{h}{b}}{(1 + n) \cdot \left(k_{\phi 1} + k_{\phi 2}\right)} \qquad F_{rP\_pt1} = 6.476 \cdot lbf \qquad \text{(Eq. F.D.1-14)}$$

bearing

$$F_{rP\_br1} := \frac{0.04 \cdot P_r}{\frac{L}{d_f}} \cdot \frac{k_{x1}}{k_{x1} + k_{x2}} \qquad F_{rP\_br1} = 66.762 \cdot lbf \qquad \text{(Eq. F.D.1-16)}$$

Side 2 / Flange 2 (#6 in 1/2in. Gypsum)

pull-through

$$F_{rP\_pt2} := \frac{0.04 \cdot P_r}{\frac{L}{d_f}} \cdot \frac{k_{\phi 2} \cdot \frac{h}{b}}{(1 + n) \cdot \left(k_{\phi 1} + k_{\phi 2}\right)} \qquad F_{rP\_pt2} = 6.522 \cdot lbf \qquad \text{(Eq. F.D.1-17)}$$

bearing

$$F_{rP\_br2} := \frac{0.04 \cdot P_r}{\frac{L}{d_f}} \cdot \frac{k_{x2}}{k_{x1} + k_{x2}} \qquad F_{rP\_br2} = 24.406 \cdot lbf \qquad \text{(Eq. F.D.1-18)}$$

Available Fastener Capacity and Strength Check

F.C.1 Available Strength of Member-Fastener-Sheahting in Bearing (draft ballot 12)

side 1, #8 in 7/16 in. OSB $P_{n\_br1} := 578 \cdot lbf$ $\phi_{br} := 0.5$ $\phi_{br} \cdot P_{n\_br1} = 289 \cdot lbf$

side 2, #6 in 1/2 in. Gyp $P_{n\_br2} := 86 \cdot lbf$ $\phi_{br} \cdot P_{n\_br2} = 43 \cdot lbf$

These nominal capacities are based on tests conducted by the author. The test setup is the same as that of draft ballot 2 for determining kx springs. See commentary and notes to draft ballot 12 for additional ideas on how to determine these capacities in other cases. Currently, to the authors knowledge, manufacturers do not regularly supply this data.

F.C.2 Available Strength of Member-Fastener-Sheahting in Pull-through (draft ballot 12)

side 1, #8 in 7/16 in. OSB $P_{n\_pt1} := 437 \cdot lbf$ $\phi_{br} := 0.5$ $\phi_{br} \cdot P_{n\_pt1} = 218.5 \cdot lbf$

side 2, #6 in 1/2 in. Gyp $P_{n\_pt2} := 40 \cdot lbf$ $\phi_{br} \cdot P_{n\_pt2} = 20 \cdot lbf$

These nominal capacities are based on tests conducted by the author. The test setup is the same as that of draft ballot 5 for determining kϕ springs. See commentary and notes to draft ballot 12 for additional ideas on how to determine these capacities in other cases. Currently, to the authors knowledge, manufacturers do not regularly supply this data. In addition, this mode of failure may be unique to cold-formed steel as in wood construction withdrawal typically controls (it seems).

Strength Check - Axial Loads

Side 1, 7/16 in. OSB with #8's

Bearing	$F_{rP\_br1} = 66.762 \cdot lbf$	<	$\phi_{br} \cdot P_{n\_br1} = 289 \cdot lbf$	OK
Pull-through	$F_{rP\_pt1} = 6.476 \cdot lbf$	<	$\phi_{br} \cdot P_{n\_pt1} = 218.5 \cdot lbf$	OK

Side 2. 1/2 in. Gyp with #6's

Bearing	$F_{rP\_br2} = 24.406 \cdot lbf$	<	$\phi_{br} \cdot P_{n\_br2} = 43 \cdot lbf$	OK
Pull-through	$F_{rP\_pt2} = 6.522 \cdot lbf$	<	$\phi_{br} \cdot P_{n\_pt2} = 20 \cdot lbf$	OK

Strength Check - Bending

Side 1, 7/16 in. OSB with #8's

Bearing	$F_{rM\_br1} = 95.079 \cdot lbf$	<	$\phi_{br} \cdot P_{n\_br1} = 289 \cdot lbf$	OK
Pull-through	$F_{rM\_pt1} = 9.852 \cdot lbf$	<	$\phi_{br} \cdot P_{n\_pt1} = 218.5 \cdot lbf$	OK

Side 2. 1/2 in. Gyp with #6's

Bearing	$F_{rM\_br2} = 34.758 \cdot lbf$	<	$\phi_{br} \cdot P_{n\_br2} = 43 \cdot lbf$	OK
Pull-through	$F_{rM\_pt2} = 9.922 \cdot lbf$	<	$\phi_{br} \cdot P_{n\_pt2} = 20 \cdot lbf$	OK

ALL FASTENERS OK FOR MAXIMUM REQUIRED DEMANDS

Note, gypsum board is near its maximum capacity in bearing, and even pull-through is close to capacity; thus one can expect with standard details Gyp board may sometimes limit the capacity of the stud from developing its full available member capacity.

Appendix: CUFSM Elastic Buckling Analysis for Design Example

Elastic buckling analysis of a nominal 362S162-68 [50ksi] with 7/16 in. OSB fastened with #8s @ 12 in. o.c. on one face and ½ in. gypsum board fastened with #6s @ 12 in. o.c. on the other face. Analysis conducted in CUFSM version 4. www.ce.jhu.edu/cufsm

The bare model of the cross-section is built and shown here:

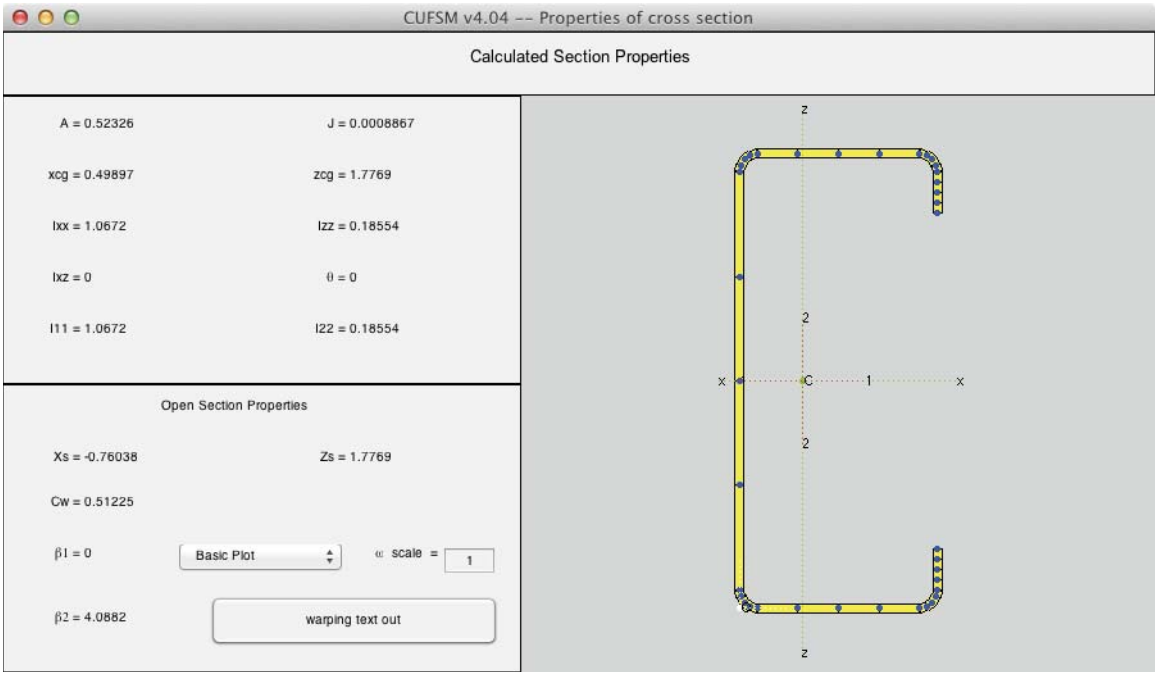

note, to check accuracy of the inputted geometry the A = 0.523 in^2 and I = 1.067in^4 above, this may be compared with SFIA tables A = 0.524 in^2 and I=1.069 in^4. The geometry is accurate.

From the work reported in the design example the sheathing are modeled as foundation springs with the following values:

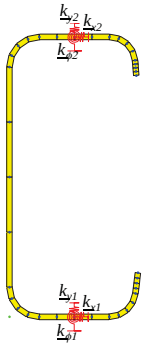

Face 2, ½ in. Gyp
k_{x2} = 0.169 kip/in. / in.
k_{y2} = 0.000041 kip/in. / in.
$k_{\phi 2}$ = 0.071 kip-in./rad / in.

Face 1, 7/16 in. OSB
k_{x1} = 0.463 kip/in. / in.
k_{y1} = 0.00018 kip/in. / in.
$k_{\phi 1}$ = 0.07 kip-in./rad / in.

Note, per proposed commentary to AISI Appendix 1, DSM, use of a foundation spring is accurate at this fastener spacing. See draft ballot 6 for additional commentary and references.

These foundation springs are introduced into the model as shown in the small Springs box below, and visually by the addition of springs depicted on the model cross-section.

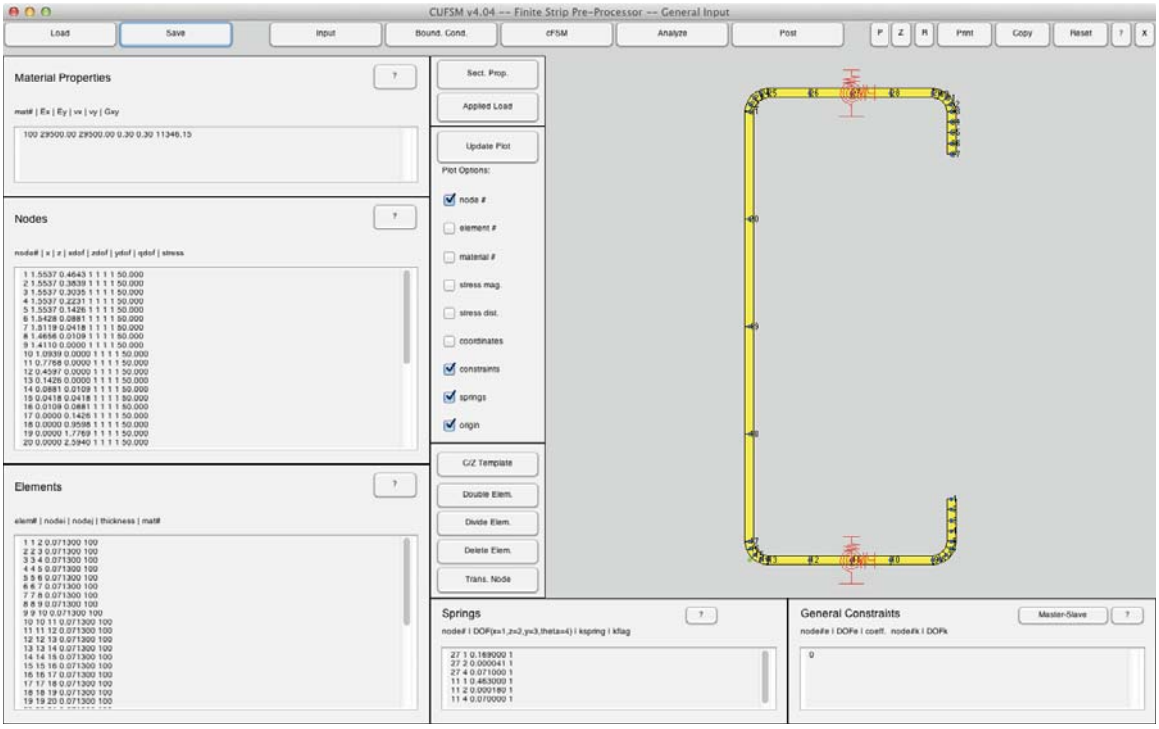

For the axial stability the member is loaded with a reference load equal to the squash load (note the applied stress = 50 ksi on all nodes in the previous screen). **Clamped-clamped boundary conditions…** The slide below shows the longitudinal terms used in the model. The analysis is not a signature curve analysis, rather like FE the analysis is conducted at the physical length (96 in.) and the modes examined.

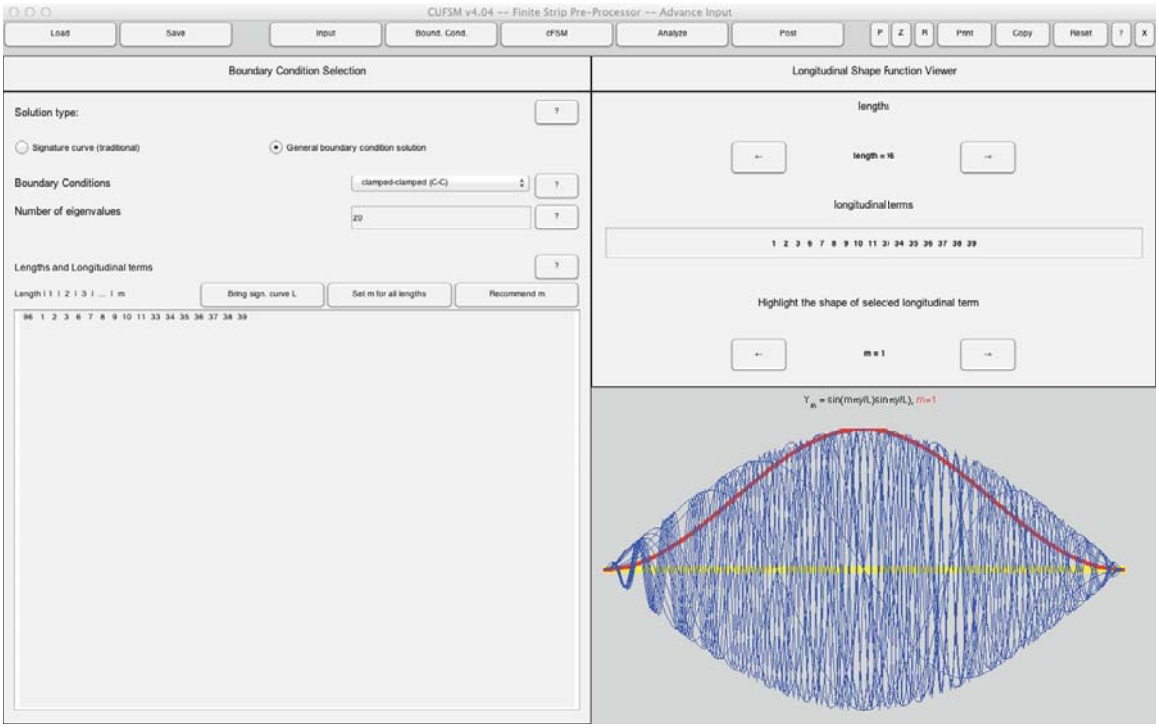

Model results Pcrℓ/Py = 1.207. In the screen below the top figure shows the buckled shape at x=0.25L along the length, second figure shows that m=34 half-waves is the dominant number of half-waves along the 96 in. length (clearly local with a typical half-wave of 96/34=2.82 in.), bottom figure shows additional results (first 20 modes provided). Note this model includes all springs, strictly the springs should be removed for the local buckling value; however in this case the elastic local buckling load is 1.2069 with all springs removed as the web is dominating local buckling so either model acceptable.

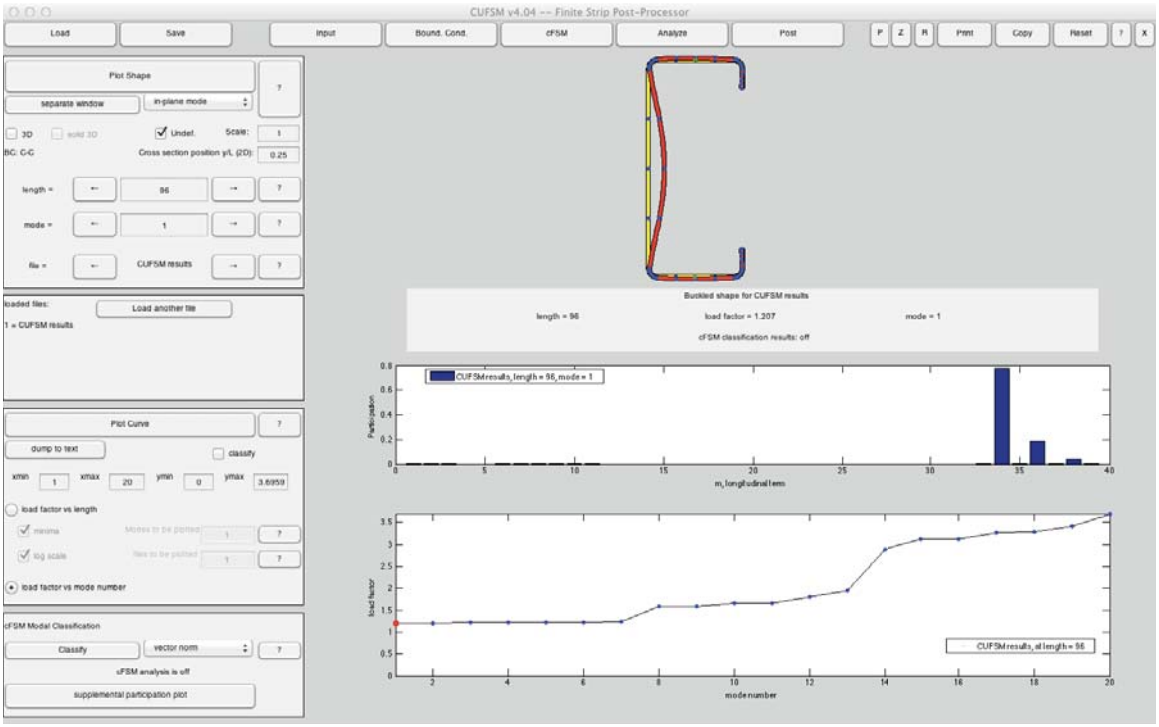

Model results Pcrd/Py = 1.579. In the screen below the top figure shows the buckled shape at x=0.2L along the length, second figure shows that m=8 half-waves is the dominant number of half-waves along the 96 in. length (clearly distortional with a typical half-wave of 96/8=12 in.), bottom figure shows additional results (first 20 modes provided).

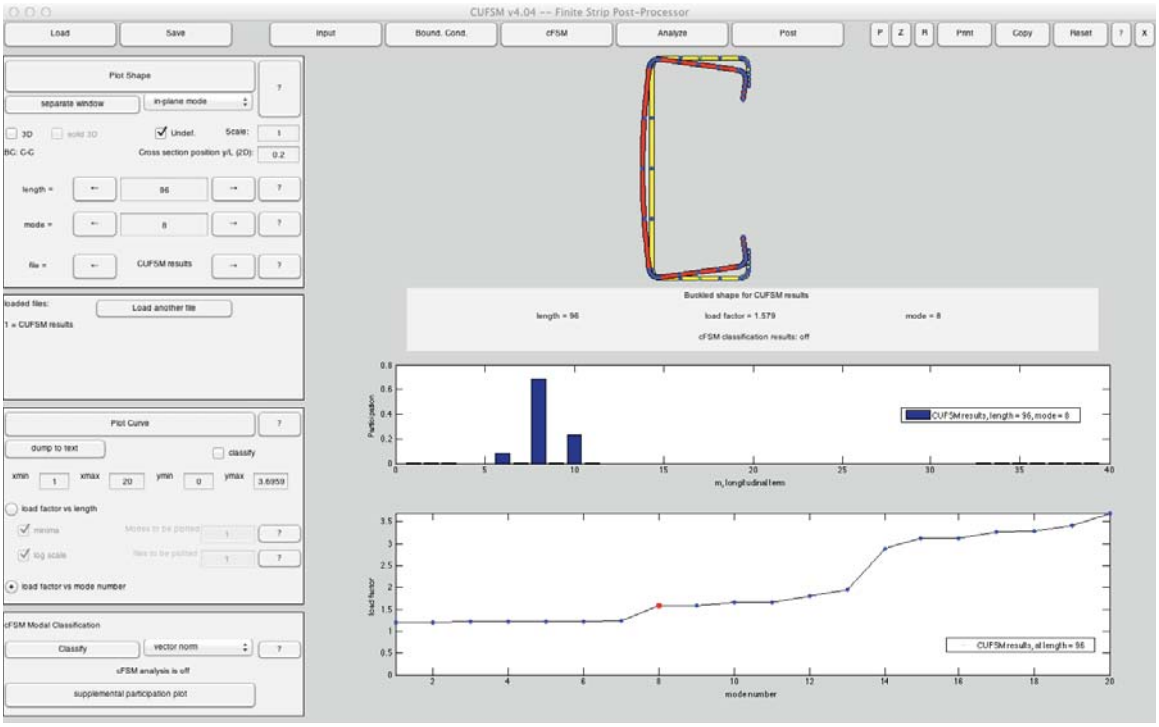

Model results Pcre/Py = 2.88. In the screen below the top figure shows the buckled shape at x=0.5L along the length, second figure shows that m=1,3 half-waves dominante, i.e. global mode is found.

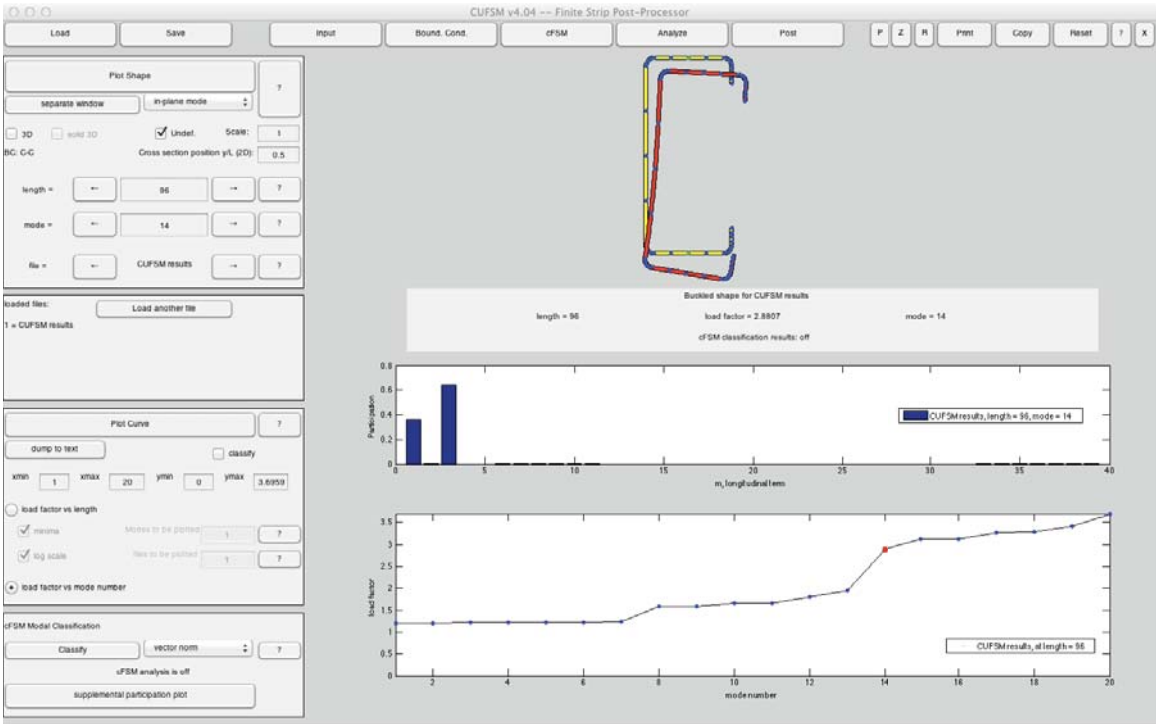

For bending stability analysis, we apply the reference M_y stress (for restrained bending). Placing the weaker (gypsum sheathed) flange in compression as the worst case bending demand.

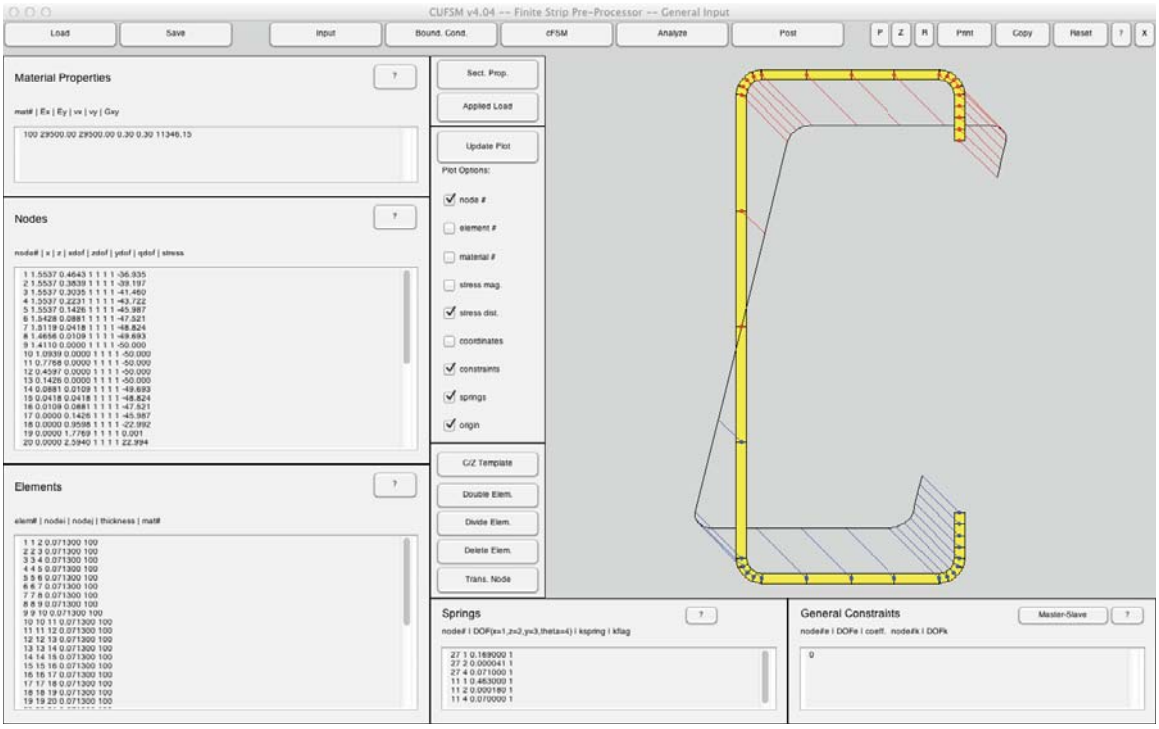

Also, we use pinned-pinned ends, so we can perform a classical signature curve analysis if desired. Results are shown below with distortional highlighted. **Mcrℓ/My=5.08, Mcrd/My=2.79, Mcre/My=4.55**. Note, the presence of springs means a minimum exists for global.

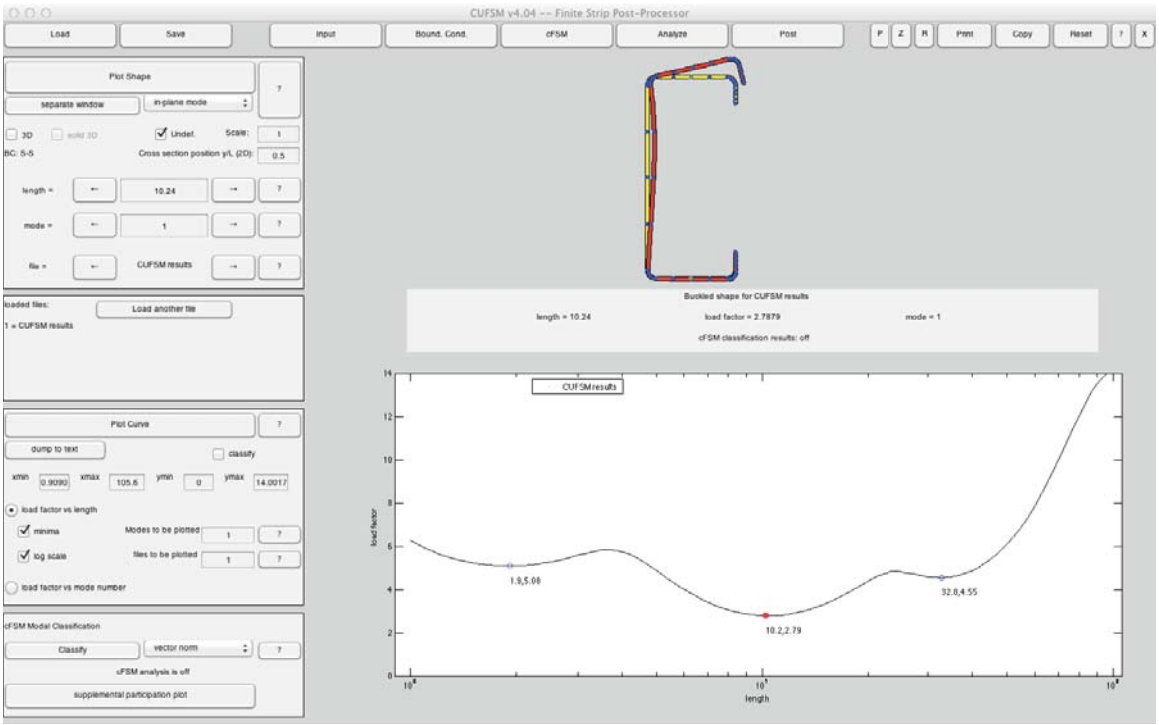

We can be more precise if desired, and perform the analysis even for pinned-pinned at the actual physical length, similar to the compression analysis under clamped-clamped. Selected *m* terms are shown:

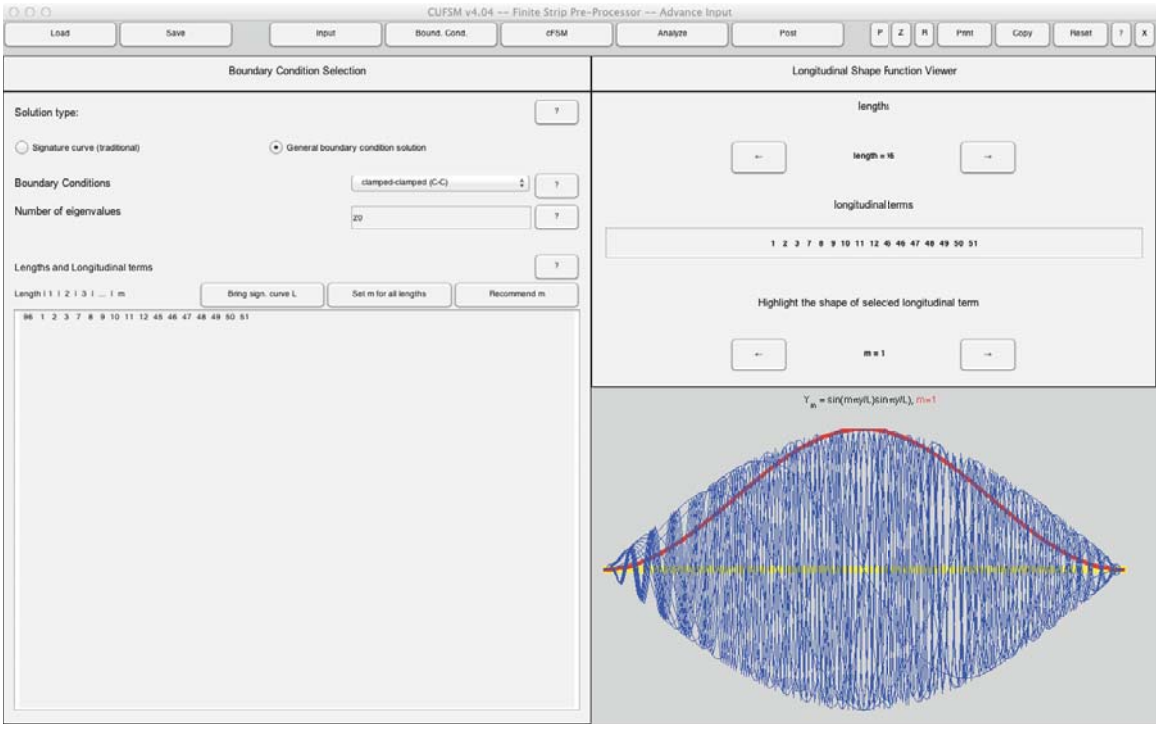

Model results Mcrℓ/My = 5.08. Note, *m*=51 half-waves is the dominant number of half-waves along the 96 in. length (clearly local with a typical half-wave of 96/51=1.88 in. same as signature curve). Also note, for this high of Mcrℓ the section will not have a local buckling reduction.

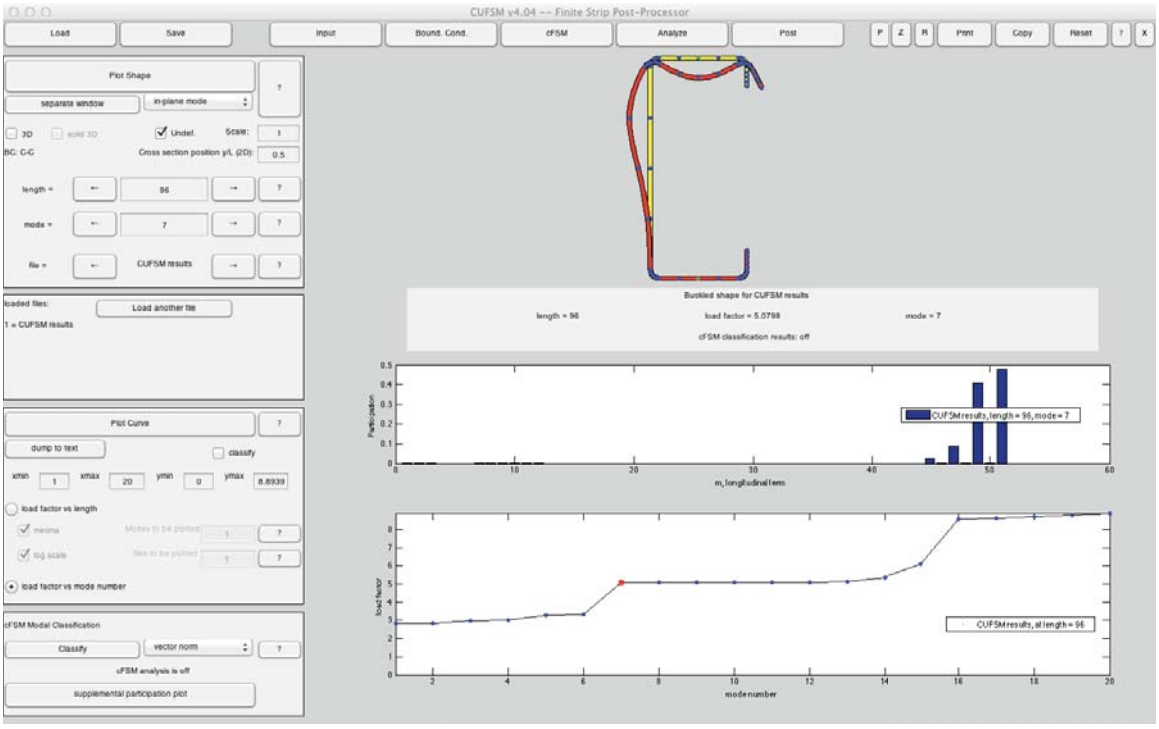

Model results Mcrd/My = 2.84. Note, *m*=9 half-waves is dominant. Results are slightly higher than signature curve (Mcrd/My = 2.79), which does not take into account end effects (i.e. when the model length is not an integer number of half-waves). Signature curve is always the most conservative if minima employed. Also note, for this high of Mcrd the section will not have a distortional buckling reduction.

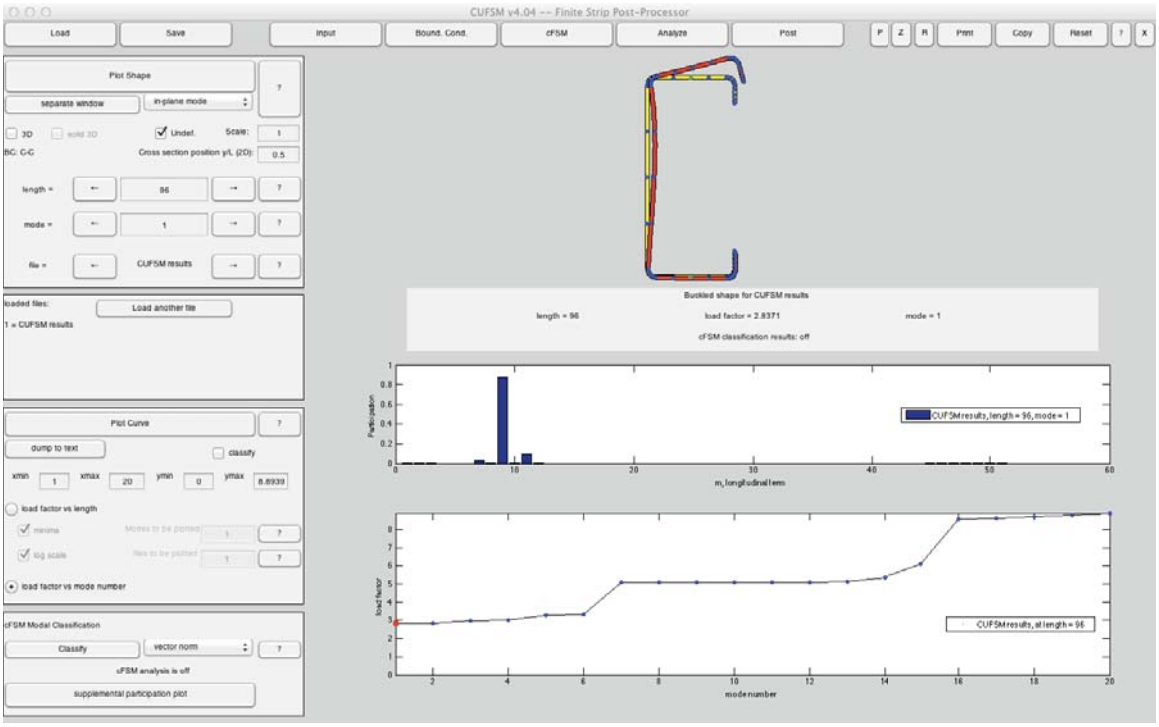

Model results Mcre/My = 5.26. Note, *m*=3 half-waves is dominant, but *m*=1 also contributes at this physical length. Results are higher than signature curve (Mcre/My = 4.55) similar to distortional case. Also note, for this high of Mcre the section will not have a global buckling reduction.

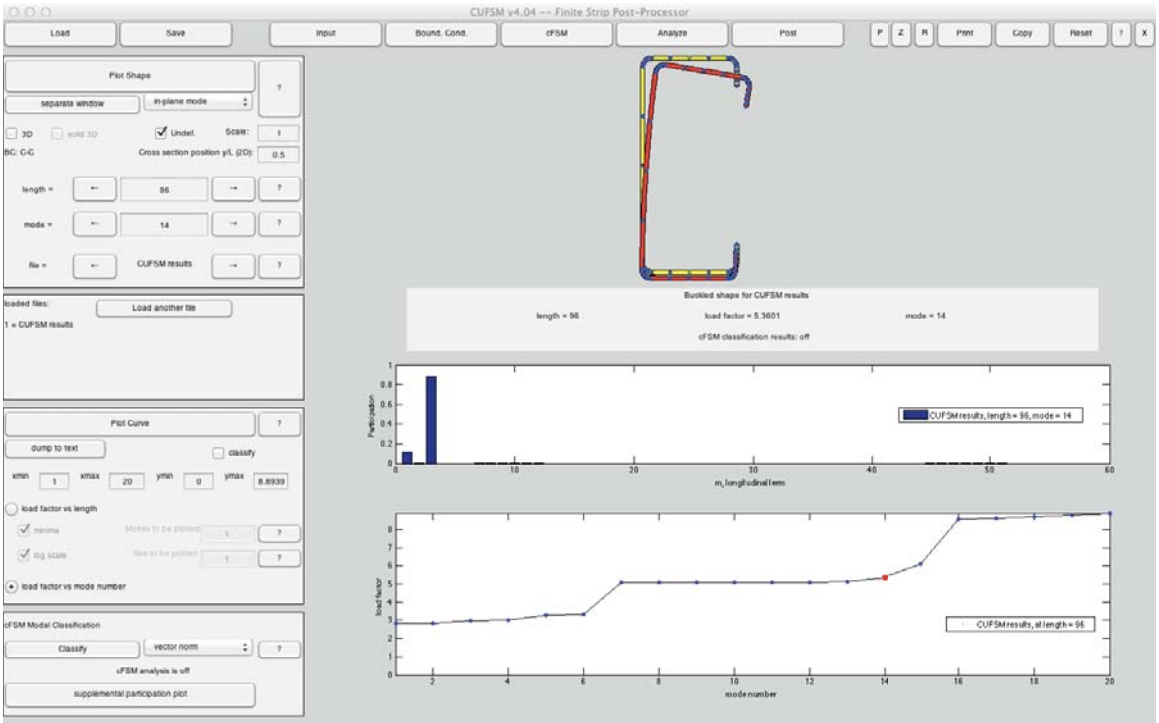

Appendix: Project Monitoring Task Group Responses

The Project Monitoring Task Group (PMTG) met in April 2012 to discuss the closeout materials provided for this project at that time. Namely this email from 21 March 2012:

From: Benjamin Schafer <schafer@jhu.edu>
Date: March 21, 2012 1:30:20 PM EDT
To: Jay Larson <JLarson@steel.org>
Cc: Debbie Lantry <dlantry1@jhu.edu>
Subject: **project closeout for AISI Sheathing Braced Design of Wall Studs**

Jay

As we discussed it is time to formally close out the Sheathing Braced Design of Wall Studs project.

I have organized and updated the project webpage so that it may provide you all closeout materials and provide a permanent repository for those interested in this work.

Specifically, in terms of a "final report", please find at

http://www.ce.jhu.edu/bschafer/sheathedwalls

at the top of the page these two summary documents:

- Vieira Jr., L.C.M. (2011) Behavior and design of cold-formed steel stud walls under axial compression, Department of Civil Engineering, Ph.D. Dissertation, Johns Hopkins University.
- Peterman, K.D.P. (2012) Experiments on the stability of sheathed cold-formed steel stud under axial load and bending, M.S. Essay, Department of Civil Engineering, Johns Hopkins University.

These two dissertations are the summary of all work completed. The page provides significant ancillary materials as well, but these two are the permanent and necessary final documentation. I will update the page as additional conference papers and journal articles are completed.

Further, I am well aware that now is the time to produce the ballots related to this work and I have begun that process as well. This work should keep us busy in COFS for some time.

If you need anything else with respect to close out of this project please let me know.

Sincerely,
Ben Schafer

Benjamin W. Schafer
Swirnow Family Faculty Scholar
Professor and Chair
Department of Civil Engineering
Johns Hopkins University
www.ce.jhu.edu/bschafer
schafer@jhu.edu 410.516.6265

The PMTG determined in April 2012 that the provided materials were insufficient for closing out the project. They provided a series of questions in a 14 April 2012 email to the PI: Ben Schafer. These questions were answered by the PI on 24 April 2012 and the PMTG and PI met on 1 May 2012 to discuss the answers.

It was determined at the 1 May 2012 meeting that a final report should be prepared, in addition to the 21 March 2012 email and that the answers to the PMTG questions should be cleaned up and included as an Appendix in that report. This is that appendix.

In the following

[…] indicates extraneous material that was removed.

`Black Courier text` is the PI's initial response

Black Times New Roman text is additional response provided in the preparation of this repot

`Blue Courier Text` is the PMTG's original questions.

From: Benjamin Schafer <schafer@jhu.edu>
Date: April 24, 2012 6:21:03 PM EDT
Additional Comments added 14 Januaruy 2013
To: Jay Larson <jlarson@steel.org>
Subject: **Re: Sheathing Braced Design of Wall Studs**

```
Just so we start off on the right foot for our meeting I provided some
short responses to the basic questions below. I look forward to
meeting with the PMTG.

On Apr 23, 2012, at 10:23 PM, Jay Larson wrote:

All –

We have scheduled the GoToMeeting® to discuss PMTG feedback on the
project closeout
[…]
A summary of PMTG feedback is in the email below.

Thank you.

Jay W. Larson, P.E., F. ASCE
Managing Director, Construction Technical
American Iron and Steel Institute
3425 Drighton Court
Bethlehem, PA 18020-1335
tel: 610.691.6334

From: Jay Larson
Sent: Saturday, April 14, 2012 9:42 AM
To: Ben Schafer (schafer@jhu.edu)
Cc: Nabil Rahman (nabil@steelnetwork.com)
Subject: Sheathing Braced Design of Wall Studs

Dear Ben –
```

As discussed on the phone on April 5th, the Project Monitoring Task Group (PMTG) met via GoToMeeting® on April 4th to discuss the project closeout. We felt that a GoToMeeting® with you would be in order to discuss PMTG feedback. To facilitate the discussion the members of the PMTG submitted comments, which are compiled below.

Generally, the PMTG would like to see a concise final report that summarizes the primary test and analysis information, conclusions and the proposed design methods from the two theses (20-25 pages). Specifically, we would like to discuss the following:

· Content of the final report; such as:
- specific recommendations
Understood
Provided in this report.

- brief outline of the proposed ballots that are going to be submitted to COFS
Understood
Provided in this report.

- design example(s) (either in the summary or with the ballots).
Understood
Provided in this report.

· Specific recommendations, such as:
- need for more information about how the role of wall length (or wall aspect ratio) will be addressed in the proposed design methods
This aspect is already embedded in the method w.r.t stud spacing and tributary area of sheet when determining spring stiffness. Brace force accumulation is less well handled. I look forward to discussing this with the PMTG so I fully understand this comment.
..try to address this at least in a design example
..accumulation? not a problem up to our 5 stud wall
..intuition of the group does not concern ourselves with the accum.
Wall length and wall aspect ratio are intrinsic to the method, specifically when determining the bracing restraint provided by the fastener-sheathing system to the studs. This issue is included in the method.

- need for a chart for the proposed design method for Axial + Bending similar to the one presented for Axial only in the 2011 thesis
Understood.
Full design method provided in this report.

· Calibration concerns; such as:
- whether the 362S162-68 used for most of the testing is sufficient for calibration (results in less LB, DB and fastener tilt than thinner and deeper members)

Definitely worth discussing, but I am confident that we have validated an overall approach and not simply the idea that local buckling always controls. To be discussed further.
..Ben asserts we are ok based on member design practice
The method provided in the report is general and checks all relevant limit states. The PI is confident that extension to other wall studs is appropriate since the approach is a direct extension of already-in-place methods for member design.

- whether inelastic reserve and composite effect of sheathing should be accounted for when studying test/predicted data
Very tricky issue, I look forward to discussing. I do not know that we will resolve this, but we can be very clear on what we did. Dominant composite action WAS removed by isolating the loading into the studs. This was shown in the early work and can be reinforced in the final writeup.
..ky spring includes potential composite action (bending only)
..what about the axial force that bleeds into the sheathing?
..Ben's argument is that the location of the failure mechanism limits the comp. action
..group would like more discussion on this point
..What about bending + axial?? Ben to think about this.
..Useful to explain that our predictions "fall where they should" as a conservative estimate should be pointed out for people to understand this.
The design method proposed herein assumes non-composite action unless one tests. If one tests, then partial composite action is allowed in terms of bracing, but not strength. Strength is always limited to the member strength, but bracing may include composite action if tests are used to determine ky. This seems like a fair compromise to the PI.
As far as inelastic reserve, additional fastener (bracing) strength checks may be required to allow the section to develop higher bending capacities. Currently the strength is limited to M_y.

- how the 2a fastener statistical treatment would be integrated into the overall calibration (phi = 0.85 required for the 2a effect alone)
To be discussed. We have not integrated this work into our design method yet.
..my argument is that this is not a unique fabrication issue
..Ben to look at fabrication factor or other possible avenues for integrating this into the design method?
The PI does not intend to include this factor uniquely in the method. The work on 2a addressed elastic buckling and the effect is much smaller for ultimate strength. Further work on reliability is needed, but the primary issue here is the reliability of the sheathing materials.

· Other uncertainties; such as:
- the composite sheathing effect, if any
let's discuss.
The design method proposed herein assumes non-composite action unless one tests. If one tests, then partial composite action is allowed in terms of bracing, but not strength. Strength is always limited to the member strength, but bracing may include composite action if tests are used to

determine ky. This seems like a fair compromise to the PI.

- whether the composite effect goes away with load cycle conditioning
let's discuss, we may only be able to point this out, our work in this project is not covering this in depth, but CFS-NEES work can be helpful in this regard.
..ky spring is the main issue here
..how to handle the testing? How to handle drywall?
..Ben's proposal here would be non-composite by calculation, and testing if you want greater brace stiffness… final report needs to address the test method.

- whether the wall tests are for flexure only and are pinned ends required
We will need to discuss this further so I fully understand.
..in the end we are satisfied that the ends acted as pinned. Should be highlighted in the final report
..what to do about axial fixed-fixed, flexure pinned-pinned
..should axial stay fixed-fixed? Final design method approach?
..mention this flexibility in final report
The final report and paper on the columns under combined axial and bending assumed axial fixed-fixed (w.r.t warping) and bending pinned-pinned (w.r.t major-axis bending) and showed the best agreement with observed behavior and strength. This is recommended as the assumptions in this case.

- whether the fastener torsion demand for uniformly distributed load instead of point load is more representative of the design case
Sure, sure. Here we are stretching our results and have not studied the uniform case. No doubt uniform case is more forgiving. We may not be able to say a great deal more on this particular aspect within this project.
..Some additional known analysis needed.
This issue is fully addressed in
Peterman, K.D., Schafer, B.W. "Sheathed Cold-Formed Steel Studs Under Axial and Lateral Load." Submitted to *Journal of Structural Engineering* (Submitted 2 January 2013).
A method is provided for extension to uniformly distributed load cases.

· Drywall reliability issues both for axial and flexure (moisture, load cycling and installation error issues)
Only studied in part in this project
..Ben has no obvious resolution
..phi factor?
..mention where we have landed and leave it beyond the scope of the report?
..let people see the data so they understand gyp board + and -
..unresolved issue at this point, load case dependent? Other design approaches? Possible rational avenues
No resolution, the current approach is to provide the information in the design method and let engineers decide if they want to rely on gypsum board in their designs.

Appendix: Vieira Jr., L.C.M., Schafer, B.W. (2013). "Behavior and Design of Sheathed Cold-Formed Steel Stud Walls under Compression." ASCE, *Journal of Structural Engineering* (DOI: 10.1061/(ASCE)ST.1943-541X.0000731). *In Press*

Behavior and Design of Sheathed Cold-Formed Steel Stud Walls under Compression

L.C.M. Vieira Jr., Ph.D.[1] and B.W. Schafer, Ph.D., P.E., A.M. ASCE[2]

Abstract

The objective of this paper is to provide a robust design method for walls framed from cold-formed steel (CFS) stud and track that utilize traditional sheathing materials as the primary means of bracing against compressive load. Existing design methods are unable to handle dis-similar sheathing attached to the CFS stud flanges (e.g., oriented strand board (OSB) on the exterior face and gypsum board on the interior face) and provide no clarity on the impact of key properties including sheathing shear rigidity and stud spacing. A series of tests on axially loaded sheathed single studs and sheathed full walls utilizing OSB, gypsum board, or an unsheathed face (and combinations thereof) are performed to elucidate the basic behavior and limit states. The stiffness that the fastener-sheathing system supplies to the stud as bracing is characterized analytically and experimentally. The characterization clarifies how both local fastener deformations and global sheathing deformations contribute to sheathing bracing. The impact of sheathing on elastic stability of the stud in local, distortional, and global buckling modes is provided. Both computational and analytical methods for stability determination including bracing stiffness from sheathing are detailed. A simple extension to current design methods that utilizes the enhanced elastic stability provided by sheathing bracing is proposed for member strength prediction. The design method is shown to agree well with the performed tests, providing consistent predictions for the limit state and the strength for walls with sheathing, including sheathing on one-side only, and dis-similar sheathing on the two stud flanges.

Keywords: cold-formed steel, sheathed wall stud

[1] Faculty, Dept. of Mechanical, Civil & Environmental Eng., University of New Haven, 300 Boston Post Road, West Haven, CT, USA, 06516, Tel.: +1.410.608.2549, email: luizvieirajr@gmail.com <Corresponding author>
[2] Professor and Chair, Department of Civil Engineering, Johns Hopkins University, 3400 N. Charles St., Baltimore, MD, USA, 21218, Tel.: +1.410.516.6265, email: schafer@jhu.edu

1 INTRODUCTION

Load bearing cold-formed steel (CFS) framed buildings utilize one of two design philosophies for bracing of the CFS studs in walls – all-steel, or sheathing-braced. The all-steel design philosophy (Figure 1a) uses discrete steel bridging to brace the stud walls. The sheathing-braced design philosophy (Figure 1b) may or may not utilize bridging for construction loads, but for design loads relies on sheathing: oriented strand board (OSB), plywood, or gypsum board to brace the stud. Since sheathing is nearly always present, accounting for the sheathing in the structural performance provides significant potential economies; however, accurate and reliable prediction of the strength of sheathing-braced stud walls can be challenging.

Recently, the first author completed a multi-year study of sheathing-braced CFS stud walls in axial compression Vieira (2011) and this work is summarized herein. Specifically, this paper provides a brief review of the theory and design approaches for the strength of sheathing-braced studs (Section 2); a summary of recent tests on sheathing-braced studs including single stud (Figure 1c) tests and full wall (Figure 1b) tests (Section 3), a summary of recent tests and analytical formulae characterizing the stiffness that fastener-sheathing systems (Figure 1d,e) supply to brace studs (Section 4), an assessment of the elastic stability of studs braced by sheathing that utilizes the determined fastener-sheathing stiffness (Section 5), member strength predictions based on the stability assessment (Section 6), and comparisons to tests as well as a discussion of fastener demands and future work (Section 7).

2 BACKGROUND

Formal design of sheathing-braced CFS studs in the AISI Specification has progressed through three periods: 1962-1980, the local stiffness approach (AISI 1962); 1980-2004 the diaphragm stiffness approach (AISI 1980); and, 2004-present a variation on the local stiffness approach focused on an unbraced length equal to twice the fastener spacing (AISI-S100 2007, AISI-S211 2007). The limitations and inherent contradictions in the existing design approaches are an important pre-text for the multi-year study summarized here; detailed examination is provided in Schafer et al. (2008) and supplemented in Vieira (2011), only summary information is provided here.

The local stiffness approach which was pioneered by Winter and his students (Green, et al. 1947, Winter 1960) had two key features: (1) the stability of the stud walls in axial compression included local translational springs (k_x springs, see Figure 1e) to account for the bracing provided by the fasteners, and (2) k_x was determined by direct experiments on small-scale stud-fastener-sheathing assemblies. The design implementation in AISI (1962) was prescriptive in nature, the weak-axis flexural buckling of the stud (P_{cry}) with the springs (k_x) included had to be greater than or equal to the column squash load (P_y), the weak-axis buckling of the stud over an unbraced length equal to twice the fastener spacing (i.e., L=2a) had to be greater than or equal to the strong-axis flexural buckling load (P_{crx}), and the fasteners had to be designed for approximately 2% of the axial demand. The local stiffness approach ignored flexural-torsional buckling and ignored distortional buckling. Further, the design rules implemented were rather arbitrary and the method was abandoned in 1980.

The diaphragm stiffness approach developed by Simaan and Peköz (1976) was adopted by the AISI Specification in 1980 and used until 2004. In this approach the bracing provided by the

fastener-sheathing system is treated in a more global manner – the local fastener stiffness is ignored (or more accurately experimentally smeared into the shear stiffness of the diaphragm) and instead the energy developed due to the in-plane shear deformation of the diaphragm as the studs deforms is included in an overall energy solution to determine the sheathing-braced buckling load. The method accounted for flexural-torsional buckling and theoretically could account for dis-similar sheathing on the two faces of the stud, though the procedure was not explicitly provided in AISI (1980). In addition, the method provides for a discrete check on the shear strain of the sheathing (though failures generally occur at fastener locations not due to basic material failure in the sheathing). The method is complex in its use, yields counter-intuitive solutions with regard to stud spacing, and did not agree well with more recent testing (Schafer, et al. 2008, Miller and Pekoz 1993, Trestain 2002). The method was abandoned in 2004.

A return to a variation on the local stiffness approach occurred in the 2004 interim update to the AISI Specification (see AISI-S100 2007, AISI-S211 2007). Bracing stiffness characterization is abandoned; instead, it is assumed that the stud should only be checked for an unbraced length equal to twice the fastener spacing (i.e. $L=2a$) and the fasteners should be checked for 2% of the axial demand – both checks utilized from 1962-1980 in the AISI Specification. Use of the method is restricted to similar sheathing on the two stud flanges. The global buckling check at $L=2a$ includes flexural-torsional buckling. The method has the advantage of extreme simplicity, but critically ignores the influence that the stiffness of the fastener-sheathing system has on the stability solution. It is assumed, regardless of fastener type, sheathing type, and stud spacing the design strength is the same. The approach has limited applicability and provides no overall philosophy for extension to stud walls with dis-similar sheathing on the two stud flanges.

3 TESTS ON SHEATHING-BRACED CFS STUDS

Testing of axially loaded CFS studs with different combinations of sheathing attached to the stud flanges was completed. The work consisted of two test series: (a) single studs with short segments of track and attached sheathing (Figure 1c) tested at lengths from 0.6 m to 2.4 m (2 ft to 8 ft), and (b) stud walls (Figure 1b) 2.4 m x 2.4 m (8 ft x 8 ft) consisting of five equally spaced studs with track and sheathing. The sheathing attached to the flanges included various combinations of OSB, gypsum board (abbreviated Gyp herein) and/or no sheathing (termed BARE herein) attached to the stud flanges.

A total of 26 sheathed single stud tests were completed and are reported in Vieira et al. (2011). A key finding from the single stud tests is that if sheathing is attached to both stud flanges, even dis-similar sheathing (e.g., OSB and Gyp), the stud fails in a limit state dominated by local buckling of the stud web. For one-sided sheathing (OSB-BARE, or Gyp-BARE), or no sheathing (BARE-BARE) the behavior is more complicated and distortional and (restrained) flexural-torsional bucking is observed, depending on the unbraced length. It was also found that the sheathing must be prevented from direct bearing on the loading platens. If bearing of the sheathing is allowed composite action develops that increases the stud capacity by as much as 20% over a stud with identical sheathing details, but not allowed to bear.

A total of 12 sheathed full wall tests were also completed, have not been previously reported, and are summarized here.

3.1 Full wall specimen details and instrumentation

The 2.4 m x 2.4 m (8 ft x 8 ft) stud walls consist of 5 equally spaced studs, track, and sheathing fastened to the flanges, as depicted in Figure 1. The studs employed throughout are 362S162-68's (50 ksi) per U.S. industry standard nomenclature (AISI-S200 2007, SSMA 2001).

Therefore, the nominal web height is 92 mm (3.62 in.), the nominal flange width is 41 mm (1.62 in.), and the nominal thickness is 1.73 mm (0.068 in.). These members also have a nominal lip length of 13 mm (0.5 in.) and an inside corner radius of 2.72 mm (0.1070 in.). The nominal track employed is a 362T125-68 (similar nomenclature). As-measured dimensions, geometric imperfections, and measured material properties for the stud and track are provided in Vieira (2011). Two types of sheathing are employed: OSB (11.1 mm, (7/16 in.), rated 24/16, exposure 1) and Gypsum (12.7 mm, (½ in.) Sheetrock Regular). Number 6 screws (Simpson DWF #6 x 41.3 mm (1 5/8 in.)) were used to connect to the Gypsum boards and number 8 screws (Simpson PPSD #8 x 49.2 mm (1 15/16 in.)) to connect to the OSB boards. The sheathing is connected to the studs and tracks every 152 mm (6 in.) along the edges, and to the studs every 305 mm (12 in.) in the field, as depicted in Figure 1.

As shown in Figure 3a the walls are tested under axial compression in the multi-degree of freedom (MDOF) testing rig in the Thin-walled Structures Laboratory at Johns Hopkins University. The testing rig is utilized only for axial testing here, the specimen (the wall) is connected to the upper (actuated) load beam and lower fixed beam of the rig through 12.7mm (½ in.) bolts through the track at every stud location. In addition, 12.7mm (½ in.) plates are used at each stud location to insure the sheathing cannot bear against the loading beams. Full details of the rig and testing are available (Vieira 2011).

In additional to the internal actuator LVDTs and load cells, simple linear position transducers (PTs) are used extensively to record the deformations of the stud. PT triplets (Figure 3b,f) are utilized along the height of the field studs in the interior of the wall to capture flexure, twist, and local deformations (the difference between the exterior and interior sensor). In some cases (given limited numbers of sensors and channels, see Figure 3c) the center PT is removed,

thus allowing only global flexure and twist to be captured. In other cases, particularly near the ends where global deformations are limited by the boundary conditions, but local bucking may still occur, only the center PT is utilized (see Figure 3d,i). Global lateral deformation of the axially compressed wall is also recorded (typically by PT 11).

3.2 General results and discussion

The observed specimen strength is summarized in Table 1 and typical axial load vs. axial displacement is provided in Figure 2. Note, the last column of Table 1 also includes the results from the single stud tests for the same height as the wall tests detailed here. Sheathing is an effective way to increase wall strength: the attachment of sheathing can increase the axial strength of the wall by as much as 91% (compare BARE-BARE to OSB-OSB). From the standpoint of strength, sheathing is always beneficial. The ascending order of values for peak load is BARE-BARE, OSB-BARE, Gyp-Gyp, OSB-Gyp and OSB-OSB. As shown in Figure 2, axial stiffness is largely unaffected by the sheathing (evidence of the success in avoiding direct composite action and direct bearing of the sheathing in the testing), but peak strength, and post-peak behavior are significantly influenced. Walls with sheathing on both sides are all dominated by local buckling limit states (Figure 3d,e,g,h) and exhibit at least some stable post-peak behavior. Variation in peak strength across the specimens sheathed on both sides is 12%. The walls with sheathing on only one side (OSB-BARE) exhibit a significant strength increase above walls without sheathing (16%), but the post-peak response is catastrophic and the wall remains unable to carry essentially any axial load (the lateral sensor rig arrested the complete collapse of these walls). More detailed examination of the tested performance for each sheathing configuration follows.

3.3 Results for an unsheathed wall

A wall tested without sheathing (i.e. BARE-BARE) is essentially a test of five independent studs. Both weak-axis flexure and flexural-torsional buckling are observed in the same wall (these two global modes have similar buckling loads for a 2.4 m (8 ft) long 362S162-68 stud). The wall tests provide a capacity 14% lower than a single stud with track (as summarized in Table 1). Although the tested strength is known to exhibit scatter, it is postulated that an important source for the lower result for the walls is that the wall fails when the weakest of the five studs in the wall fails, as without sheathing, redistribution is nearly impossible.

The end conditions of the stud-to-track are of great interest as they are highly influential for global buckling. The observed performance, under the tested conditions (i.e. perfect bearing against steel plates in the presence of axial load) is that of a member with fixed end conditions. It is observed that the axial load present is large enough to fully seat the stud (note the change in stiffness in Figure 2 after the stud seats) and provide warping and bending fixity to the member ends. This issue is examined further in Section 4 and is consistent with the experiments and modeling from the single stud tests reported in Vieira et al. (2011).

3.4 Sheathing on one-side only

Walls tested with OSB sheathing on one-side only (OSB-Bare, see Figure 3a) suffer from restrained axis flexural-torsional buckling and post-peak behavior with no reserve. As Figure 4 indicates for the 1-OSB-BARE test, the twist, i.e. the difference between PT7 and 9, increases dramatically as failure is approached. Variation in the load response of the OSB-BARE tests was relatively high (see Table 1). In test 6-OSB-BARE, which had the highest peak load of the OSB-BARE tests, what occurred during the test was that one of the studs started to twist towards the flange side instead of towards the lip side (the usual side that buckles). After the other studs all

buckled towards the lip side the stud had to reverse its initial twist before finally twisting to the lip side and failing along with the rest of the wall. Thus, providing a physical demonstration of the imperfection sensitivity of this failure mode.

The most important feature of the OSB-BARE wall tests was the pronounced lack of post-buckling reserve. The failures were dramatic, in sharp contrast even to the single column tests with the same sheathing configuration. The load-displacement response of Figure 2 does not do justice to the violent nature of the observed collapse, even in displacement controlled loading. Given the nature of this collapse the common practice of using strap on the BARE side may not be sufficient to restrict this mode (i.e., blocking or sheathing may be necessary).

3.5 Similar sheathing on both sides

The walls with gypsum sheathed on both sides (Gyp-Gyp) or OSB sheathing on both sides (OSB-OSB) failed in a limit state dominated by local buckling. For the gypsum sheathed walls the local buckling (Figure 3d) causes significant damage in the gypsum (Figure 3e). After local buckling, distortional buckling is present in some of the gypsum-sheathed tests as Figure 3i shows for the 7-Gyp-Gyp test after failure. The distinction between local buckling and distortional buckling can be quite subtle and the preceding discussion relies primarily on the (half-) wavelength of the observed deformations.

Local buckling in an OSB sheathed specimen (test 9-OSB-OSB) is shown in Figure 3g after the test and after removing one side of the sheathing. Failure occurred at the member ends: top in 9-OSB-OSB, bottom in 5-OSB-OSB. The PTs captured the amplification of displacements during local buckling. For example for the 5-OSB-OSB test Figure 5 shows the measurement location and reading from all PTs and for PTs 8,9, and 10 (mounted as depicted in Figure 3d or i)

as the axial displacement increases these PTs undergo the large displacements associated with the local buckling failure.

The OSB-OSB tests carried 12% more load than the Gyp-Gyp tests even though the studs fail in the same local buckling limit state dominated by web deformations near the member ends. As demonstrated further in Section 4 since the sheathing, which is connected to the flanges, has little to no influence on the local buckling of these studs the additional capacity must derive from the sheathing itself carrying a modest amount of axial load (and the stiffer, stronger OSB sheathing carrying more than gypsum board). This occurs despite the fact that the sheathing is not allowed to directly bear on the loading or support beams and instead must transfer its axial load to the track via fasteners in shear back to the stud.

3.6 Dis-similar sheathing on the two sides

Walls with dis-similar sheathing, OSB on one side and Gypsum on the other (OSB-Gyp) present an interesting response: limit state (local buckling), strength (Table 1) and axial load-displacement (Figure 2) is essentially the same for all tests, but deformations observed in the post-peak behavior vary. Test 3-OSB-Gyp failed in local buckling (Figure 6d), but in the post-peak regime also exhibited flexural-torsional buckling (stud S14, Figure 7c). Test 10-OSB-Gyp also failed in local buckling; however, post peak one stud was also observed to fail in distortional buckling (Figure 3i). Test 8-OSB-Gyp failed in local buckling alone. OSB and gypsum board restrain the stud with different stiffness and strength, this leads to fastener tearing (bearing failures) in the Gypsum board (Figure 6b,c) as the stud twists about the more restrained OSB face. Though the imbalance in sheathing stiffness creates this demand, the observed limit state remains local buckling and the observed strength is consistent with walls with similarly sheathed studs.

3.7 Comparison between wall tests and single stud tests

The observed limit states in the single stud tests of (Vieira, et al. 2011) are the same as for the wall tests reported here. However, as indicated in Table 1, the peak load is usually slightly lower in the complete wall tests (except for the OSB-Bare tests). Postulated reasons for the slight decrease in the full-scale wall tests, when compared with the single columns tests: (a) the tributary area of the board designated to each stud in the wall as engaged for sheathing resistance is modestly less than in the single column tests, (b) bracing forces in the sheathing accumulate and may have a modestly detrimental influence, (c) when the weakest of the 5 studs in the wall fail the forces must be carried by the other studs, thus strength may be more of a weakest link strength as opposed to an idealized redistribution of a fully parallel system.

For the OSB-Bare case the failure is in flexural-torsional buckling and the full wall actually has a higher observed per stud mean strength than the single column, this may be due to the increased torsional resistance at the ends of the studs in a full wall, but the variability is significant and the failure mode in the full walls and one-sided sheathed single studs is similar.

4 FASTENER-SHEATHING STIFFNESS

The bracing forces that are supplied to a sheathed stud occur at the fastener locations. Thus, Winter's basic idea of a stud braced by springs (Figure 1d) still provides the conceptually correct beginning. However, many types of springs exist (not just those restricting lateral translation, see Figure 1e) and perhaps more importantly, the springs represent a fastener-sheathing system and not just local fastener stiffness. A contribution of the work of Vieira (Vieira 2011), summarized here, is the marriage of local and diaphragm stiffness in the determination of the fastener-sheathing stiffness and the formalization of experimental and simplified analytical methods for determining this stiffness.

Theoretically, the fastener-sheathing system supplies three translation and three rotational springs at every fastener location bracing the stud. Practically, a more limited set of springs in the plane of the cross-section, as shown in Figure 1e, consisting of lateral translation (k_x) which is in the plane of the sheathing, "vertical" translation (k_y) which is out of the plane of the sheathing, and rotational stiffness (k_ϕ) which is in the plane of the cross-section are the most important. The k_x springs restrain against buckling modes associated with weak-axis flexure and torsion, while k_ϕ springs restrains flange distortion (distortional buckling), and k_y springs restrain strong-axis flexure and account for flexural composite action. The translational spring along the length (k_z) is neglected because the fastener-sheathing system is not allowed to provide an independent vertical load path. The rotational spring about the fastener ($k_{\phi y}$) is neglected since the fasteners are largely free to twist in the sheathing. The out-of-plane rotational spring about the x-axis ($k_{\phi x}$) may be approximated as the same as k_ϕ (the mechanisms are similar) but is generally neglected because restriction of in-plane (cross-section) deformations are of the most importance.

4.1 Lateral translational stiffness (k_x)

Resistance to lateral translation at the fastener location from the fastener-sheathing system consists of two parts: local resistance as the fastener tilts and bears into the sheathing, and diaphragm resistance as the stud undergoes bending which is resisted by shear in the diaphragm equilibrated by differential lateral forces at the fasteners. These two mechanisms are fully detailed in Vieira and Schafer (2012); in particular, it is shown that they act in series and thus the lateral translational stiffness k_x is determined by combining the local translational stiffness ($k_{x\ell}$) and diaphragm translational stiffness (k_{xd}) via:

$$k_x = 1/\left(1/k_{x\ell} + 1/k_{xd}\right) \tag{1}$$

The local translational stiffness ($k_{x\ell}$) was the focus of Winter's pioneering work (Green, et al. 1947, Winter 1960) and the most direct means to determine $k_{x\ell}$ is by test. Figure 8 shows a simple test of two horizontal studs connected by sheathing fastened to the flanges where the studs are pulled apart (perpendicular to the long axis of the stud). This test was preferred by Winter and by the authors, but other valid methods exist (Fiorino, et al. 2007, Okasha 2004, Chen, et al. 2006). The observed bearing response in the simple fastener test is similar to the wall tests, as shown in Figure 8b and c.

Alternatively, $k_{x\ell}$ may be approximated by a lower bound formula:

$$k_{x\ell} = \frac{3Ed^4t^3\pi}{4t_{board}^2(9d^4\pi + 16t_{board}t^3)} \tag{2}$$

where: E = Young's modulus of the steel stud, d = fastener diameter, t = flange thickness, and t_{board} = board or sheathing thickness. The expression assumes that a tributary width of the stud flange and the fastener form a frame, that in bending resist the lateral movement of a force applied at the fastener head (a distance t_{board} from the flange). Though approximate, and only accounting for the sheathing in terms of its thickness, the expression is found to provide a useful lower bound (Vieira and Schafer 2012).

The lateral diaphragm resistance developed at the fasteners as the studs attempt to bend in a single half sine wave about the weak-axis, k_{xd}, is:

$$k_{xd} = \frac{\pi^2 G t_{board} d_f w_{tf}}{L^2} \tag{3}$$

where: G = shear modulus of the sheathing, and may be found through testing by ASTM-D2719-89 (ASTM 2002a), or utilizing tabulated values from NDS (NDS 2005), w_{tf} = fastener tributary width, d_f = distance between fasteners, and L = sheathing height. Derivation and validation of the expression is available (Vieira and Schafer 2012).

The marriage of the local and diaphragm stiffness is critical to the method's robustness. The local stiffness accounts for the stud (E, t) the fastener (d) and its length (t_{board} is the fastener length in bending) while the diaphragm stiffness brings in the critical issues of sheathing shear stiffness (G) and stud spacing (w_{tf}). If the diaphragm is stiff enough sheathing shear rigidity and stud spacing are irrelevant and only local mechanisms dominate, but if the sheathing is weak in shear, as shown analytically and experimentally in Vieira and Schafer (2012), the opposite occurs. Thus, as an example, even for the same stud the importance of stud spacing may be great for one type of sheathing and irrelevant for another. This explains the sometime contradictory existing results regarding stud spacing and unites the fundamentals of the local approach used in the AISI Specification from 1962-1980 and the diaphragm approach from 1980-2004.

4.2 Out of plane translational stiffness (k_y)

Translational stiffness k_y, restricts deformations out of the plane of the sheathing, and is typically ignored in derivations related to sheathing bracing. However, in flexural-torsional buckling of studs the flexure is in the strong-axis and even small resistance to vertical (out-of-plane) movement can be influential. If composite action is ignored then k_y is the stiffness from bending of the sheathing about its own axis. For a stud bending about its strong axis in a single half sine wave sheathing bent in the same mode will contribute:

$$k_y = \frac{(EI)_w \pi^4 d_f}{L^4} \tag{4}$$

where: $(EI)_w$ = sheathing rigidity per APA-D510C (APA-D510C 2008) for OSB and plywood sheathing, and GA-235-10 (GA-235-10 2010) for gypsum sheathing, d_f = distance between fasteners, and L = sheathing height. For fully composite action $(EI)_{wc}$ replaces $(EI)_w$ in Eq. (4):

$$\left(EI\right)_{wc} = \left(EI\right)_w + E_w w_{tf} t_{board} \left(\tfrac{1}{2} h + \tfrac{1}{2} t_{board}\right)^2 \tag{5}$$

where E_w may be back-calculated from the tabled $(EI)_w$ as

$$E_w = 12\left(EI\right)_w / w_{tf} t_{board}^3 \tag{6}$$

w_{tf} = tributary width of the fastener, t_{board} = thickness of the board, and h = out-to-out depth of the stud.

Determination of partial composite action (the most realistic situation) requires testing. For non-structural stud walls it is common practice to determine the stiffness of the composite wall system via ASTM-E72 (ASTM 2002b) tests, a similar test is recommended here. The strong-axis bending rigidity of the composite stud-sheathing system ($(EI)_{system}$) may be found from the results of ASTM-E72 tests in one of the two loading alternatives:

$$(EI)_{system} = \frac{11HL^3}{384\delta} \text{ (two point loads) or } = \frac{5wL^4}{384\delta} \text{ (uniform load)} \tag{7}$$

where: H = concentrated load applied perpendicular to the wall, L = height of the wall, w = uniform load perpendicular to the wall, and δ = maximum measured displacement for the respective loading case (H or w). The stiffness of the stud must be removed from the system stiffness to determine k_y, also recognizing that sheathing is on two sides (i.e. k_y is on the two flanges) the sheathing bending rigidity $(EI)_{wpc}$ that should be used in Eq. (4) for partially composite action is:

$$\left(EI\right)_{wpc} = \tfrac{1}{2}\left[\left(EI\right)_{system} - \left(EI\right)_{stud}\right] \tag{8}$$

4.3 Rotational Stiffness (k_ϕ)

Rotational stiffness restricts cross-section torsion and flange rotation/distortion. For sheathing on both flanges the k_x pair is more effective in resisting torsion than k_ϕ, so in practical cases the importance of k_ϕ is in restricting flange rotation associated with distortional buckling. The rotational stiffness develops as the flange attempts to rotate against the sheathing and a

moment couple consisting of contact at the stud flange/web juncture and pull-through at the fastener location develops. This mechanism is fully explored in Schafer et al. (2010) along with experiments utilizing an augmented version of AISI-TS-1 (2002) and a simple analytical formulation that in 2011 was adopted in AISI-S210 in a tabular form. The rotational stiffness is separated (similar to lateral stiffness) into two components the local fastener (connector) foundation stiffness $\underline{k}_{\phi c}$ and the sheathing stiffness $\underline{k}_{\phi w}$, and the two are combined as springs in series:

$$\underline{k}_{\phi c} = 0.00035Et^2 + 75 \text{ (note: } E \text{ in lbf/in}^2\text{, } t \text{ in in.)} \quad (9)$$

$$\underline{k}_{\phi w} = (EI)_w / d_f \quad (10)$$

$$\underline{k}_{\phi} = 1/(1/\underline{k}_{\phi c} + 1/\underline{k}_{\phi w}) \quad (11)$$

where: E = Young's modulus of the steel stud, t = flange thickness, d_f = distance between fasteners, and $(EI)_w$ = sheathing rigidity per APA-D510C (APA-D510C 2008) for OSB and plywood sheathing, and GA-235-10 (GA-235-10 2010) for gypsum sheathing. Note, for $(EI)_w$ the appropriate sheathing orientation must be selected: horizontal for $\underline{k}_{\phi w}$ and vertical for k_y. In addition, if the discrete rotational stiffness at the fastener is desired, i.e., k_ϕ then $\underline{k}_\phi$ is simply multiplied times the fastener tributary length along the stud, i.e. d_f.

4.4 Fastener-sheathing stiffness for tested members

The fastener-sheathing stiffness k_x, k_y and k_ϕ was determined for the details consistent with the sheathed stud and wall testing of Section 3. For k_x the small scale experimental values as detailed in Vieira and Schafer (2012) are selected for $k_{x\ell}$, and k_{xd} and k_x are determined per Eq. 3 and 1 respectively. For k_y non-composite and composite limits based on Eq.'s 4 and 5 are used, and for $\underline{k}_\phi$ Eq.'s 9-11 are used. In addition, the discrete springs k_x and k_y are smeared into foundation stiffnesses (divided by fastener tributary length of the stud) which is denoted with an

underbar, i.e. $\underline{k}_x$, $\underline{k}_y$, The rotational stiffness of Eq. 11 is a foundation stiffness. Summary results and key assumptions are provided in Table 2 and complete details and further discussion are available in Vieira (2011).

5 ELASTIC STABILITY

The elastic stability of a CFS stud is significantly altered by the presence of sheathing. An unsheathed CFS stud such as the 362S162-68 studied in detail here has a classical finite strip signature curve (Schafer and Adany 2006) and the three typical stability modes: local, distortional, and global buckling as provided in Figure 9. The global buckling mode is either weak-axis flexural buckling, or flexural-torsional buckling – both are at similar elastic buckling loads. At practical lengths flexural-torsional buckling is the minimum (slightly lower than weak-axis flexure), while at extreme lengths (greater than 3 m) weak-axis flexural buckling is the minimum. If spring foundations are introduced into the finite strip model to account for the sheathing (per Section 4, numerical values in Table 2) then the influence of the sheathing may be observed to alter the signature curve. Note, comparison between shell finite element models with discrete springs and FSM models with smeared (foundation) springs indicate satisfactory accuracy for the smeared spring model up to fastener spacing as large as 203 mm (8 in.) in the studied cases (Iourio and Schafer 2008).

For the case of one-sided sheathing (OSB-Bare, Figure 10a) local buckling is largely unchanged, distortional buckling is slightly elevated, and global buckling is (a) elevated, (b) exhibits minima, (c) is dominated by restrained axis flexural-torsional buckling, and (d) shows significant sensitivity to the magnitude of $\underline{k}_y$ (i.e. the level of composite action in strong-axis flexure). The elevated elastic global buckling values provide an increase in strength. The global minimum (just like minima for local and distortional buckling) indicate that the half-wavelength

at which the particular (restrained axis flexural-torsional) global mode will repeat itself along the length (increases to the right of a minima for the same mode should be ignored). The dominance of flexural-torsional buckling is to be expected given the highly unsymmetric nature of the sheathing restraint. The sensitivity to $\underline{k}_y$ indicates the important role that the coupling of torsion and strong-axis flexure play in flexural-torsional buckling.

For the case of two-sided OSB sheathing (OSB-OSB, Figure 10b) local buckling is largely unchanged, distortional buckling is modestly elevated, and global buckling is (a) significantly elevated, (b) exhibits minima, and (c) shows sensitivity to the magnitude of $\underline{k}_y$ only when significant composite action is present. Comparison of the global stability with and without the non-composite (lower bound) $\underline{k}_y$ shows little change; indicating that the lateral stiffness ($\underline{k}_x$) supplied to the two flanges provides the primary resistance needed against both flexural-torsional and weak-axis flexural buckling at practical lengths. If no $\underline{k}_y$ is present at extreme lengths strong-axis flexure controls. If $\underline{k}_y$ is present a restrained flexural-torsional mode with a global minimum results – and this restrained mode is dependent on the magnitude of $\underline{k}_y$. At the fully composite limit global buckling is restrained (elastic global buckling values are extremely high). Note, if testing for partially composite action is not completed then the lower bound non-composite action for $\underline{k}_y$ should be employed in design predictions.

An important aspect of the elastic stability not provided in the finite strip signature curves of Figure 9 and Figure 10 is the impact of end boundary conditions. As detailed in Vieira et al. (2011) and discussed in Section 3.2 a fully seated stud bearing against a level steel plate (as in the testing conducted herein) develops bending and warping fixed end conditions. The finite strip signature curve is for pinned end conditions. It is possible to extend the finite strip method to general end conditions (Li and Schafer 2010a), but as a result the meaning of the signature curve

is lost and analysis is only useful at physical lengths (similar to a finite element method analysis of a member discretized as shell elements). Specific guidance on finding the elastic buckling loads for a sheathed stud follow.

5.1 Local Buckling ($P_{cr\ell}$)

Sheathing does not affect local buckling. The sheathing restrains the flange, but local buckling is largely driven by the web. Theoretically, $\underline{k}_x$ and $\underline{k}_\phi$ (if located at the exact mid-width of the flange) have no influence on local buckling, only $\underline{k}_y$. The out-of-plane stiffness, $\underline{k}_y$, is derived consistent with global bending resistance and not localized resistance. For local buckling predictions it is recommended to ignore the sheathing. Due to the short wavelength of the buckling mode, end conditions also have little influence on local buckling. Thus, a conventional finite strip signature curve result completed on the bare stud (or similar shell finite element model) is adequate for finding the local elastic buckling load, $P_{cr\ell}$. For industry standard studs $P_{cr\ell}$ has been tabled (Li and Schafer 2011); and practical modeling guidance and analytical hand solutions (if desired) are available (Schafer 2006).

5.2 Distortional Buckling (P_{crd})

Sheathing provides beneficial rotational restraint against distortional buckling, and $\underline{k}_\phi$ as discussed in Section 4.3 should be included when determining the elastic distortional buckling load (P_{crd}). For studs with deep webs (and narrow flanges) the additional restraint supplied by $\underline{k}_x$ may be influential – its inclusion is optional, but if included requires the use of computational stability solutions. Stiffness $\underline{k}_y$ should not be included when determining distortional buckling. In distortional buckling $\underline{k}_y$ would be engaged, but as derived, $\underline{k}_y$'s deformations are consistent with strong-axis stud flexure, not rotation of the flange. Further, $\underline{k}_\phi$ already accounts for the moment couple that develops between $\underline{k}_y$ at the fastener and bearing between the flange and sheathing.

End conditions have influence on distortional buckling at practical lengths. General end conditions may be treated in the finite strip solution (Li and Schafer 2010a), in shell finite element models, or by using a correction factor (D_{boost} in (Moen 2008)) for fixed-fixed end conditions on a simply-supported model. In some cases the distortional buckling mode can be difficult to identify in a finite strip model, in such cases the constrained FSM is recommended (Li and Schafer 2010a, 2010b).

For industry standard studs, tables are provided to aid in the determination of $\underline{k}_\phi$ and P_{crd} along with full design examples of the available analytical hand solutions (Li and Schafer 2011, Schafer 2008) including the P_{crd} solutions adopted in AISI-S100 (2007).

5.3 Global Buckling (P_{cre})

Sheathing greatly influences the global buckling load (P_{cre}). For determining P_{cre} inclusion of all available fastener-sheathing springs ($\underline{k}_x$, $\underline{k}_y$, $\underline{k}_\phi$) is recommended, but $\underline{k}_x$ is critical as it provides the primary fastener-sheathing restraint for both weak-axis flexure and torsion (when present on both flanges). Experimental determination of $k_{x\ell}$ may well be warranted for maximum efficiency; otherwise the lower bound solution of Eq. (2) combined with Eq.'s (3) and (1) may be used to determine $\underline{k}_x$. Flexural composite action can be beneficial and if tests are available can be utilized as detailed in Section 4.2; otherwise, the non composite value for $\underline{k}_y$ (Eq. 4) should be used.

End conditions (in the testing conducted here fixed ends are appropriate) should be accounted for in determining P_{cre}. To include the impact of fixed end conditions (and the bracing springs) the recently developed finite strip model for general end conditions (Li and Schafer 2010a) or shell finite element models may be utilized. Alternatively, classical analytical solutions with appropriate effective length factors may be employed. An analytical solution for global buckling of an unsymmetric section with multiple springs is not generally available. Timoshenko

(1961) provides the necessary fundamentals, but not the details for this particular case. A solution is provided for P_{cre} in the Appendix, including the appropriate effective length factors K_x, K_y, and K_t for the member buckling terms and K_{x_spring}, K_{y_spring}, and K_{t_spring} for the spring terms (see Appendix and Figure 11).

Comparison of the classical (Appendix) solution for P_{cre} to numerical solutions using FSM for general end boundary conditions, i.e. (Li and Schafer 2010a) are provided in Figure 11. For simply supported end boundary conditions the solutions are in exact agreement. For fixed-fixed end conditions the analytical solution is provided for a single buckling half-wave, i.e. m=1 and for two buckling half-waves m=2 with appropriate effective length (K) factors. Agreement is excellent, but care must be taken to use the m solution with the lowest P_{cre}. Computational solutions are preferred by the authors, but for cases where formal analytical solutions must be provided (and ultimately programmed), the analytical solution provides the correct answer.

6 MEMBER STRENGTH DETERMINATION

The basic method proposed for strength determination is to correct the elastic buckling loads for the presence of the sheathing and then to use existing design expressions; either the Direct Strength Method (DSM) of Appendix 1 of AISI-S100, or the Effective Width Method (EWM) of the main specification of AISI-S100 to find the strength. Determining the fastener-sheathing stiffness $\underline{k}_x$, $\underline{k}_y$, $\underline{k}_\phi$ per Section 4 is the first step. Finding the elastic buckling loads $P_{crℓ}$, P_{crd}, P_{cre} with appropriate inclusion of $\underline{k}_x$, $\underline{k}_y$, $\underline{k}_\phi$ per Section 5 is the second step. The final step is to utilize existing design expressions to convert the elastic buckling loads (and knowing the squash load, P_y) to predict the nominal strength P_n.

6.1 DSM Approach for finding P_n

The Direct Strength Method requires that the engineer provide the elastic buckling loads ($P_{cr\ell}$, P_{crd}, P_{cre}) by rational analysis. With those loads determined the predicted nominal capacity is a direct application of the available design expressions in Appendix 1 of AISI-S100, specifically global strength P_{ne} is found by:

$$P_{ne} = \begin{cases} 0.658^{\lambda_c^2} P_y & \text{for } \lambda_c \le 1.5 \\ 0.877 P_{cre} & \text{for } \lambda_c > 1.5 \end{cases} \quad \text{and } \lambda_c = \sqrt{P_y / P_{cre}} \tag{12}$$

Local-global interaction is accounted for utilizing:

$$P_{n\ell} = \begin{cases} P_{ne} & \text{for } \lambda_c \le 0.766 \\ \left[1 - 0.15\left(\frac{P_{cr\ell}}{P_{ne}}\right)^{0.4}\right]\left(\frac{P_{cr\ell}}{P_{ne}}\right)^{0.4} P_{ne} & \text{for } \lambda_c > 0.766 \end{cases} \quad \text{and } \lambda_\ell = \sqrt{P_{ne} / P_{cr\ell}} \tag{13}$$

Distortional buckling is found as follows

$$P_{nd} = \begin{cases} P_y & \text{for } \lambda_c \le 0.561 \\ \left[1 - 0.25\left(\frac{P_{crd}}{P_y}\right)^{0.6}\right]\left(\frac{P_{crd}}{P_y}\right)^{0.6} P_y & \text{for } \lambda_c > 0.561 \end{cases} \quad \text{and } \lambda_d = \sqrt{P_y / P_{crd}} \tag{14}$$

Finally the capacity is the minimum (note, $P_{n\ell}$ is strictly less than or equal to P_{ne}, P_{ne} is just an intermediary calculation):

$$P_n = \min\left(P_{ne}, P_{n\ell}, P_{nd}\right) \tag{15}$$

6.2 EWM Approach for Finding P_n

The main body of the AISI Specification utilizes the EWM approach for local buckling, which leads to a modestly different implementation for the strength. To account for local-global interaction an effective area (A_e) utilizing the design expressions in AISI-S100 Chapter B must be found at the long column stress F_n.

$$P_{nC4.1} = A_e F_n \tag{16}$$

$$F_n = \begin{cases} 0.658^{\lambda_c^2} F_y & \text{for } \lambda_c \le 1.5 \\ 0.877 F_e & \text{for } \lambda_c > 1.5 \end{cases} \quad \text{and } \lambda_c = \sqrt{F_y / F_e} \text{ and } F_e = P_{cre} / A_g \tag{17}$$

474 Note, F_n is identical to P_{ne}/A_g from the DSM method, $P_{nC4.1}$ is directly comparable to $P_{n\ell}$, and the
475 key modification is the introduction of a long column elastic buckling stress, F_e, that accounts for
476 sheathing restraint (i.e. P_{cre} as per Section 5 includes the benefit of sheathing). Distortional
477 buckling, found in C4.2 of the main Specification of AISI-S100 is identical to the DSM method:

$$P_{nC4.2} = \begin{cases} P_y & \text{for } \lambda_c \le 0.561 \\ \left[1 - 0.25\left(\frac{P_{crd}}{P_y}\right)^{0.6}\right]\left(\frac{P_{crd}}{P_y}\right)^{0.6} P_y & \text{for } \lambda_c > 0.561 \end{cases} \quad \text{and } \lambda_d = \sqrt{P_y / P_{crd}} \tag{18}$$

478 Finally, the strength is simply the minimum of the two

$$P_n = \min\left(P_{n-C4.1}, P_{n-C4.2}\right) \tag{19}$$

479 ## 7 COMPARISON WITH TESTS AND DISCUSSION

480 ### 7.1 Strength Comparison

481 In this section the observed axial capacity of the 0.6 m to 1.8 m (2 ft to 6 ft) tall sheathed
482 single stud tests (Vieira, et al. 2011) and the 2.44 m (8 ft) tall sheathed stud and wall tests (Table
483 1) are compared against the predicted member strength. Consider first the comparison for
484 specimens sheathed on one-side only (OSB-Bare) as provided in Figure 12. The figure provides
485 comparison to design predictions with pinned and fixed end conditions, as well as predictions
486 with no sheathing, with sheathing and a lower bound non composite flexural action assumption,
487 and with sheathing and upper bound composite flexural action assumed. The test data most
488 closely follows the assumption of fixed-fixed end conditions (this was also observed of bare-bare
489 specimens (Vieira, et al. 2011)). In fact, up to 183 cm (72 in.), the end conditions are more

490 influential than the sheathing restraint. For longer columns the importance of the sheathing
491 restraint grows significantly. For the fixed-fixed end conditions, the lower bound (non
492 composite) approximation for the sheathing contribution to the major–axis bending of the stud is
493 sufficiently accurate.

494 For the columns and walls with sheathing restraint on both sides: Gyp-Gyp, OSB-Gyp and
495 OSB-OSB Figure 13 provides a comparison with potential design assumptions (to provide some
496 clarity the spring values employed in the design curves are those for OSB-OSB alone, additional
497 curves with all combinations are provided subsequently). All of the tested columns fail in local
498 buckling, at approximately the same per stud strength. In stark contrast to the case with one-
499 sided sheathing (OSB-Bare) having springs on both flanges dramatically decreases the impact of
500 the end boundary conditions. Even when only considering the in-plane resistance ($\underline{k}_x$ and $\underline{k}_\phi$)
501 this restraint is enough to strongly restrict weak-axis bending and torsion. However, for longer
502 lengths the major-axis bending becomes increasingly important to restrain the stud. The
503 assumption of fixed-fixed end conditions and the noncomposite lower bound for $\underline{k}_y$ is again
504 found to be a good predictor of the behavior. Pin-pin end conditions and only in-plane resistance
505 (in essence the traditional model) is observed to be (a) a conservative predictor, and (b) one that
506 reasonably follows the observed experimental trends.

507 Finally, the proposed design method (using DSM and employing fixed-fixed end conditions,
508 $\underline{k}_x$ and $\underline{k}_\phi$ in-plane restraint and the non composite $\underline{k}_y$ lower bound resistance) is compared to
509 the tests and other currently available design methods. The test data compares well with the
510 proposed method and the small differences between OSB-OSB, OSB-Gyp, and Gyp-Gyp are
511 even reflected in the predicted strength, along with the relatively pronounced decrease as a
512 function of length for the one-sided sheathing case: OSB-Bare. The strength prediction is a

significant improvement over (a) ignoring the sheathing and end conditions (labeled AISI-S100-07 in Figure 14), (b) the diaphragm stiffness model used from 1980-2004 (labeled AISI-S100-01 in sheathing as Figure 14), and (c) the empirically simplified variation on the local stiffness approach adopted in 2004 (labeled AISI-S210-07 in Figure 14).

7.2 Fastener Demands

In all of the completed axial testing, member failure (not fastener failure) was the first observed limit state: flexural-torsional for tests without sheathing or one-sided sheathing, and local buckling for tests with sheathing on both flanges. In the post-peak collapse regime both local bearing failures in the sheathing and pull-through of the fastener through the sheathing are observed. The fastener demands due to global buckling, including those deriving from one-sided sheathing or dis-similar sheathing, may be predicted from an analytical method as provided in the Appendix. The method is dependent on the ratio of the axial load to the buckling load, the size of imperfection, and the mode shape itself. The method can readily be extended to FSM solutions as well (the FSM mode shapes and P_{cre} replace the analytical solution).

An extensive study of fastener demand using detailed shell finite element models of the stud, track, and sheathing, and discrete springs for the fasteners is provided in Vieira (2011). In global buckling fastener forces predicted by the analytical method agree reasonably well with the more detailed finite element model. The finite element model also provides fastener demands that develop due to local buckling and accumulation of fastener forces. These final two points warrant further study, but it is worth recalling that in the 2.4 m x 2.4 m (8 ft x 8 ft) CFS wall studied here fastener (and related) limit states did not control.

7.3 Discussion

Both practical and research work remains related to the design of axially loaded sheathed CFS studs. Development or augmentation of formal test standards for $k_{x\theta}$, k_y, and $k_{\phi c}$ are needed. Formal code-approved interfaces for the use of *EI* and *G* for gypsum board, plywood, oriented strand board and other sheathing materials are needed. The lower bound expressions provided herein for stiffness need adoption by the AISI Specification. The appropriate selection of end boundary conditions for imperfect bearing surfaces needs further study, as the analysis here shows that fixed end boundary conditions are possible against steel surfaces. Though preliminary work is complete formal methods are needed in the AISI Specification for predicting all fastener demands and for predicting capacities for various sheathing materials (particularly, bearing and pull-through). Extensions are possible, and needed, for (a) systems that use both steel bridging and sheathing to brace studs; (b) to account for brace force accumulation, and (c) for beam-columns where fastener demands to resist direction torsion can be much greater than those observed here for axial loads alone.

8 CONCLUSIONS

Studs of load bearing cold-formed steel framed walls may be adequately braced by sheathing. Characterization of the sheathing-bracing requires careful consideration of local fastener deformations and global sheathing deformations. This insight of the dual sources (local and global) for sheathing-bracing leads to a unification of proposed analytical and design methods which focused exclusively on either local fastener deformations (Winter's method) or global deformations (shear diaphragm method). Analytical formulae are provided for characterizing the stiffness of sheathing-bracing and may be augmented by material and small-scale fastener tests for greater accuracy as described herein. With the correct stiffness of the sheathing-bracing

established local, distortional, and global buckling of the sheathing-braced studs may be readily predicted; including cases of one-sided or dis-similar sheathing, in addition to studs with similar sheathing attached to the two stud flanges. Both computational and analytical methods are provided for the elastic buckling determination and specific guidance is provided for appropriately including the sheathing-bracing springs in each of the local, distortional, and global buckling modes. It is proposed to use the sheathing-braced elastic buckling values in design, and both Direct Strength and Effective Width procedures for doing so are detailed. A series of full-scale tests on 2.4 m x 2.4 m (8 ft x 8 ft) cold-formed steel framed walls with combinations of oriented strand board, gypsum board, and no sheathing were tested to failure in axial compression. All tests with sheathing attached to both stud flanges (oriented strand board, gypsum, or a combination of the two) failed in local buckling. Tests with sheathing on one side only, failed in a dramatic restrained-axis flexural-torsional buckling mode. Comparison of the tested capacities with the proposed design method demonstrates good agreement across the member lengths and sheathing conditions studied. Further, the proposed method is a significant improvement over existing and past Specification methods. Work remains to simplify the fastener demand predictions, explicitly incorporate brace force accumulation, and extend the approach to allow for discrete bridging and sheathing-bracing to both be included in the design – a highly desired feature for practice.

9 ACKNOWLEDGMENTS

For all their help in the lab acknowledgments are extended to Senior Instrument Designer Nickolay Logvinovsky and undergraduate researchers: Hannah Blum, Mo Alkyasi, Lauren Thompson, Linda Wan and Maggie Wildnauer. For providing materials and equipment thanks are also extended to the Steel Stud Manufacturers Association and Simpson Strong Tie. Finally, the American Iron and Steel Institute and the Steel Stud Manufactures Association are acknowledged for funding the research. Any opinions, findings, and conclusions or recommendations expressed in this material are those of the authors only and do not necessarily reflect the views of the sponsors, or material suppliers.

10 REFERENCES

[1] Vieira, L. C. M. J. (2011). "Behavior and Design of Sheathed Cold-Formed Steel Stud Walls under Compression." Doctor of Philosophy, Johns Hopkins University, Baltimore.

[2] AISI (1962). "Light Gage Cold-Formed Steel Design Manual." *American Iron and Steel Institute*.

[3] AISI (1980). "Light Gage Cold-Formed Steel Design Manual." *American Iron and Steel Institute*.

[4] AISI-S100 (2007). "North American Specification for the Design of Cold-Formed Steel Structural Members." *American Iron and Steel Institute*.

[5] AISI-S211 (2007). "North American Specification for the Design of Cold-Formed Steel Structural Members." *American Iron and Steel Institute*.

[6] Schafer, B. W., Iourio, O., and Vieira Jr, L. C. M. (2008). "Notes on AISI Design Methods for Sheathing Braced Design of Wall Studs in Compression." *A supplemental report for AISI-COFS Project on Sheathing Braced Design of Wall Studs*, The Johns Hopkins University, Baltimore.

[7] Green, G. G., Winter, G., and Cuykendall, T. R. (1947). "Light Gage Steel Columns in Wall-braced Panels." *Cornell University Engiineering Experiment Station*, 35, 1-50.

[8] Winter, G. (1960). "Lateral Bracing of Beams and Columns." *Journal of the Structural Division*.

[9] Simaan, A., and Pekoz, T. B. (1976). "Diaphragm Braced Members and Design of Wall Studs." *ASCE J Struct Div*, 102(1), 77-92.

[10] Miller, T. H., and Pekoz, T. (1993). "Behavior of cold-formed wall stud-assemblies." *Journal of structural engineering New York, N.Y.*, 119(2), 641-651.

[11] Trestain, T. (2002). "AISI Cold-Formed Steel Framing Design Guide CF02-1." American Iron and Steel Institute, Washigton D.C.

610 [12] Vieira, L. C. M. J., Shifferaw, Y., and Schafer, B. W. (2011). "Experiments on sheathed
611 cold-formed steel studs in compression." *Journal of Constructional Steel Research*.
612 [13] AISI-S200 (2007). "North American Standard for Cold-Formed Steel Framing - General
613 Provisions." *American Iron and Steel Institute*, AISI-S200-07.
614 [14] SSMA (2001). "Product Technical Information, ICBO ER-4943P." S. S. M. Association, ed.
615 [15] Vieira, L. C. M. J., and Schafer, B. W. (2012). "Lateral Stiffness and Strength of Sheathing
616 Braced Cold-Formed Steel Stud Walls." *Engineering Structures*(Accepted for Publication).
617 [16] Fiorino, L., Della Corte, G., and Landolfo, R. (2007). "Experimental tests on typical screw
618 connections for cold-formed steel housing." *Engineering Structures*, 29(8), 1761-1773.
619 [17] Okasha, A. F. (2004). "Okasha, A.F., Performance of Steel Frame/Wood Sheathing Screw
620 Connections
621 Subjected to Monotonic and Cyclic Loading, 2004, McGill University." M.S., McGill
622 University, Montreal.
623 [18] Chen, C. Y., Okasha, A. F., and Rogers, C. A. (2006). "Analytical Predictions Of Strength
624 and Deflection Of Light Gauge Steel Frame/Wood Panel Shear Walls." *Advances in Engineering*
625 *Structures, Mechanics & Construction*, 381-391.
626 [19] ASTM (2002a). "Standard Test Method for Structural Panels in Shear Through-the-
627 Thickness." *ASTM D2719-89*, American Society for Testing and Materials, West Conshohocken,
628 PA.
629 [20] NDS (2005). "National Design Specification (NDS) for Wood Construction, ANSI/AF&PA
630 NDS." A. F. a. P. Association, ed.Washington, DC.
631 [21] APA-D510C (2008). "Panel Design Specification." A.-T. e. W. Association, ed.Tacoma,
632 Washington, USA.
633 [22] GA-235-10 (2010). "Gypsum Board Typical Mechanical and Physical Properties." Gypsum
634 Association, Hyattsville, MD, USA.
635 [23] ASTM (2002b). "Standard Test Methods of Conducting Strength Tests of Panels for
636 Building Construction." *E 72-98*, American Society for Testing and Materials, West
637 Conshohocken, PA.
638 [24] Schafer, B. W., Vieira Jr, L. C. M., Sangre, R. H., and Guan, Y. (2010). "Rotational
639 Restraint and Distortional Buckling in Cold-Formed Steel Framing Systems." *Revista Sul-*
640 *Americana de Engenharia Estrutural (South American Journal of Structural Engineering)*, 7(1),
641 71-90.
642 [25] AISI-TS-1-02 (2002). "Rotational-Lateral Stiffness Test Method for Beam-to-Panel
643 Assemblies." *AISI Cold-Formed Steel Design Manual*.
644 [26] Schafer, B. W., and Adany, S. "Buckling analysis of cold-formed steel members using
645 CUFSM: Conventional and constrained finite strip methods." *Proc., Eighteenth International*
646 *Specialty Conference on Cold-Formed Steel Structures: Recent Research and Developments in*
647 *Cold-Formed Steel Design and Construction*, 39-54.
648 [27] Iourio, O., and Schafer, B. W. (2008). "FE modeling of elastic buckling of stud walls."
649 *research report to American Iron and Steel Institute*, Johns Hopkins University, Baltimore, MD,
650 42.
651 [28] Li, Z., and Schafer, B. W. "Buckling analysis of cold-formed steel members with general
652 boundary conditions using CUFSM: conventional and constrained finite strip methods." *Proc.,*
653 *Twentieth International Specialty Conference on Cold-Formed Steel Structures*.
654 [29] Li, Z., and Schafer, B. W. (2011). "Local and Distortional Elastic Buckling Loads and
655 Moments for SSMA Stud Sections." Cold-Formed Steel Engineers Institute, 5.

[30] Schafer, B. W. (2006). "Direct Strength Method Design Guide." American Iron and Steel Institute, Washington, D.C., 171.
[31] Moen, C. D. (2008). "Direct strength design for cold-formed steel members with perforations." Ph.D., Johns Hopkins University, Baltimore, MD USA.
[32] Li, Z., and Schafer, B. W. (2010b). "Application of the finite strip method in cold-formed steel member design." *Journal of Constructional Steel Research*, 66(8-9), 971-980.
[33] Schafer, B. W. (2008). "Design Aids and Examples for Distortional Buckling." *Tech Note*, Cold-Formed Steel Engineers Institute, 22.
[34] Timoshenko, S. P., Gere, James M. (1961). *Theory of Elastic Stability*, McGraw-Hill, New York.
[35] Zeinoddini, V. M., and Schafer, B. W. (2011). "Global Imperfections and Dimensional Variations in Cold-Formed Steel Members." *International Journal of Sructural Stability and Dynamics*, (Accepted 2011).

11 GLOSSARY OF VARIABLES

See Figure 15 for axis definition

$k_{x\ell}$ = local (fastener) translational stiffness in x
k_{xd} = lateral diaphragm stiffness in x
k_x = discrete lateral fastener-sheathing stiffness in x
$\underline{k}_x$ = foundation lateral fastener-sheathing stiffness in x
k_y = discrete lateral fastener-sheathing stiffness in y
$\underline{k}_y$ = foundation lateral fastener-sheathing stiffness in y
$k_{\phi c}$ = local rotational fastener (connector) stiffness in the x-y plane
$k_{\phi w}$ = sheathing rotational stiffness in the x-y plane
k_ϕ = discrete rotational fastener-sheathing stiffness in the x-y plane
$\underline{k}_\phi$ = foundation rotational fastener-sheathing stiffness in the x-y plane
h_{xi} = x-distance from centroid to spring i
h_{yi} = y-distance from centroid to spring i
h_{xs} = x-distanced from shear center to spring i
h_{ysi} = y-distance from shear center to spring i
I_o = polar moment of inertia of stud ($I_o = I_x + I_y + A\left(x_o^2 + y_o^2\right)$)
A = cross-sectional area of the stud
E = Young's modulus of steel
E_w = Young's modulus of sheathing
G = Shear modulus of sheathing
J = St. Venant Torsional Constant of stud
I_x = Moment of inertia about x-axis of stud
I_y = Moment of inertia about y-axis of stud
C_w = Warping constant of stud
x_o = x distance from centroid to shear center
y_o = y distance from centroid to shear center
K_x = effective length about x-axis
K_y = effective length about y-axis
K_t = effective length in torsion about shear center
$K_{x,spring}$ = effective length for the spring foundation about x-axis
$K_{y,spring}$ = effective length for the spring foundation about y-axis
$K_{t,spring}$ = effective length in torsion for the spring foundation about shear center
d = fastener diameter
t = flange thickness
t_{board} = board or sheathing thickness
w_{tf} = fastener tributary width
d_f = distance between fasteners
L = sheathing height
$(EI)_w$ = sheathing rigidity per APA-D510C (APA-D510C 2008) for OSB and plywood sheathing, and GA-235-10 (GA-235-10 2010) for gypsum sheathing (for fully composite action $(EI)_{wc}$ replaces $(EI)_w$)
$(EI)_{wpc}$ = sheathing bending rigidity for partially composite action

715 $(EI)_{system}$ = strong-axis bending rigidity of the composite stud-sheathing system found from the
716 results of ASTM-E72 tests
717 h = out-to-out depth of the stud
718 H = concentrated load applied perpendicular to the wall for composite action testing
719 L = stud length or height of the wall
720 w = uniform load perpendicular to the wall for composite action testing
721 δ = maximum measured displacement at mid-height for the respective loading case (H or w)
722 P = axial reference load in buckling analysis
723 $P_{cr\ell}$ = local elastic buckling load
724 P_{crd} = distortional elastic buckling load
725 P_{cre} = global elastic buckling load
726 P_y = squash load
727 P_n = nominal strength
728 P_{ne} = global strength
729 $P_{n\ell}$ = local strength
730 P_{nd} = distortional strength
731 P_{crx} = global elastic buckling load in x
732 P_{cry} = global elastic buckling load in y
733 $P_{cr\phi}$ = torsional elastic buckling load about shear center
734 λ_c = column non-dimensional slenderness
735 A_e = effective area
736 $P_{nC4.1}$ = local buckling strength, found in C4.1 of the main Specification of AISI-S100
737 $P_{nC4.2}$ = distortional buckling strength, found in C4.2 of the main Specification of AISI-S100
738 F_n = nominal stress (long column) = P_{ne}/A_g
739 K_e = elastic stiffness matrix
740 λ = eigenvalue
741 K_g = geometric stiffness matrix
742 Φ = eigenvector
743 P_{crj} = buckling loads for the buckling modes (j=1, 2, 3)
744 λ_j = eigenvalues for the buckling modes (j=1, 2, 3)
745 u_{crj} = eigenvector in the x direction for the buckling modes (j=1, 2, 3)
746 v_{crj} = eigenvector in the y direction for the buckling modes (j=1, 2, 3)
747 ϕ_{crj} = eigenvector on the plane x-y for the buckling modes (j=1, 2, 3)
748 u_λ = buckling mode shape along the length in the x direction
749 v_λ = buckling mode shape along the length in the y direction
750 ϕ_λ = buckling mode shape along the length in the x-y plane
751 u_0 = mid-height bow
752 v_0 = mid-height camber
753 ϕ_0 = mid-height twist
754 u_{imp} = initial imperfection shape along the length in the x direction
755 v_{imp} = initial imperfection shape along the length in the y direction
756 ϕ_{imp} = initial imperfection shape along the length in the x-y plane
757 β_j = amplification of deflection for any buckling mode (j=1, 2, 3)
758 δ_{xi} = amplification of the deformation in the x direction at fastener location i at the mid-height
759 δ_{yi} = amplification of the deformation in the y direction at fastener location i at the mid-height

760 ϕ_{xyi} = amplification of the twist in the *x*-*y* plane at fastener location *i* at the mid-height
761 u_i = deformation along the length in the *x* direction at fastener location *i*
762 v_i = deformation along the length in the *y* direction at fastener location *i*
763 ϕ_i = twist along the length in the plane *x*-*y* at fastener location i

12 APPENDIX: GLOBAL BUCKLING AND FASTENER DEMANDS

The following provides an extension to Timoshenko (1961) Article 5.6. Consider the stability of an axially loaded member with an arbitrary number of $\underline{k}_{xi}$, $\underline{k}_{yi}$, $\underline{k}_{\phi i}$ foundation springs attached at location *i* in the cross-section as depicted in Figure 15. The axial stability is an eigen problem:

$$\left(K_e - \lambda K_g\right)\Phi = 0 \tag{A1}$$

where the elastic stiffness including the contribution from the foundation springs is:

$$K_e = \begin{bmatrix} P_{cry} + \frac{(K_{y,spring}L)^2}{m^2\pi^2}\sum_{i=1}^{n}\underline{k}_{xi} & 0 & \frac{(K_{y,spring}L)^2}{m^2\pi^2}\sum_{i=1}^{n}\underline{k}_{xi}h_{ysi} \\ & P_{crx} + \frac{(K_{x,spring}L)^2}{m^2\pi^2}\sum_{i=1}^{n}\underline{k}_{yi} & -\frac{(K_{x,spring}L)^2}{m^2\pi^2}\sum_{i=1}^{n}\underline{k}_{yi}h_{xsi} \\ sym & & \frac{I_0}{A}P_{cr\phi} + \frac{(K_{t,spring}L)^2}{m^2\pi^2}\sum_{i=1}^{n}\underline{k}_{xi}(h_{ysi})^2 + \frac{(K_{t,spring}L)^2}{m^2\pi^2}\sum_{i=1}^{n}\underline{k}_{yi}(h_{xsi})^2 + \frac{(K_{t,spring}L)^2}{m^2\pi^2}\sum_{i=1}^{n}\underline{k}_{\phi i} \end{bmatrix} \tag{A2}$$

$$P_{crx} = \frac{m^2\pi^2 EI_x}{(K_xL)^2}, \quad P_{cry} = \frac{m^2\pi^2 EI_y}{(K_yL)^2}, \text{ and } \quad P_{cr\phi} = \frac{A}{I_o}\left(GJ + \frac{m^2\pi^2 EC_w}{(K_tL)^2}\right)$$

Further, the geometric stiffness under reference load *P* is:

$$K_g = P\begin{bmatrix} 1 & 0 & y_o \\ & 1 & -x_o \\ sym & & \frac{I_o}{A} \end{bmatrix} \tag{A3}$$

The three buckling loads P_{cr1}, P_{cr2}, P_{cr3} are found from the eigenvalues (λ's) as follows:

$$\begin{bmatrix} P_{cr1} & 0 & 0 \\ 0 & P_{cr2} & 0 \\ 0 & 0 & P_{cr3} \end{bmatrix} = \begin{bmatrix} \lambda_1 & 0 & 0 \\ 0 & \lambda_2 & 0 \\ 0 & 0 & \lambda_3 \end{bmatrix} P \tag{A4}$$

and the buckling modes from the eigenvectors (columns of Φ):

$$\Phi = \begin{bmatrix} \begin{Bmatrix} u_{cr1} \\ v_{cr1} \\ \phi_{cr1} \end{Bmatrix} & \begin{Bmatrix} u_{cr2} \\ v_{cr2} \\ \phi_{cr2} \end{Bmatrix} & \begin{Bmatrix} u_{cr3} \\ v_{cr3} \\ \phi_{cr3} \end{Bmatrix} \end{bmatrix} \tag{A5}$$

774 Note, for convenience the columns of Φ are normalized such that $\sqrt{u_{cr}^2 + v_{cr}^2 + \phi_{cr}^2} = 1$. The

775 buckling mode shape along the length is defined as:

$$u_\lambda = u_{cr} \sin(\pi z / L),\ v_\lambda = v_{cr} \sin(\pi z / L), \text{ and } \phi_\lambda = \phi_{cr} \sin(\pi z / L) \tag{A6}$$

776
777 Global initial imperfections may be defined based on the mid-height bow (u_o) camber (v_o)

778 and twist (ϕ_o) imperfections:

$$u_{imp} = u_o \sin(\pi z / L),\ v_{imp} = v_o \sin(\pi z / L), \text{ and } \phi_{imp} = \phi_o \sin(\pi z / L) \tag{A7}$$

779 statistics of measured global imperfections (u_o, v_o, ϕ_o) of CFS studs are available (Zeinoddini and

780 Schafer 2011). Amplification of deflection for any global mode (j = 1, 2, 3) follows from

$$\beta_j = \frac{P / P_{crj}}{1 - P / P_{crj}} \tag{A8}$$

781 Specifically, at fastener location i the mid-height deflection accounting for imperfections, the

782 three buckling modes, and the amplification of the deformations is:

$$\delta_{xi} = \sum_{j=1 \text{ to } 3} \beta_j \left(u_o u_{crj} + \phi_o h_{ysi} \phi_{crj} \right) \tag{A9}$$

$$\delta_{yi} = \sum_{j=1 \text{ to } 3} \beta_j \left(\delta_{oy} v_{crj} + \phi_o h_{xsi} \phi_{crj} \right) \tag{A10}$$

$$\phi_{xyi} = \sum_{j=1 \text{ to } 3} \beta_j \left(\phi_o \phi_{crj} \right) \tag{A11}$$

783 and along the length at fastener location i the deformations are:

$$u_i = \delta_{xi} \sin(\pi z / L),\ v_i = \delta_{yi} \sin(\pi z / L), \text{ and } \phi_i = \phi_{xyi} \sin(\pi z / L) \tag{A12}$$

784 These displacements may be multiplied times fastener-sheathing stiffness k_x, k_y, k_ϕ at any fastener

785 location to determine predicted fastener forces. Given the nature of the deformed shapes, mid-

786 height forces typically control.

TABLES

Table 1 – Condensed summary of test results (ascending order of mean peak load)

Test #	Sheathing Front	Sheathing Back	Limit State[1]	Wall Tests Peak Load Total (kN)	per stud (kN)	per stud mean	per stud CoV	Single Stud Tests[2] Peak Load (kN)
2	Bare	Bare	FT and F	250.6	50.1	50.1	-	57.1
12	OSB	Bare	FT	362.8	72.6			
1	OSB	Bare	FT	396.8	79.4			
6	OSB	Bare	FT	410.2	82.0	78.0	0.063	69.6
7	Gyp	Gyp	L	418.4	83.7			
11	Gyp	Gyp	L	429.9	86.0			
4	Gyp	Gyp	L	437.9	87.6	85.7	0.023	95.1
10	OSB	Gyp	L	458.4	91.7			
3	OSB	Gyp	L	470.2	94.0			
8	OSB	Gyp	L	471.4	94.3	93.3	0.015	99.9
5	OSB	OSB	L	471.7	94.3			
9	OSB	OSB	L	487.3	97.5	95.9	-	102.7

(1) Primary limit state observed at peak strength, FT=flexural-torsional, F=weak-axis flexural, L=local buckling

(2) Single stud tests 2.44 m (8 ft) in length as reported in Vieira and Schafer (2011)

Table 2 – Spring foundation stiffness and properties considered

Sheathing Material	$\underline{k}_x$ (N/mm/mm)	$\underline{k}_y$-fully composite (N/mm/mm)	$\underline{k}_y$-non-composite (N/mm/mm)	$\underline{k}_\phi$ (kN.mm/mm/rad)
OSB	3.185	0.3172	0.001227	0.313
Gypsum	1.172	0.0579	0.000284	0.315

$\underline{k}_x$ – t_{board} = 1.11 cm, w_{tf} = 61 cm, d_f = 30.5 cm, L = 244 cm, OSB – G = 1310 MPa, $k_{x\ell}$ = 1241 N/mm, k_{xd} = 4490 N/mm, Gyp – G = 552 MPa, $k_{x\ell}$ = 426N/mm, k_{xd} = 2147N/mm

$\underline{k}_y$ – b_w = 92mm, OSB – $(EI)_{w\text{-parallel}}$=736N.m^2/m , Gyp – E = 993 MPa

$\underline{k}_s$ – laboratory test

802 FIGURES

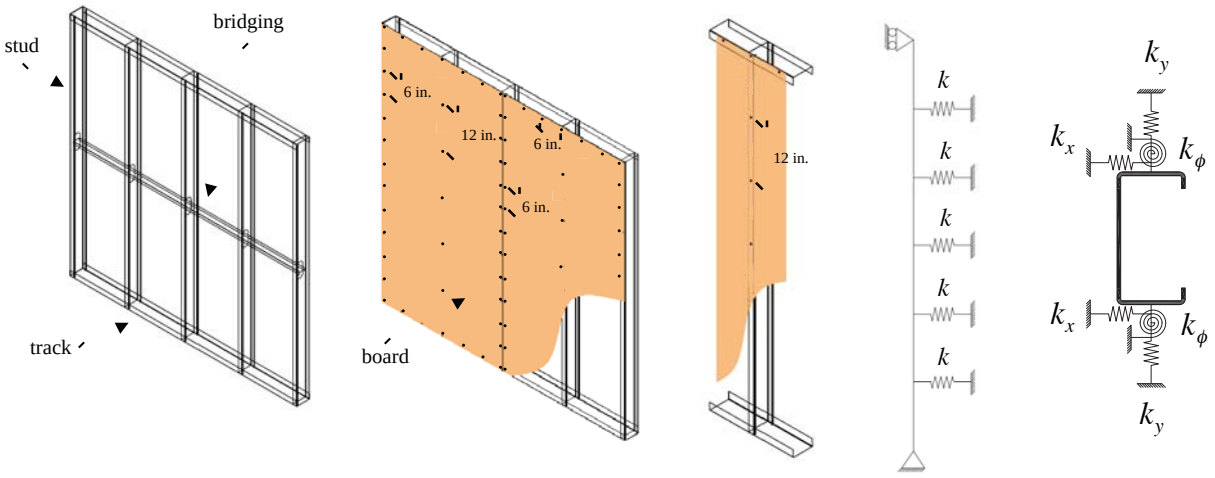

803

804 Figure 1 – Cold-formed steel walls and bracing of the studs: (a) all steel wall, (b) sheathed wall,
805 (c) sheathed single stud, (d) schematic of stud with springs as bracing at fastener locations, (e)
806 detail of springs bracing the stud cross-section.
807

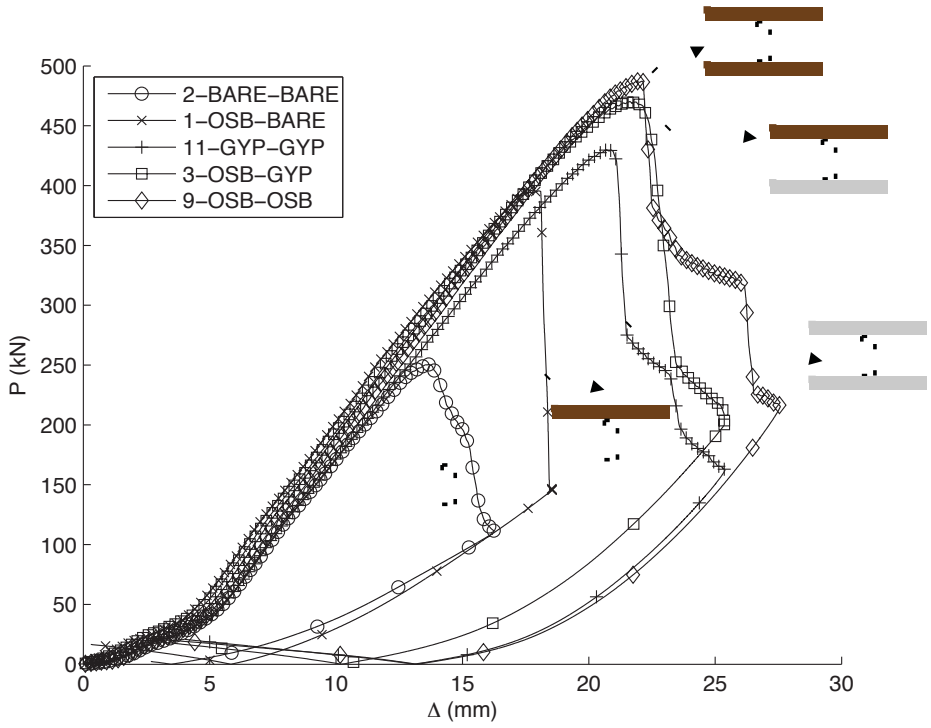

808

809 Figure 2 – P-Δ curve of full-scale walls comparing different sheathing combinations (note, Δ is
810 overall axial machine displacement, i.e. change in actuator position)

Figure 3 – Tests of sheathed cold-formed steel stud walls under compression: (a) side view of wall in MDOF testing rig before testing; (b) and (c) PT sensors for measuring stud deformations; (d) Gyp-Gyp wall opened after test to show local buckling at the ends; (e) local buckling tearing gypsum board; (f) flexural-torsional buckling of unsheathed Bare-Bare wall; local buckling (g) at the top of OSB-OSB wall, (h) at the bottom of OSB-Gyp wall, (i) followed by distortional buckling on Gyp-Gyp wall.

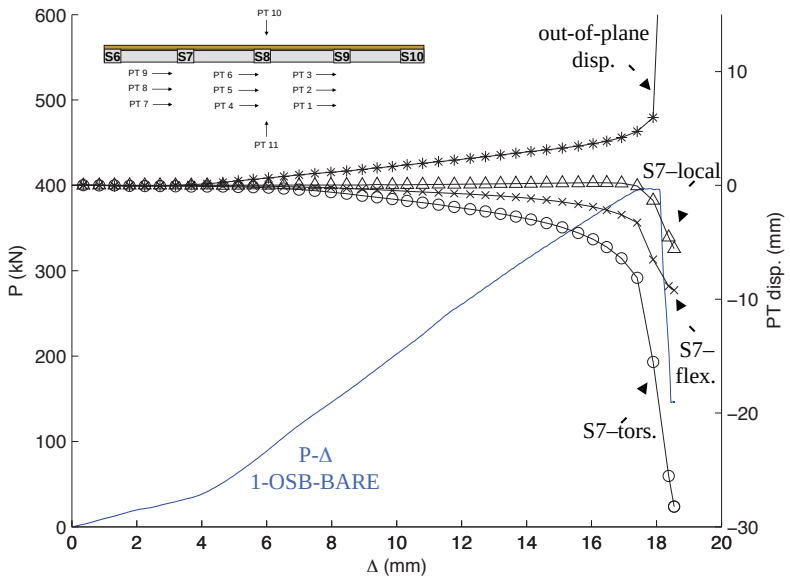

819

820 Figure 4 – Measured PT displacements and axial load vs. axial machine displacement for wall 1-
821 OSB-BARE, note dominance of torsion in response
822

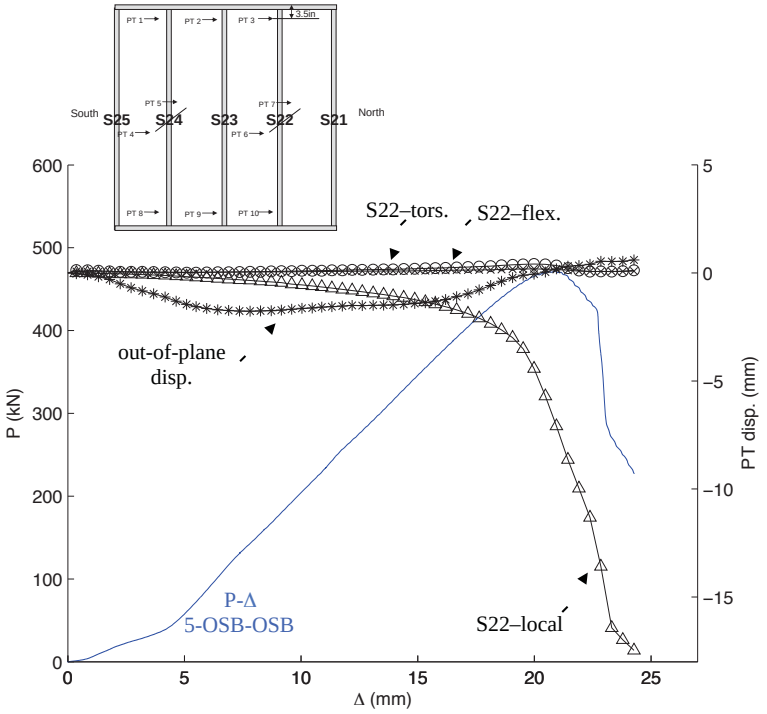

823

824 Figure 5 – Measured PT displacements and axial load vs. axial machine displacement for wall 5-
825 OSB-OSB, note dominance of local buckling in response
826

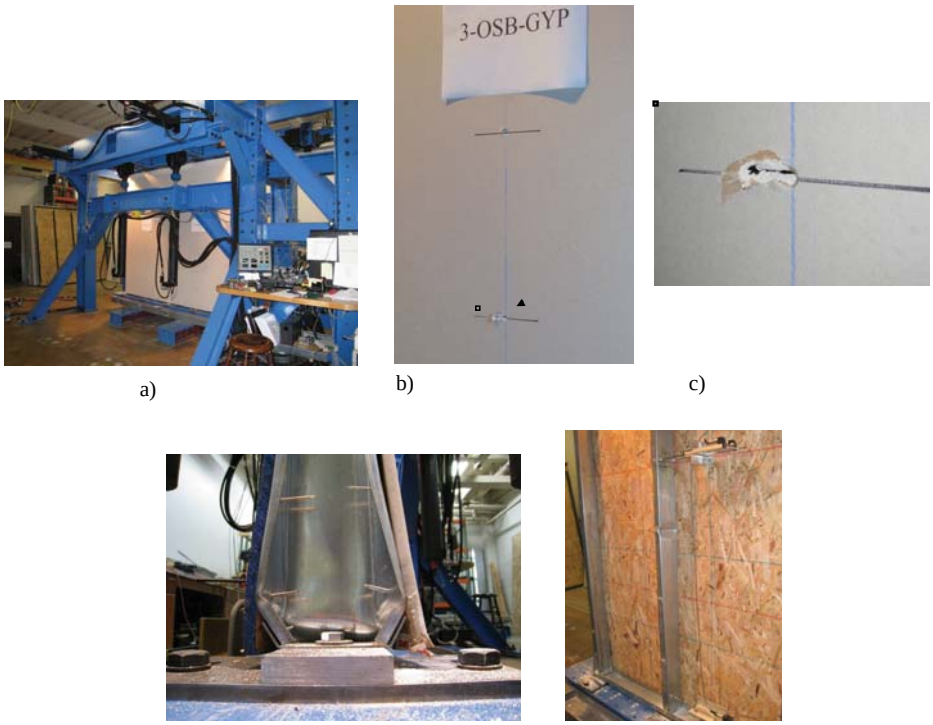

827

828 Figure 6 – Response of specimen 3-OSB-Gyp: (a) side view; (b) bearing failure / screw tearing
829 out board; (c) close-up view of bearing failure; (d) local buckling; (e) wall opened after test.
830

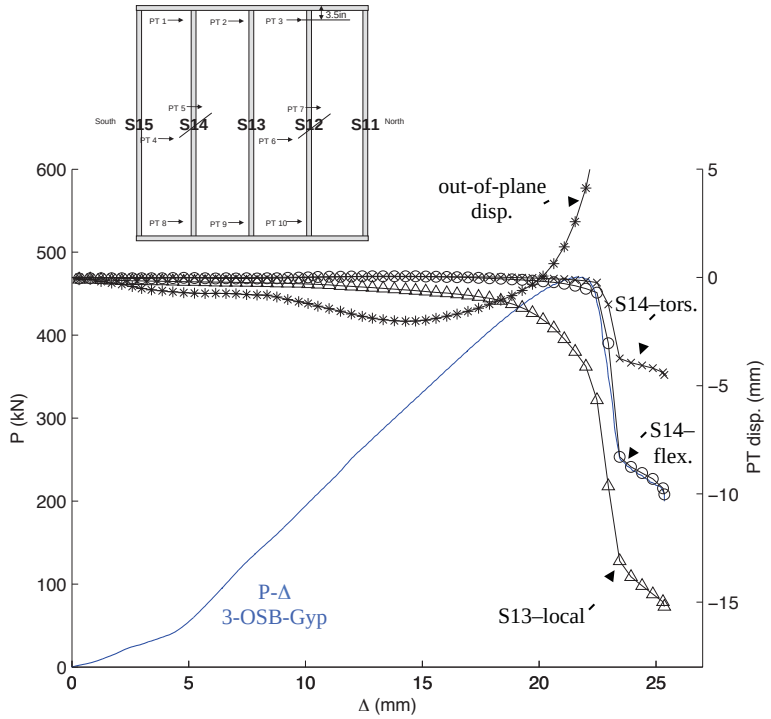

Figure 7 – Measured PT displacements and axial load vs. axial machine displacement for wall 3-OSB-Gyp, note dominance of local buckling and presence of other modes

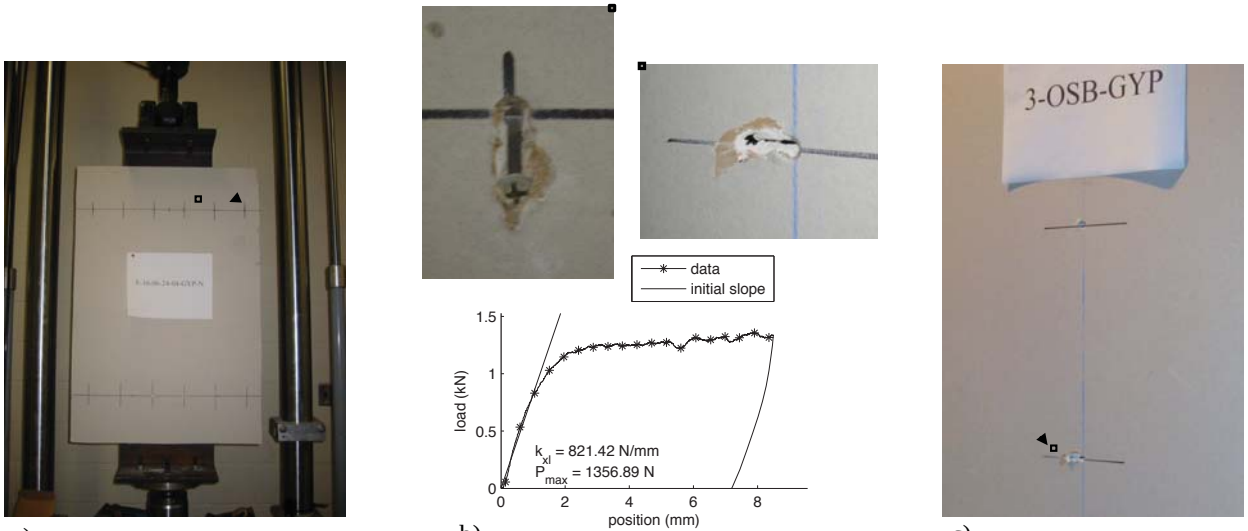

a) b) c)

Figure 8 – Small scale test for local lateral stiffness: (a) test setup with gypsum sheathing, (b) load-displacement response, local lateral stiffness (per fastener $k_{x\ell}$ = 821.42/2 = 410.71N/mm, and peak load (per fastener P_{max} = 1356.89/4 = 339.23N), (c) similarity in bearing failure for full-scale wall with dissimilar sheathing and small scale test for local lateral stiffness.

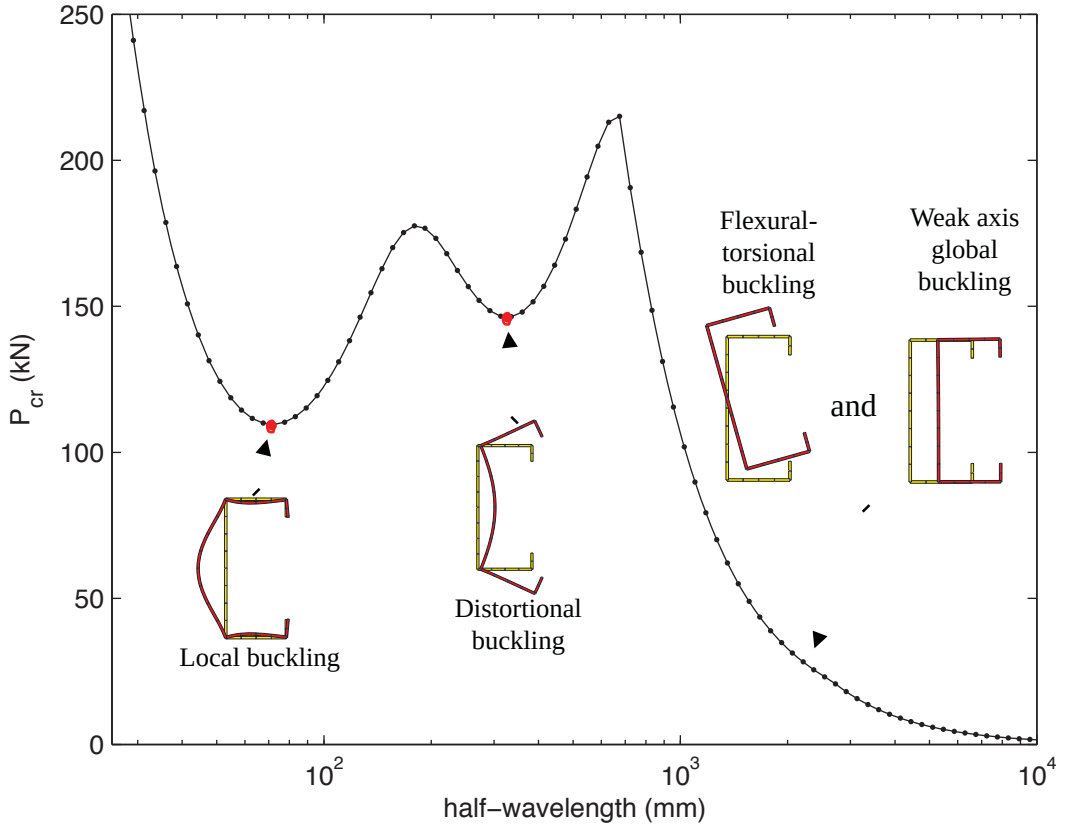

841

842 Figure 9– Buckling curve and modes for pin-pin, unrestrained 362S162-68 cross-section. (Note,
843 dimensions as cataloged (SSMA 2001) except thickness as measured: 1.665 mm (0.0655 in.)).
844

845

846

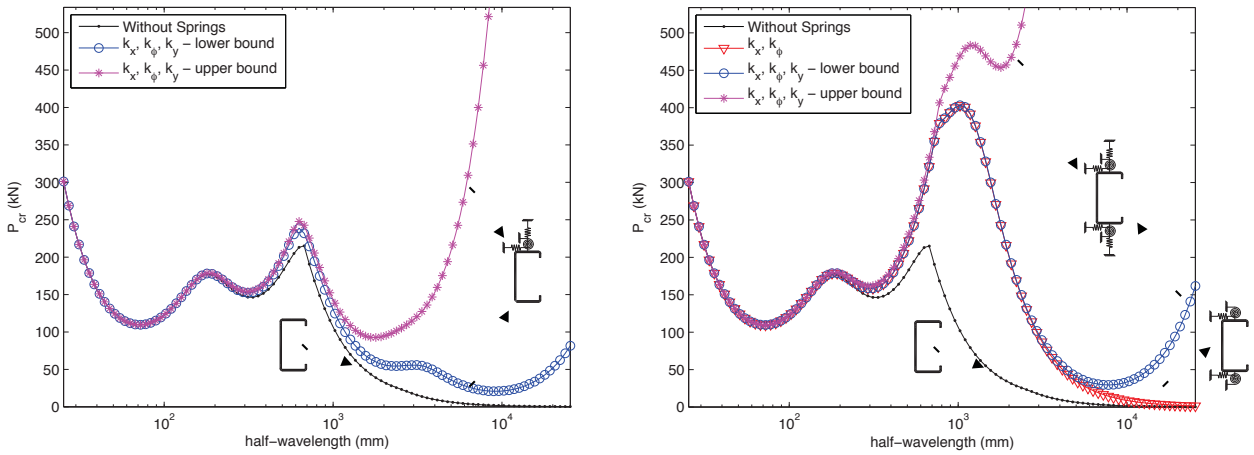

847

848 Figure 10 – Comparison of buckling curves for studs with bracing (spring) restraints: (a) springs
849 on one flange only (i.e., OSB-Bare); (b) springs on both flanges (OSB-OSB).
850

851

852

853

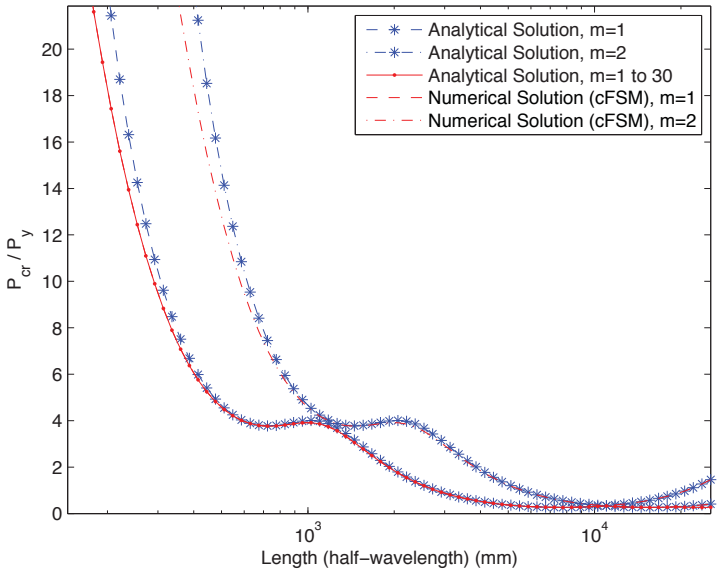

a)

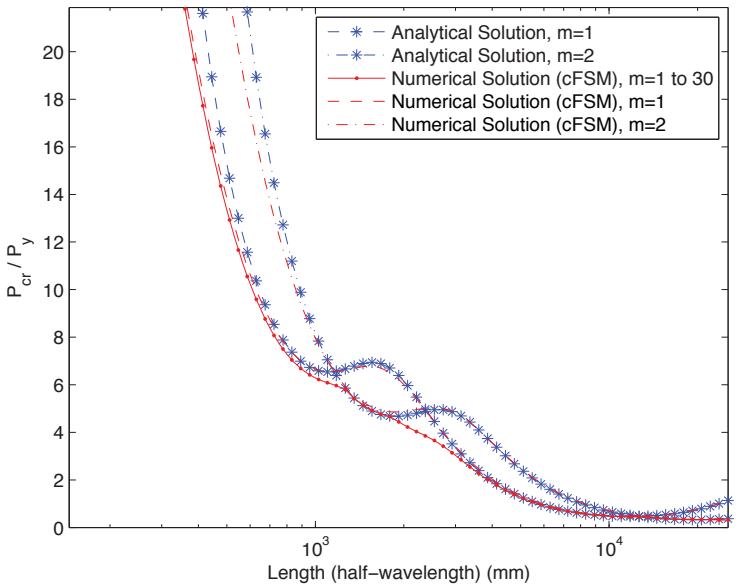

b)

Figure 11 – Comparison between numerical and analytical solution for global buckling of a 362S162-68 column with OSB-OSB springs (Table 2): (a) simply-supported boundary conditions, (b) fixed-fixed boundary conditions (K_x=K_y=K_t=0.5 for m=1, K_x=K_y=K_t=0.7 for m=2, and $K_{x,spring}$=$K_{y,spring}$=$K_{t,spring}$= $\sqrt{3}/2$ =0.866 for all m)

859

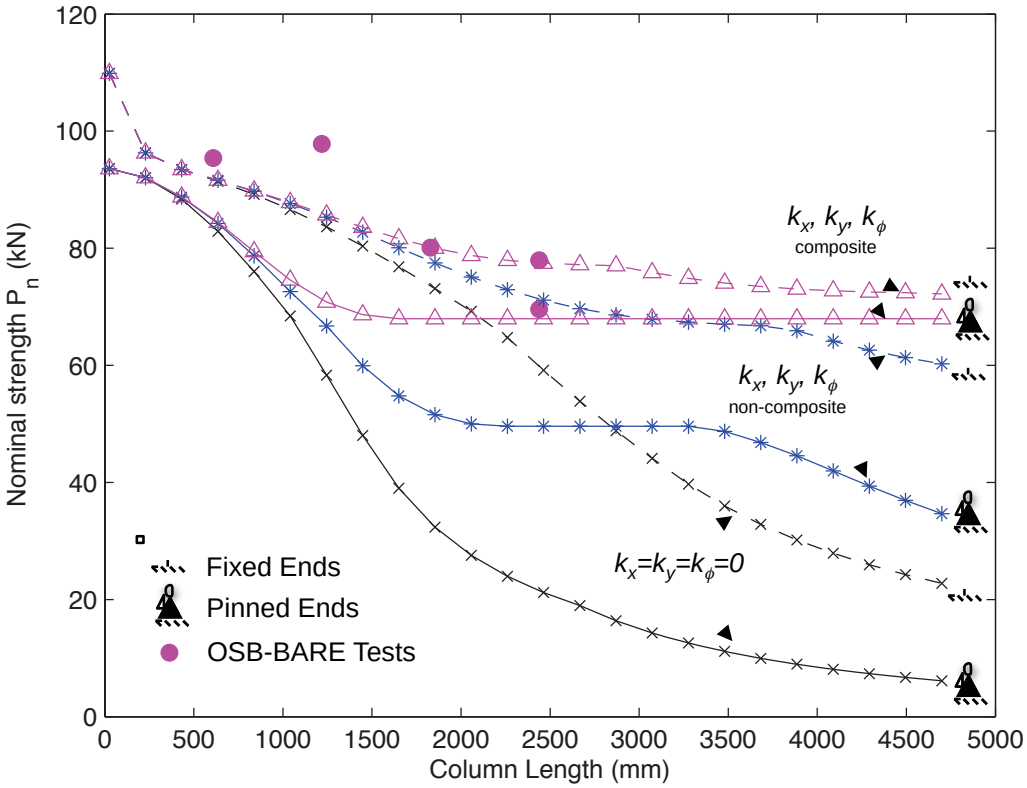

860

861 Figure 12 – Comparison of test results on one-sided (OSB-Bare) sheathed studs with proposed
862 design strengths as a function of end conditions and assumptions about bracing (spring) restraint
863 provided by the sheathing (i) ignored k_x=k_y=k_ϕ=0, (ii) non-composite k_y, and (iii) composite k_y
864

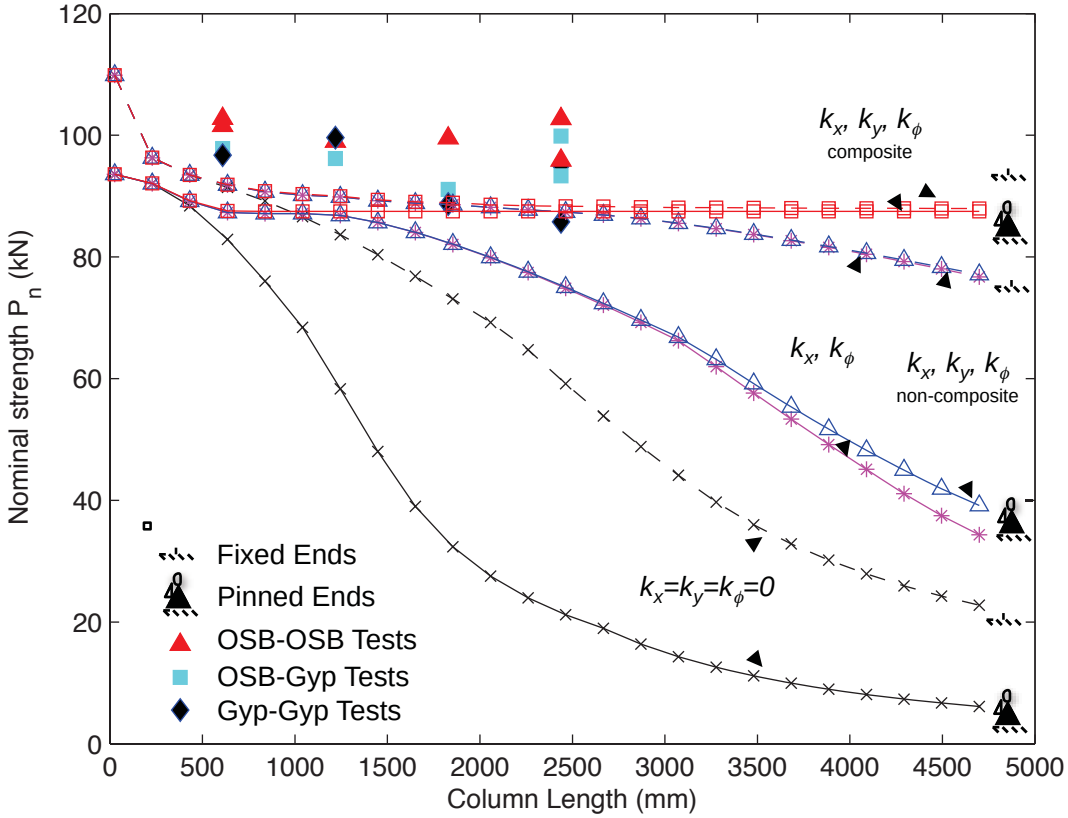

865

866 Figure 13 – Comparison of test results on two-sided (OSB-OSB, OSB-Gyp, Gyp-Gyp) sheathed
867 studs with proposed design strengths as a function of end conditions and assumptions about
868 bracing (spring) restraint provided by the sheathing (i) ignored k_x=k_y=k_ϕ=0, (ii) in-plane only k_x
869 and k_ϕ as appropriate, (iii) in-plane and non-composite k_y, and (iv) in-plane and composite k_y
870
871

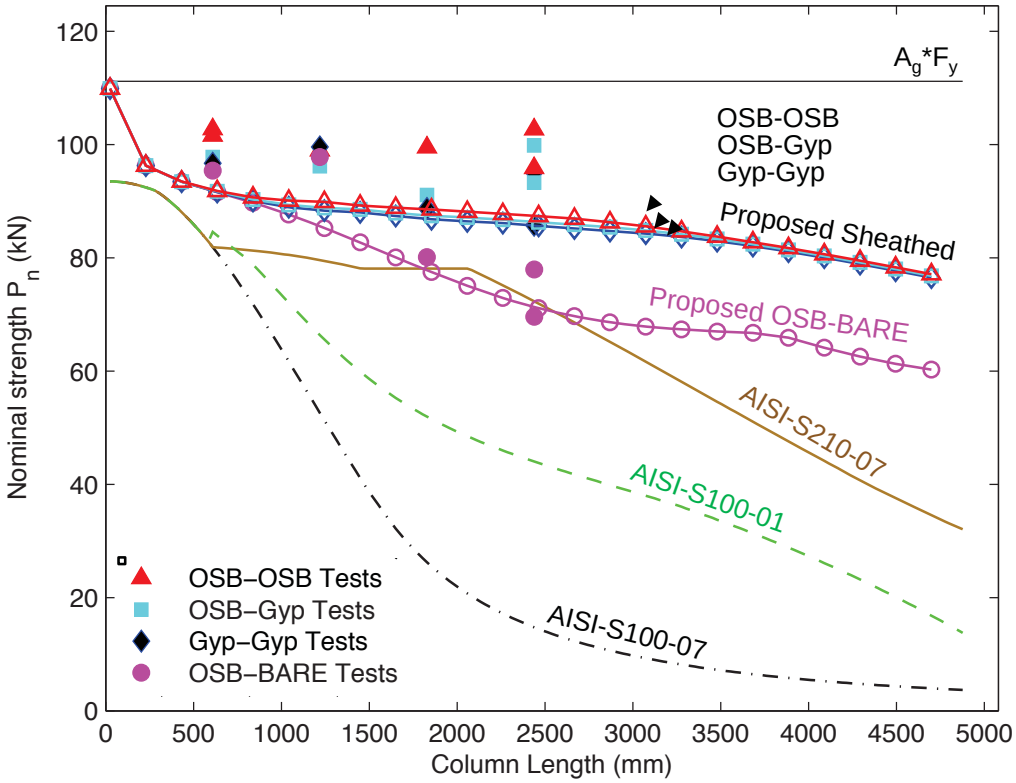

872

873 Figure 14 – Comparison of test results to former, current and proposed design methods
874

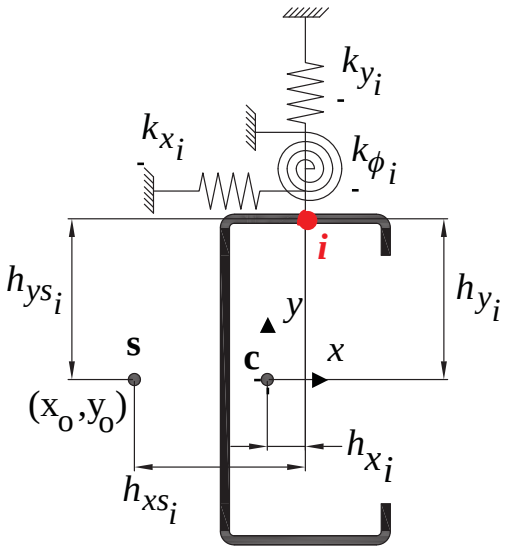

875

876 Figure 15 – Coordinate system and nomenclature for spring *i* on a stud
877

Appendix: Peterman, K.D., Schafer, B.W. "Sheathed Cold-Formed Steel Studs Under Axial and Lateral Load." Submitted to *Journal of Structural Engineering* (Submitted 2 January 2013).

Sheathed Cold-Formed Steel Studs Under Axial and Lateral Load

K.D. Peterman[1], B.W. Schafer[2]

1. Graduate Research Assistant, Department of Civil Engineering, Johns Hopkins University, Baltimore MD, USA <kdpeterman@gmail.com>
2. Professor and Chair, Department of Civil Engineering, Johns Hopkins University, Baltimore MD, USA <schafer@jhu.edu>

Abstract

This research aims to identify and characterize the behavior of dissimilarly sheathed, load bearing, cold-formed steel studs under axial and lateral load. A series of tests on single studs, set in track, and sheathed with either oriented strand board, gypsum board, or combinations thereof are completed. The tests approximate the behavior of a sheathed stud, within a larger wall. In each test a pre-determined level of axial load (or displacement) is introduced into the stud and a lateral load is then applied until failure. This configuration results in axial load, bending, and (potentially) torsion on the stud. Observed failure modes for studs sheathed on only one face include torsion and/or fastener pull-through. For studs sheathed on both faces, failure modes include torsion, local buckling, fastener pull-through, and bearing (particularly for gypsum sheathed studs). Analysis of the torsional response indicates the important role of the sheathing in limiting torsion and in determining the demands on the member and fastener. The observed member limit states compared favorably with the Direct Strength Method of design even when direct torsion is not explicitly considered. New models for strength prediction in the connection limit states are explored. A model based on the torsional capacity of the fastener-sheathing system limited by first failure in either pull-through or bearing provides the best agreement with the observed testing. Recommendations for design are provided.

Introduction

Cold-formed steel (CFS) members are widely used in light-framed construction for both structural (load bearing) and non-structural members. Vertical CFS members (studs) are commonly capped in horizontal members (track) and sheathed in wood or gypsum board to frame the walls. For partition (non-structural) walls it is common practice to rely on the sheathing to provide bracing for the CFS studs. For structural walls, typically steel bridging running through holes in the studs provide the required flexural and torsional bracing. Recently, Vieira and Schafer (2012) explored the use of sheathing to supply bracing to structural studs and demonstrated that oriented strand board (OSB) or gypsum board can provide sufficient bracing to axially loaded studs. This research extends that work to sheathed walls with lateral as well as axial loads applied.

Research in the behavior of sheathed CFS stud walls under axial load originated with Winter (e.g., Green et al. 1947) and focused on determining the stiffness that sheathing could supply to a stud to restrict weak-axis flexural buckling. This work was followed by examinations of the role of sheathing shear stiffness (Simman and Pekoz 1976) and the use of gypsum and plaster board for bracing the studs (Miller and Pekoz 1993,1994, Lee and Miller 2001, Telue and Mahendran 2001). Vieira and Schafer (2013) demonstrated that sheathing supplies a local restraint (dominated by deformations at the fastener) and a shear diaphragm restraint (dominated by the shear modulus of the sheathing material) to the stud, and that if these restraints are properly incorporated into the elastic buckling analysis of the stud accurate strength predictions using the Direct Strength Method result.

Research on sheathed CFS structural stud walls under out-of-plane lateral load has seen relatively little study; however, the role of sheathing in restraining CFS floor joists has long been

studied (e.g., Winter 1960, Schafer et al. 2009) and is strongly related to the performance of walls under lateral load. Characterizing the stiffness of the sheathing as it fully or partially restrains torsion of the joist, due to the fact that in C-sections (e.g. studs or joists) the shear center and lateral load are not aligned, is the key issue in this previous work. Recent research on CFS stud walls under lateral load has been focused primarily on the unique problems associated with blast (Salim et al. 2005, Aviram et al. 2012) and is not the focus here. Work on CFS stud walls under combined axial and lateral load has seen limited study for a specialized CFS section (Pham et al. 2006), but no general methods developed. It is worth noting that extensive work has been conducted on in-plane laterally loaded walls, i.e., CFS sheathed shear walls, including combined axial and shear tests; however, this mode of behavior is not the focus of the work here.

This paper begins with an overview of the setup for the conducted experiments on sheathed CFS stud walls under axial and lateral load. This is followed by analysis of the experimental results focusing on the observed limit states and capacities, the member end conditions, and the lateral load application point. This is followed by torsional analysis of the assembly to determine the relative torsion between the stud and the fastener-sheathing system. Next, prediction methods for the member limit states and connector limit states are explored. In the case of connector limit states new methods are developed and compared to the experiments. The paper concludes with a discussion of extensions to distributed lateral loads, and a critical discussion of the developed method for design.

Experimental Setup

Consider an isolated, unsheathed (bare) stud, under axial and lateral load as depicted in Figure 1. The applied loads result in axial force, bending moment, shear, and direct torsion (due to lack of alignment between the lateral load and the shear center of the stud). Thus, although the applied

loads are relatively simple the resulting internal actions can be complicated. For typical end details and stud length, shear does not control and is thus not studied further here; instead, axial force, bending moment, and torsion are the focus.

Previous research on axially loaded stud walls demonstrated that tests on a single stud with a tributary width of attached sheathing and track provides the same capacities and limit states as tests on a full 2.4 x m 2.4 m [8 ft x 8 ft] wall with five studs (Vieira and Schafer 2013). Therefore, a single stud, with a tributary width of sheathing and track was employed for the combined axial plus lateral load tests conducted here. However, special attention was paid to the ends of the track and their connection to the testing rig as the track plays an important role in resisting the bending and torsion that results from the laterally applied load.

As illustrated in Figure 2, the test specimens consisted of a 2.4 m [96 in.] long 362S162-068 (AISI-S200 (2007) nomenclature) stud, with average dimensions and properties as reported in Table 1, connected to 0.6 m [24 in.] long 362T125-068 track at top and bottom. The track bears on three 19 mm [¾ in.] thick plates, 152 mm [6 in.] long, and 92 mm [3 5/8 in.] wide - the same width as the web of the track, thus insuring the sheathing cannot bear against the plates or testing rig. At mid-length the track is bolted to the 19 mm [¾ in.] plate with a 15.8 mm [5/8 in.] bolt. The track ends are blocked and clamped over a 76 mm [3 in.] length between two 19 mm [¾ in.] plates to restrict twist.

The entire specimen is mounted in a multi degree of freedom wall testing rig (see Vieira 2011 for full details). The top beam of the rig is actuated and provides axial load to the specimen. A 152 mm [6 in.] diameter circular bar is affixed to an actuator and supplies a mid-height lateral load on the specimen. Loading is performed in displacement control at a typical rate of 1.2 mm/min [0.047 in./min] slower rates are used near peak capacity.

Where desired sheathing is attached to the stud and track as detailed in Figure 2b. The sheathing utilized includes 11 mm [7/16 in.] oriented strand board (24/16 rated, exposure 1), and 12.7 mm [1/2 in.] gypsum board (sheetrock). The boards were stored in the laboratory with an average humidity of 56% and temperature of 22°C (71°F) over 102 days. Simpson Quikdrive No. 6 x 41 mm [1⅝ in.] fasteners were used for attaching gypsum to the stud while Simpson Quikdrive No. 8 x 49 mm [1 $^{15}/_{16}$ in.] were used for attaching the oriented strand board (OSB).

Seven different sheathing combinations were tested: OSB-OSB (OO), gypsum-gypsum (GG), OSB-gypsum (OG), gypsum-OSB (GO), OSB-bare (OB), and bare-OSB (BO). In the nomenclature used herein, the second letter signifies the laterally loaded face of the specimen (e.g., a GO specimen is loaded on the OSB side). It should be noted that in specimens left bare (B) on the laterally loaded face, the lateral load is then applied directly to the stud.

Vieira et al. (2012) provide results for a similar specimen setup under axial load alone. Here we find the lateral load that causes failure given an applied axial load of 10%, 40%, 60%, or 80% of the axial-only capacity, for the seven different sheathing combinations. Complete details of the test setup including measured drawings of the end details, sensor locations and numbering, as-measured dimensions of all stud and track, imperfection measurements, etc. are provided in Peterman (2012).

Experimental Results

Peak loads and limit states

The tests were conducted by applying a pre-determined amount of axial load, and then increasing the lateral load until failure occurred. As the tests were typically conducted in displacement control the axial displacement (not load) was held constant during the lateral load application;

however in two tests the axial load was maintained. The difference in the two loading protocols and the resulting response is provided in Figure 3. Under lateral load the member shortens slightly and a constant axial displacement test results in a slowly decreasing axial force. Regardless of the selected protocol, a failure point, in terms of axial force and lateral force, is established for each specimen.

A summary of the tested capacities and observed limit states for the twenty-seven specimens is provided in Table 2 along with the previously conducted axial-only tests on similarly detailed specimens. The peak results are plotted in terms of lateral peak load vs. axial peak load for the seven different sheathing configurations in Figure 4. The presence of sheathing leads to a clear increase in capacity for all combinations of axial and lateral load, with bare (BB) and one-sided sheathed specimens (BO and OB) being the weakest. For the two-sided specimens with similar sheathing gypsum (GG) is considerably weaker than OSB (OO) and the difference is greatest in bending dominated (low axial load) cases. For the two-sided specimens with dis-similar sheathing it is superior to have the loaded face with OSB (GO) as opposed to the loaded face with gypsum (OG), and this difference is again greatest in bending dominated cases.

Examples of the limit states highlighted in Table 2 are provided in Figures 5 and 6. Figure 5 provides the member limit states: torsion for the bare and one-sided sheathed specimens, and local buckling (combined with yielding) for the OO and most of the GO and OG specimens. Figure 6 provides the connection limit states: pull-through for the fasteners on the laterally loaded face and bearing for the fasteners on the non-loaded face. Fastener limit states were particularly pronounced in the gypsum sheathed specimens (i.e., GG, GO, OG).

Member end conditions

To accurately resolve the applied lateral load (H) into moment in the specimen, it is necessary to characterize the end conditions for strong-axis bending. The intent of the detailing of the track end condition is to simulate a stud in a complete wall system and the expectation, after previously conducted axial testing (Vieira et al. 2012, Vieira and Schafer 2013), was that this would supply fixed ends. Although the intent was met and the authors believe the stud-to-track-to-sheathing end condition is close to field conditions, the expectation of fixed end conditions in strong-axis flexure was not met.

The measured horizontal force (H) and mid-height displacement (δ) is compared against theoretical fixed, pinned, and semi-rigid solutions in Figure 7. For the semi-rigid end conditions the stud strong-axis rotational end restraint is provided by the torsional stiffness of the short segment of track with either warping free or warping fixed ends. The track is torsionally weak, with warping free end conditions for the track the mid-height moment is 99% of the pinned case, with warping fixed end conditions for the track the mid-height moment is 95% of the pinned case. As Figure 7 illustrates, for all practical purposes, due to the torsionally weak track, the boundary condition for major-axis bending of the stud is pinned.

Lateral load location

As illustrated in Figure 8, load eccentricity from the shear center, e, changes as the stud twists. Experimental evidence based on scoring of the load bar against the specimen (Figure 8b) shows the point of load application moving from approximately mid-flange to the edge of the flat width of the flange as the twist progresses. As detailed in Figure 8c, for small but finite twist the distance from the shear center to the termination of the corner radius (e = 23.1 mm [0.91 in.]) is utilized in this work. This e is an approximation. The exact e depends on the specific cross-

160 section and construction details; further, the cross-section does not remain rigid as it twists, and
161 in addition the load application does not follow the twist of the stud, therefore the resulting
162 eccentricity decreases as the stud twists. Nonetheless, an estimate of *e* is necessary for exploring
163 the torsional demands.

164 **Torsional Response and Analysis**

165 For an unsheathed (bare) stud loaded laterally (with *H)* eccentric from the shear center
166 (by a distance *e*) the torsional demand (*He*) is distributed as shown in Figure 1. Warping restraint
167 provides the primary torsional resistance of the stud. This warping restraint creates additional
168 longitudinal (σ_w) and shear stresses in the cross-section. For a known bimoment (*B*) these
169 longitudinal warping stresses are found from:

170 $$\sigma_w = B\omega / C_w \quad (1)$$

171 where ω is the sectoral coordinates, C_w is the warping torsion constant, and *B* is the bimoment.
172 The distribution of σ_w is proportional to ω and is provided for the as-measured 362S162-68
173 cross-section in Figure 9a. The distribution of σ_w is static, but scales with *B*, which may be
174 determined from appropriate differentiation of the twist, or more generally is available in
175 numerical beam finite element solutions.

176 For a sheathed stud it is typical in design to assume that the fastener-sheathing system
177 will supply full torsional resistance to the stud. Thus, it is assumed that the stud does not twist,
178 the bimoment is zero, and the fasteners carry the full torsional moment. However, in the
179 experiments the studs experienced finite torsion (Peterman 2012 provides detailed
180 measurements) most noticeably in the specimens sheathed on one-side only, but also in the two-
181 sided sheathed specimens.

To assess the relative sharing in resisting the applied torsion a structural analysis model is created in MASTAN using 14 DOF beam finite elements capable of incorporating warping torsion (McGuire et al. 1999). The 362S162-68 stud is modeled as warping continuous along its height and warping fixed at its end. Rotational springs of stiffness k_θ are included in the model every 305mm [12 in.] to simulate the fastener-sheathing restraint. A torque is applied at mid-height, and the resulting torsional moment diagram and torsion in the springs (fasteners) are summarized in Figure 10a-d as a function of the fastener-sheathing stiffness k_θ. The limits are clear: for small k_θ the stud twists significantly, develops a large bimoment (and related stresses) at mid-height, and sees little of the torsion carried by the springs (fasteners); for large k_θ the stud twist is limited, the bimoment (and related stresses) are smaller, and the applied torsion is carried directly in the springs (fasteners). For realistic spring (fastener-sheathing) stiffness the behavior falls somewhere in between these ideal limits.

The member and fastener-sheathing attachments relevant for resisting torsion are summarized in Figure 9b and c. The primary resistance comes from bearing and the associated lateral springs k_{x1} and k_{x2}. Pull-through and its related torsional resistance is determined from a rotational restraint test, and $k_{\phi 1}$ and $k_{\phi 2}$ incorporate this resistance. The equivalent rotational spring, k_θ, for the fastener-sheathing system is:

$$k_\theta = k_{\phi 1} + \tfrac{1}{4} k_{x1} d^2 + k_{\phi 2} + \tfrac{1}{4} k_{x2} d^2 \quad (3)$$

The stiffness provided to the stud by the fastener-sheathing combinations are known from experiments: for OSB k_x = 971 N/mm [5.52 kip/in.] and k_ϕ = 95309 N-mm/rad [0.84 kip-in./rad] and for gypsum board k_x = 427 N/mm [2.43 kip/in.] , and k_ϕ = 95987 N-mm/rad [0.85 kip-in./rad]. See Vieira and Schafer 2013 for a summary, Vieira and Schafer 2012 for details on k_x, and Schafer et al. 2010 and Vieira 2011 for details on k_ϕ.

The stiffness of the sheathing combinations is indicated as vertical lines in Figure 10e. As Figure 10e indicates, one-sided sheathing is relatively ineffective, while two-sided sheathing provides significant, if incomplete, torsional restraint. To more directly gauge the relative effectiveness of the sheathing the member mid-height rotation (θ_{mid}) is estimated from the model. The demand torsion, *He*, is based on the maximum observed *H* for each sheathing type. For the bare case (BB) θ_{mid} is 9.6 deg., for the one-sided sheathing cases (OB, BO) θ_{mid} is a maximum of 10.1 deg., and for the two-sided sheathing cases (GG, GO, OG, OO) θ_{mid} is a maximum of 1.7 deg. at the peak *He* demand.

To explore the expected impact of the warping longitudinal stresses on the cross-section capacity the bending strength reduction ratio, *R*, of AISI-S100 (2012) Section C3.6 is calculated for the various sheathing configurations. *R* is the ratio of the maximum bending stress to the sum of the bending (σ_b) and warping (σ_w) stresses, specifically:

$$R = \frac{(\sigma_b)_{\max}}{|\sigma_b + \sigma_w|} \le 1.0 \tag{4}$$

The ratio is limited to one, as locations where the bending and warping stresses counteract are assumed non-detrimental to the member capacity. From, Eq. (1), and assuming the cross-section is in the *xy* plane, for the general case:

$$R = \frac{My^* / I}{|My / I + B\omega(x,y) / C_w|} \le 1.0 \tag{5}$$

where y^* is the distance to the extreme fiber, and *I* is the moment of inertia. For the specific case of a laterally applied mid-height load, *H*, the moment $M = HL/4$ and the bimoment, *B*, can be determined from analysis (i.e. Figure 10) and is denoted as $B = cHe$ where *c* is the analysis dependent constant and *He* the applied torsion. Note, in this configuration the maximum *B* and *M* both occur at mid-height. For this specific case, Eq. (5) becomes:

$$R = \frac{Ly^{*}/4I}{\left|Ly/4I + ce\omega(x,y)/C_{w}\right|} \leq 1.0 \quad (6)$$

The resulting ratio is independent of H and only a function of the section, length, and bracing.

The bending reduction factor, R, is supplied for all sheathing configurations in Figure 11. For the bare (BB) case the warping stresses are large, and the minimum R = 0.51 indicating the expected bending capacity is 0.51 of the pure bending capacity (ignoring torsion). For one-sided sheathing, (BO, OB) modest relief from torsion is provided, but the minimum R is still 0.64; indicating a strong reduction. For two-sided sheathing the reductions are generally small. For the GG case R is 0.91 in the tension flange and 0.94 in the compression flange. For the OO case R is 0.94 in the tension flange and 0.96 in the compression flange. Longitudinal warping stresses exist in the cases with two-sided sheathing and their absolute magnitude is not small; however, the maximum location at the tip of the lips, (Figure 9a) is not at the location of maximum bending stress, and the reduction ratio R indicates the expected impact is modest. These stress predictions are approximate as they rely on small deflection analysis, ignore cross-section deformations, and utilize relatively coarse estimates of the fastener-sheathing stiffness. Nonetheless, they provide an important relative sense of the importance of the warping torsional stresses and indicate that they are not a primary concern for studs with two-sided sheathing. Design methods for the observed member and fastener limit states are addressed in the following sections.

Capacity Predictions for Member Limit States

The member limit states of local, distortional, and global buckling (with appropriate interactions) are considered in assessing the member capacity. As detailed in Vieira and Schafer (2013) sheathing greatly influences global buckling, modestly influences distortional buckling, and has

249 little influence on local buckling (due to its short buckling wavelength). To specifically assess
250 the influence of the sheathing, the stiffness supplied from the fastener-sheathing combination
251 must be known and included in an elastic stability analysis of the member.

252 The cross-section model including the fastener-sheathing springs of Figure 9b is utilized
253 in an elastic buckling finite strip analysis. The lateral and rotational springs k_x and k_ϕ are provided
254 in the previous section, for OSB k_y = 0.374 N/mm [0.0021 kip/in.], and for gypsum, k_y = 0.087
255 N/mm [0.00049 kip/in.]. The stiffness values are derived for the specific fastener-sheathing
256 combinations and may be determined experimentally (stiffness determined at 40% of ultimate),
257 or using closed-form lower bound solutions as discussed in Vieira and Schafer (2013). The
258 lower-bound, non-composite action stiffness is employed for k_y. The per fastener values are
259 divided by the tributary width of the fasteners (305 mm [12 in.]) to convert from spring stiffness
260 to foundation stiffness values $\underline{k}_x$, $\underline{k}_y$, and $\underline{k}_\phi$ which are then used in the finite strip analysis.

261 Elastic buckling analysis for pure compression and pure bending is completed for the
262 finite strip model in CUFSM (Li and Schafer 2010). The local (ℓ), distortional (d), and global (e)
263 buckling loads in compression (P_{cr}) and bending (M_{cr}) are provided in Table 3. With the elastic
264 buckling values known the nominal strength (P_n and M_n) may be predicted using the Direct
265 Strength Method formulation of AISI-S100 (2007) Appendix 1. Assuming a simple linear
266 interaction (as employed in AISI-S100) and ignoring second order-effects the nominal capacity
267 is compared to the tests via:

268
$$\frac{P}{P_n}+\frac{M}{M_n}\le 1 \overset{M=HL/4}{\rightarrow} \frac{P}{P_n}+\frac{H}{H_n}\le 1 \qquad (7)$$

269 The resulting linear interaction expression, which is dependent on the sheathing type, is
270 compared against the test data in Figure 12.

In comparing the nominal predictions to the tests in Figure 12, first note that the axial-only experimental results are from Vieira et al. (2012), and although the nominal cross-section is the same, the as-measured sections for Vieira's tests were smaller (area and yield stress in Vieira's tests are both 93% of the as-measured specimens reported here) thus the disagreement between the predictions and the tests along the axial-only (vertical) axis are due to this difference in as-measured properties, see Peterman (2012) for further details.

For the remaining sections, which have a combination of axial and lateral load, the predicted member capacities are a conservative approximation of the observed capacities. The strength prediction for studs sheathed on one-side demonstrates sensitivity of the method to the sheathing details, the BO case where the fastener-sheathing is connected to the compression flange provides far greater bending capacity than the OB case. However, while the experimental results provide a clear difference between the GO, OG, GG, and OO cases the design method does not and instead predicts essentially all two-sided sheathing cases are able to develop the moment at first yield, (i.e. $M_n = M_y$). It is worth noting that the GG case is unconservatively predicted for bending dominant response; indicating a need to consider fastener limit states in addition to member limit states.

Capacity Predictions for Connector Limit States

As discussed in the Torsional Analysis and Response section, it is typical to assume in design that the full torsional demand (*He*) is carried by the fasteners. However, for practical fastener-sheathing stiffness the demand on the fasteners is typically less than *He*. As Figure 10 shows, for two-sided sheathing, the demand is around 0.4*He*. The exact torsional demand on the fasteners may be determined by a torsional analysis model, similar to that of Figure 10.

293 The torsional demand is carried by the fasteners in a combination of bearing and pull-
294 through resistance as depicted in the free-body diagram of Figure 9c. Specifically, if subscript "*i*"
295 refers to face 1 and 2, the pull-through resistance supplies a torsional resistance (T_{pt}) as the
296 section undergoes twist θ of:

297 $$T_{pti}(\theta) = k_{\phi i}\theta$$

298 which has a maximum value based on the pull-through capacity (P_{pt}) that occurs at θ_{pt}:

299 $$(T_{pti})_{\max} = P_{pti}(b/2) = k_{\phi i}\theta_{pti}$$

300 The torsional resistance developed from the bearing mechanism (T_{br}) as a function of twist is:

301 $$T_{bri}(\theta) = k_{xi}\left(d^2/4\right)\theta$$

302 which has a maximum value based on the bearing capacity (P_{br}) that occurs at θ_{br}:

303 $$(T_{bri})_{\max} = P_{bri}(d/2) = k_{xi}\left(d^2/4\right)\theta_{bri}$$

304 Two models for the torsional capacity are considered. The first model (T_1) assumes the capacity
305 of the fastener-sheathing system is based on first failure in either pull-through or bearing, on
306 either face:

307 $$\theta_f = \min\left(\theta_{pt1}, \theta_{br1}, \theta_{pt2}, \theta_{br2}\right)$$

308 $$T_1 = T(\theta_f) = T_{pt1}(\theta_f) + T_{br1}(\theta_f) + T_{pt2}(\theta_f) + T_{br2}(\theta_f)$$

309 The second model (T_2) is based on fully ductile failure response in the fastener-sheathing system,
310 and thus based on the maximum strength:

311 $$T_2 = (T_{pt1})_{\max} + (T_{br1})_{\max} + (T_{pt2})_{\max} + (T_{br2})_{\max}$$

312 Strength in bearing (P_{br}) and pull-through (P_{pt}), unfortunately, is not generally available.
313 Bearing strength's upperbound is the screw shear strength, which is available from
314 manufacturers, but bearing is governed by the sheathing and fastener size. Average experimental
315 bearing strength (P_{br}) from lateral stiffness tests reported in Vieira and Schafer (2012) are 2570
316 N [578 lbf] for a #8 in OSB and 380 N [86 lbf] for a #6 in gypsum. Pull-through strength's
317 upperbound is the screw tensile strength, also available from manufacturers (but essentially
318 irrelevant), as pull-through is governed by the sheathing and the fastener head details. Pull-
319 through capacities can be determined from the failure load in a rotational restraint test (e.g., per
320 AISI-TS-1 (2002)) test. The tests detailed in Vieira and Schafer (2012) only provide the stiffness,
321 the data was revisited as detailed in Peterman (2012), and the average pull-through capacity (P_{br})
322 determined as 1944 N [437 lbf] for a #8 in OSB and 178 N [40 lbf] for a #6 in gypsum.
323 Utilizing the preceding formulation, torsional capacity for models T_1 and T_2 are provided
324 for the different sheathing configurations in Table 4. To compare against the tests the torsional
325 capacity must be converted to lateral capacities H_1 and H_2. This may be done either by the
326 typical design assumption that all of the torsion is borne by the fasteners, $T = He$, or by a torsion
327 analysis (i.e. Figure 10) which results in a reduced torsion demand, $T = rHe$, where r is
328 determined from the analysis and is approximately 0.4 for two-sided sheathing cases. Per Table
329 4, assuming the full torsion demand is borne by the fasteners ($T = He$) leads to unrealistically
330 low fastener limit state strength, regardless of whether first failure (T_1) or maximum capacity
331 (T_2) is employed. A torsional analysis is necessary for determining the proper demand.
332 For similarly sheathed specimens GG or OO first failure (T_1 or H_1) and maximum
333 capacity (T_2 or H_2) provide similar strength. For dis-similarly sheathed specimens GO or OG the
334 gypsum fails much earlier than the OSB and the two models diverge. As Table 4 shows first

failure (T_1 or H_1) occurs in the gypsum at 1.1 deg. while the OSB does not fail until 24 deg.. Experimental observation of the limit state is more consistent with the first failure model (T_1 or H_1), i.e., failure in the gypsum is equivalent to failure of the specimen.

The predicted capacity for the model based on first failure (T_1 or H_1) utilizing the analysis-based torsional demand ($T = rHe$) is provided in Table 4 and compared across all tests and against the member limit states in Figure 12. This model predicts that connector limit states will not control for the BO, OB, or OO sheathed cases. However, connector limit states may control in the gypsum sheathed cases GG, GO, or OG. As Figure 12 illustrates the connector limit state is dominant under moderate bending demands in the GG case, but only controls for high bending demands in the GO and OG case. The experiments indicated that the GG case was controlled by connector limits both in terms of observed limit states and capacity. The resulting failure surface (minimum of the member and connector limit states) provides a rational progression in its results and is qualitatively similar to the test results.

Discussion

Extension to distributed lateral loads

The most common design case for a sheathed stud under axial load and bending is for a distributed lateral load as opposed to the point load studied here. A torsion analysis, similar to that described in the Torsional Analysis and Response section (Figure 10) was conducted to provide preliminary findings for this case. The results are provided in Figure 13. Figure 13e compares the earlier results for the point torque (He) directly to the distributed torque (He/L). The distributed torque allows more fasteners to be involved in resisting the twist and the results are far more effective. For the same total torque the case with the distributed torque twists less,

has lower bimoment (and hence lower warping stresses), and more evenly distributes the demand to the fasteners compared with a point torque. This is a promising finding, as it suggests that a torsional stiffness analysis may not be required for design under distributed loads, instead it is satisfactory to assume the fasteners see their full tributary demand, and that the warping stresses can be ignored. These assumptions would greatly simplify design.

Recommendations for Design

The method explored for checking the member limit states is relatively sophisticated: all three buckling classes are explored and the role of sheathing is explicitly included in the elastic stability analysis. However, it is also approximate: direct torsion stresses are ignored, shear stress are ignored, stability analysis is only conducted for pure compression or pure bending not for the actual combined stress states, second-order effects are ignored, inelastic reserve in bending is ignored, and composite action in bending is ignored. Despite these crude simplifications the results are useful in a practical sense as the method incorporates the essential increase in strength that occurs for a sheathed specimen – note the capacity increases 107% in pure bending from the unsheathed case to the sheathed on both sides case. Even without direct torsional stresses incorporated the weakness of the section in torsion is included through the stability analysis. Also, the explored design method does not rely on tools or analysis currently unavailable to design engineers. Until a more fundamental and detailed prediction method is developed the approach provided here is recommended for design against the key member limit states in a sheathed stud.

In the method developed for exploring the connector limit states the fasteners are designed only against the direct torsional demand, not the second-order forces from bracing the member. This is based on the assumption that the direct torsional demands are greater. This is

supported by the axial tests of Vieira and Schafer (2013) that do not exhibit fastener limit states. A more advanced method would include contributions both from second-order forces (dependent on bracing stiffness and different for axial and bending) as well as the direct torsional forces considered here. Alternative mechanisms for resisting torsion were explored in Peterman (2012), only the most promising models were summarized here. Despite the significant simplifications utilized here the developed connector limit state model is found to usefully predict the potential for connector limit states in the tests.

The recommended procedure for design of a sheathed stud wall under axial and bending is as follows. First determines the stiffness and strength of the fastener-sheathing system that will be providing resistance to the stud. Preferably this is done by test, or alternatively using simplified closed-formed solutions (see Vieira and Schafer 2013 for a summary). Second, the member stability in local, distortional, and global buckling must then be assessed. Preferably this is done by computational analysis (e.g., CUFSM), or alternatively closed-form solutions are available, but may be involved (e.g., see Vieira and Schafer 2013). Third, the member stability analyses are used to assess the member limit states using either effective width or Direct Strength Method approaches. Direct Strength Method is followed herein. Direct torsion was not considered in the member limit state analyses performed herein, but is included in the fastener limit states. Fourth, the fastener-sheathing capacities must be determined for pull-through and bearing limit states. The authors were unable to find generally available methods or industry reported values for these limit states and thus instead relied on our own direct testing (see Vieira and Schafer 2012 and Peterman 2012). Fifth, to determine the fastener demands one may assume all the torsion must be carried by the fasteners, (however this may be too conservative) or perform a torsional stiffness analysis to determine the proportion carried by the member vs. that

carried by the fastener-sheathing combination. Finally, the minimum of the member and fastener limit states controls the strength.

Conclusions

This paper explores the behavior and design of load-bearing cold-formed steel stud walls, where only sheathing supplies bracing of the stud, under axial and out-of-plane lateral load. A series of tests were conducted on 2.4 m [8 ft] high 362S162-68 studs, set in 362T162-68 track with special blocking details. The stud was tested as (a) unsheathed, (b) sheathed on one-side only with oriented strand board, and (c) sheathed on two sides with all combinations of oriented strand board and/or gypsum board. The results demonstrate that sheathing has a definitive and positive impact on the stability and strength of the stud. The unsheathed studs experienced severe twist, due to the lateral load's lack of alignment with the member shear center, and failed in a torsion limit state. The studs with sheathing on one-side developed greater capacity, but still suffered from excessive twist and eventually pull-through of the fasteners through the sheathing. The studs with sheathing on both sides are generally able to develop member limit states of local buckling or yielding, and have limited twisting. Connector limit states of pull-through and bearing are also observed, typically as the specimen strength descends under displacement. The gypsum sheathed specimens exhibit significantly more damage near the fasteners and are not able to develop full member capacity in all cases.

An analysis of the stud and fastener-sheathing restraint under the torsional demand induced by the eccentric horizontal load demonstrates how the torsional demand is shared between the stud and the fastener-sheathing bracing. In all cases the mid-height fastener is not predicted to carry the full torsional demand. This observation is found to be significant when

investigating connector limit states, as it is overly conservative to assume the fasteners carry the full demand. Further, it is found that the longitudinal warping stresses induced by the torsion in the member are only significant for the unsheathed and one-sided sheathed studs.

Investigation of the design considered both member and connector limit states. The member limit states of local, distortional, and global buckling were considered. Elastic stability assessment of the stud must include the restraint from the fastener-sheathing system, and when this is included the progression in predicted capacity from the unsheathed to two-sided sheathed cases is reasonable. A new model was developed for assessing the connector limit states, based on the manner in which fastener pull-through and bearing resist the induced torsional demand. The total torsional resistance supplied by the fastener sheathing system is included, but first failure in either pull-through or bearing limits the total connector capacity. The torsional demand on the fasteners is based on a torsional stiffness analysis as detailed herein. This approach predicts connector limit states only control for high levels of primary bending in the gypsum sheathed specimens, consistent with the testing.

Extension of the overall design approach to distributed lateral loads (as opposed to a point lateral load) is provided. Further, the limitations and assumptions of the developed design method are fully detailed. Significant advancements are still possible as tested capacity exceeds predicted capacity in many cases; however, for the time being the proposed method provides a design approach that includes all essential features and provides limit state predictions consistent with the tests. In summary, it is shown that cold-formed steel stud walls braced by sheathing alone and subjected to axial and lateral loads can provide the full member capacity (i.e. the local buckling limited strength) if properline nly detailed.

Acknowledgments

This paper was prepared as part of the American Iron and Steel Institute (AISI) sponsored project: Sheathing Braced Design of Wall Studs. The project also received supplementary support and funding from the Steel Stud Manufacturers Association (SSMA). Any opinions, findings, and conclusions or recommendations expressed in this publication are those of the authors and do not necessarily reflect the views of AISI, nor SSMA.

References

AISI-S100 (2007). "North American Specification for the Design of Cold-Formed Steel Structural Members." American Iron and Steel Institute, Washington, D.C.

AISI-S100 (2012). "North American Specification for the Design of Cold-Formed Steel Structural Members." American Iron and Steel Institute, Washington, D.C.

AISI-S200 (2007). "North American Standard for Cold-Formed Steel Framing – General Provisions." American Iron and Steel Institute, Washington, D.C.

AISI-TS-1 (2002) "Rotational-Lateral Stiffness Test Method for Beam-to-Panel Assemblies" Cold- Formed Steel Design Manual, 2002 Edition, American Iron and Steel Institute, Washington, D.C.

Aviram, A., Mayes, R.L., Hamburger, R.O. (2012). "Enhanced Blast-Resistance of an Innovative High-Strength Steel Stud Wall System." Proceedings of the 2012 SEAOC Convention, 12 pp.

Green, G.G., Winter, G., and Cuykendall, T.R. (1947). "Light Gage Steel Columns in Wall-braced Panels." Cornell University Engineering Experiment Station, 35, 1-50.

Lee, Y., Miller, T.H. (2001). "Axial Strength Determination for Gypsum-Sheathed, Cold-Formed Steel Wall Stud Composite Panels." ASCE, Journal of Structural Engineering, 127 (6) 608-615.

Li, Z., Schafer, B.W. (2010) "Buckling analysis of cold-formed steel members with general boundary conditions using CUFSM: conventional and constrained finite strip methods." Proceedings of the 20th Int'l. Spec. Conf. on Cold-Formed Steel Structures, St. Louis, MO. November, 2010. 17-32.

Vieira, L.C.M., Schafer, B.W. (2013). "Behavior and Design of Sheathed Cold-Formed Steel Stud Walls under Compression." ASCE, Journal of Structural Engineering, Preview Manuscript, (doi: http://dx.doi.org/10.1061/(ASCE)ST.1943-541X.0000731)

Miller, T.H., Pekoz, T. (1993). "Behavior of Cold-Formed Steel Wall Stud Assemblies." ASCE, Journal of Structural Engineering, 119 (2) 641-651.

Miller, T.H.. Pekoz, T. (1994). "Behavior of Gypsum-Sheathed Cold-Formed Steel Wall Studs." ASCE, Journal of Structural Engineering, 120 (5) 1644-1650.

Peterman, K.D. (2012). “Experiments on the Stability of Sheathed Cold-Formed Steel Studs Under Axial Load and Bending.” M.S. Thesis. Johns Hopkins University.

Pham, M.M., Miles, J.E., Zhuge, Y. (2006). “Experimental Capacity Assessment of Cold-Formed Boxed Stud and C Stud Wall Systems Used in Australian Residential Construction.” ASCE, Journal of Structural Engineering, 132 (4) 631–635.

Salim, H., Muller, P., Dinan, R. (2005). “Response of Conventional Steel Stud Wall Systems under Static and Dynamic Pressure.” ASCE, Journal of Performance of Constructed Facilities, 19 (4) 267-276.

Schafer, B.W. Vieira Jr., L.C.M., Sangree, R.H., Guan, Y. (2010) "Rotational Restraint and Distortional Buckling in Cold-Formed Steel Framing Systems." Revista Sul-Americana de Engenharia Estrutural (South American Journal of Structural Engineering), Special issue on cold-formed steel structures, 7 (1) 71-90.

Simaan, A., Pekoz, T. (1976). “Diaphragm Braced Members and Design of Wall Studs.” ASCE, Journal of the Structural Division, 102 (1) 77-92.

Vieira Jr., L.C.M., Schafer, B.W. (2012). “Lateral Stiffness and Strength of Sheathing Braced Cold-Formed Steel Stud Walls.” Elsevier, Engineering Structures. 37, 205–213

Vieira Jr., L.C.M., Shifferaw, Y., Schafer, B.W. (2011) “Experiments on Sheathed Cold-Formed Steel Studs in Compression.” Elsevier, Journal of Constructional Steel Research. 67 (10) 1554-1566.

Vieira, L.C.M. (2011). “Behavior and Design of Sheathed Cold-Formed Steel Stud Walls under Compression.” Ph.D. Dissertation. Johns Hopkins University.

Winter, G. (1960). "Lateral Bracing of Beams and Columns." ASCE, Transactions, Vol. 125 Paper No. 3044, 807-826.

McGuire, W., Gallagher, R., Ziemian, R. (1999). Matrix Structural Analysis, With MASTAN2.

Table
Click here to download Table: KDP_BWS_SheathedBC_ JSE _2012_Tables.pdf

List of Tables

Table 1 Nominal and average (across 27 specimens) measured dimensions for 362S162-68 stud, See Peterman (2012) for individual specimen measurements and full statistics

Parameter	Nominal	Measured
	(mm)	(mm)
h	92.1	93.5
b_A	41.3	43.2
b_B	41.3	43.0
d_A	12.7	16.4
d_B	12.7	14.2
t	1.811	1.816
$r_{hb\text{-}B}$	2.7	8.9
$r_{db\text{-}B}$	2.7	7.5
$r_{hb\text{-}A}$	2.7	8.8
$r_{db\text{-}A}$	2.7	7.8
	(deg.)	(deg.)
$\theta_{hb\text{-}B}$	90.0	88.1
$\theta_{db\text{-}B}$	90.0	85.3
$\theta_{hb\text{-}A}$	90.0	87.3
$\theta_{db\text{-}A}$	90.0	83.1
	(MPa)	(MPa)
F_y	345	413

Table 2 Observed failure loads and limit states for previously conducted axial-only test and current axial plus lateral load tests reported here

NOMINAL LOADING		**SHEATHING** (B=BARE, G=GYPSUM, O=OSB)																				
P	**H**	**BB**			**OB**						**GG**			**OG**						**OO**		
		L (m)	**P_{test}** (kN)	**LS**	**L** (m)	**P_{test}** (kN)	**LS**				**L** (m)	**P_{test}** (kN)	**LS**	**L** (m)	**P_{test}** (kN)	**LS**				**L** (m)	**P_{test}** (kN)	**LS**
100%	0	0.6	87.9	D	0.61	95.4	L				0.6	96.7	L	0.6	97.8	L				0.6	101.6	L
		1.2	84.6	FT	1.219	97.8	L				1.2	99.6	L	1.2	96.2	L				1.2	99.0	L
		1.8	60.5	FT	1.829	80.1	FT				1.8	88.7	L	1.8	91.1	L				1.8	99.5	L
		2.4	57.1	F	2.438	69.6	FT				2.4	95.0	L	2.4	99.9	L				2.4	102.7	L
		BB			**OB**			**BO**			**GG**			**OG**			**GO**			**OO**		
L=2.4 m axial + lateral tests		**P_{test}** (kN)	**H_{test}** (kN)	**LS**	**P_{test}** (kN)	**H_{test}** (kN)	**LS**	**P_{test}** (kN)	**H_{test}** (kN)	**LS**	**P_{test}** (kN)	**H_{test}** (kN)	**LS**	**P_{test}** (kN)	**H_{test}** (kN)	**LS**	**P_{test}** (kN)	**H_{test}** (kN)	**LS**	**P_{test}** (kN)	**H_{test}** (kN)	**LS**
~80%P	to failure	-	-	-	-	-	-	-	-	-	77.3	3.4	Y	-	-	-	-	-	-	80.9	4.7	L,PT,Y
$\Delta_{80\%P}$	to failure	-	-	-	44.1	4.3	T	50.8	3.2	T,PT	64.7	3.2	PT,B,Y	68.0	4.4	L,PT,Y	65.3	5.1	PT,B,Y	66.4	6.0	L,PT,Y
$\Delta_{60\%P}$	to failure	28.5	2.4	T	28.9	3.4	PT	32.0	3.5	PT	51.6	4.4	PT,B,Y	45.1	5.2	PT,Y	45.2	6.5	B,L,Y	50.9	6.7	L,Y,PT
$\Delta_{40\%P}$	to failure	10.6	2.6	T	20.3	3.4	PT,T	20.1	4.8	PT,T	30.4	4.8	PT,B	29.8	5.8	L,PT,Y	33.2	6.8	PT,B,Y	33.7	6.9	L,Y
$\Delta_{10\%P}$	to failure	-	-	-	2.2	5.0	T	-	-	-	7.7	5.5	PT,B	7.7	6.1	L,B,T,Y	8.1	7.3	PT,L,B	10.8	7.4	L,Y

(1) shaded results are from axial only tests of Vieira et al. (2011) on the same nominal stud and similar test setup

(2) limit states (LS): member limit states: L = local buckling, D = distortional buckling, FT = flexural-torsional buckling, F = weak-axis flexural buckling, T = torsion, Y = yielding
connector limit states: PT = pull-through of the fastener head through the sheathing, B = bearing damage in the sheathing from fastener

Table 3 Predicted axial and bending member capacity based on average stud dimensions and including restraint from sheathing

AXIAL						BENDING						
sheathing	P_y (kips)	$P_{cr\ell}/P_y$	P_{crd}/P_y	P_{cre}/P_y	P_n[1] (kN)	**sheathing**	M_y (kN-mm)	$M_{cr\ell}/M_y$	M_{crd0}/M_y	M_{cre0}/M_y	C_bM_{cre0}/M_y	M_n[2] (kN)
BB	31.3	1.17	1.30	0.58	**67.6**	BB	4015	5.70	2.35	0.37	0.48	**1927**
OB/BO	31.3	1.17	1.34	0.86	**85.5**	OB	4015	>5.70	>2.35	0.80	1.06	**3292**
						BO	4015	>5.70	>2.35	>8	>8	**4015**
GG	31.3	1.17	1.38	2.37	**110.4**	GG	4015	>5.70	>2.35	>8	>8	**4015**
OG/GO	31.3	1.17	1.38	2.56	**111.4**	OG	4015	>5.70	>2.35	>8	>8	**4015**
						GO	4015	>5.70	>2.35	>8	>8	**4015**
OO	31.3	1.17	1.39	2.92	**112.9**	OO	4015	>5.70	>2.35	>8	>8	**4015**

(1) calculated per AISI-S100-07 Appendix 1 (DSM) with $\underline{k}x$, $\underline{k}y$, $\underline{k}\phi$ springs included in CUFSM4 models for finding $Pcr\ell$, Pcrd, Pcre

(2) calculated per AISI-S100-07 Appendix 1 (DSM) with $\underline{k}x$, $\underline{k}y$, $\underline{k}\phi$ springs included in CUFSM4 models for finding $Mcr\ell$, Mcrd, Mcre

(3) the number of longitudinal (*m*) terms kept in the CUFSM analysis is 1-10 and 31-37 for P runs, and 1-11 and 39-45 for M runs

(4) axial capacities assumed fixed end conditions consistent with Vieira and Schafer 2012 findings

(5) bending capacities assume major-axis pinned end conditions consistent with findings herein

(6) max moment M=HL/4, utilized for conversion to P vs. H space for visualizing interaction

Table 4 Predicted strength of fastener-sheathing system

	fastener torsional capacity calculation				fastener capacity in terms of lateral load H				
					demand T=He		demand T=rHe [b]		test
	θ_f	$T_1=T(\theta_f)$	T_2=sum(T)	$\theta(T_2)$	$H_1=T_1/e$	$H_2=T_2/e$	$H_1=T_1/re$	$H_2=T_2/re$	H [a]
sheathing	(deg)	(kN-mm)	(kN-mm)	(deg)	(kN)	(kN)	(kN)	(kN)	(kN)
BB	-	-	-	-	-	-	**-**	-	**2.62**
OB	24.1	40	40	24.1	1.73	1.73	**12.06**	12.06	**4.98**
BO	24.1	40	40	24.1	1.73	1.73	**12.06**	12.06	**4.80**
GG	1.1	39	42	2.2	1.68	1.84	**4.19**	4.57	**5.47**
OG	1.1	61	179	24.1	2.65	7.76	**5.87**	17.19	**6.14**
GO	1.1	61	179	24.1	2.65	7.76	**5.87**	17.19	**7.25**
OO	3.3	247	316	24.1	10.70	13.69	**21.93**	28.04	**7.38**

(a) Maximum horizontal load observed in testing, generally for 10%P_{axial}, see Table 2 for fulltest results.

(b) Demand on fasteners determined from torsional analysis model, for 2 sided sheathing r ~ 0.4, see Figure 10

List of Figures

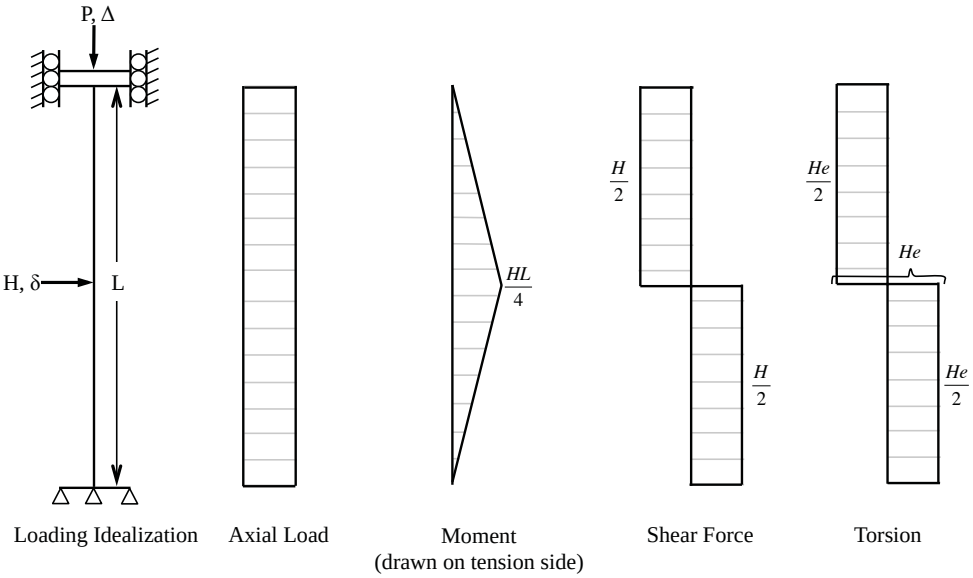

Figure 1 Loading and internal actions for unsheathed (bare) specimen

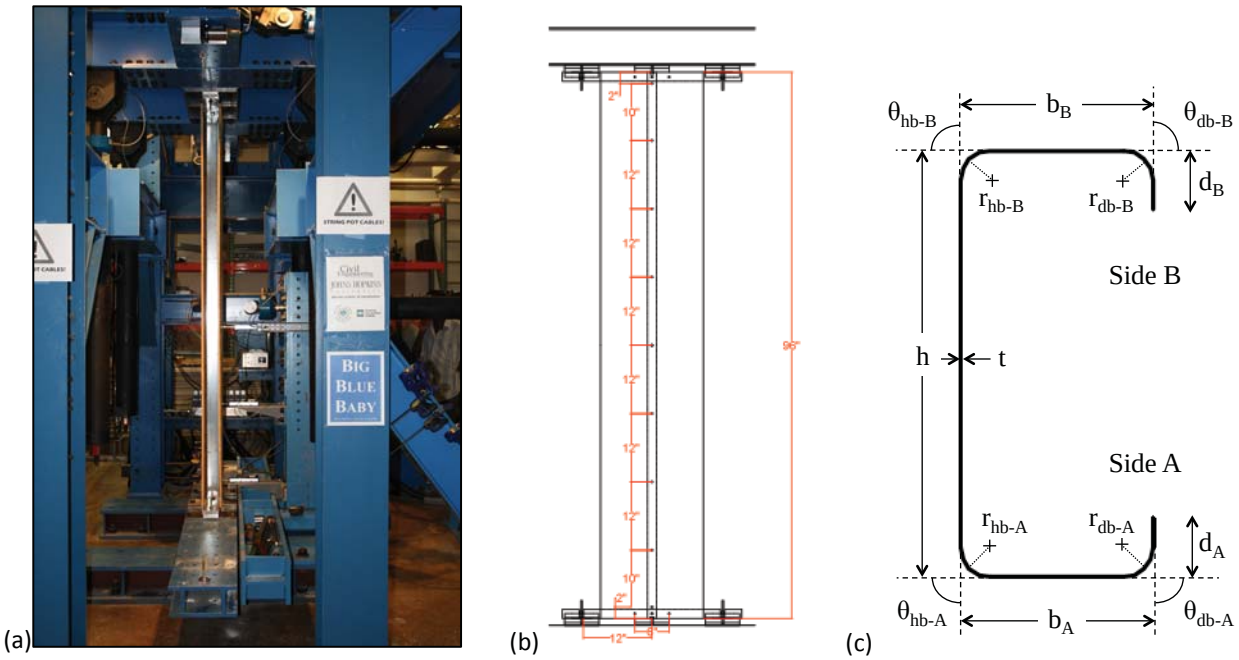

Figure 2 Typical specimen, tested under applied axial and lateral load (a) end elevation in testing rig, top beam is actuated, and lateral load applied by circular bar, (b) side elevation with fastener spacing and track to testing rig detailed, (c) dimensional nomenclature of tested stud

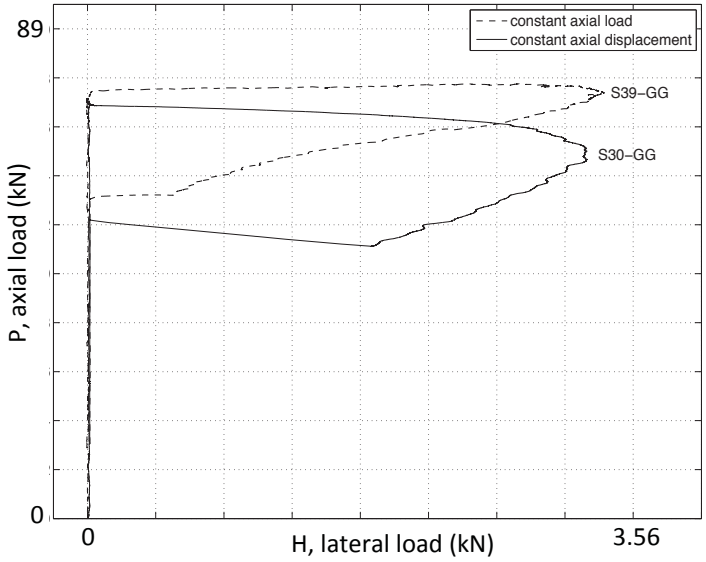

Figure 3 Force and moment response for gypsum sheathed specimens under different load protocols: constant axial displacement, and constant axial load

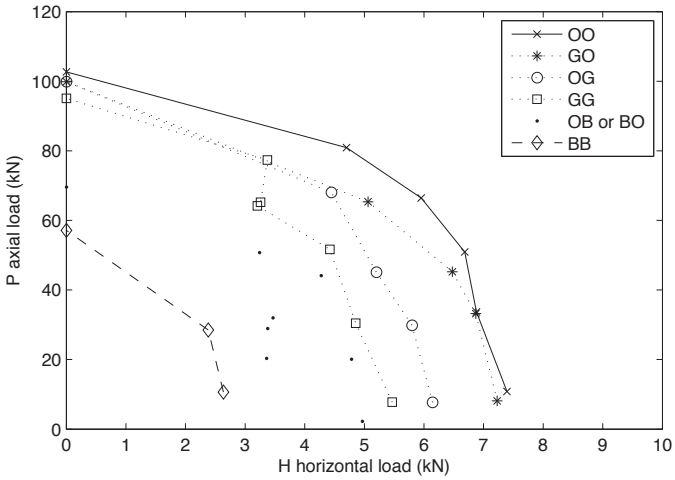

Figure 4: Observed axial and lateral failure loads of tested 362S162-68 studs with various sheathing configurations on the two stud flanges (B = Bare, O = OSB, G = Gypsum)

(a) local bucking (L) limit state in OG specimen, similar for OO specimens

(b) detail of (a) at point of lateral load application, connection damage limited

(c) torsion (T) in stud, typical for bare or one-sided sheathing cases, BO case shown

Figure 5 Observed member limit states in axial and lateral load testing

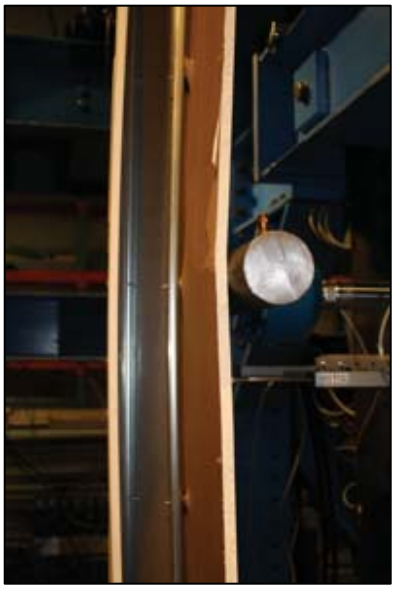

(a) GG specimen exhibiting pull-through (PT) failures on loaded board

(b) same GG specimen as (a) exhibiting bearing (B) failures on non-loaded board

(c) GO specimen exhibiting pull-through (PT) failures on loaded OSB board

Figure 6 Observed connection limit states in axial and lateral load testing

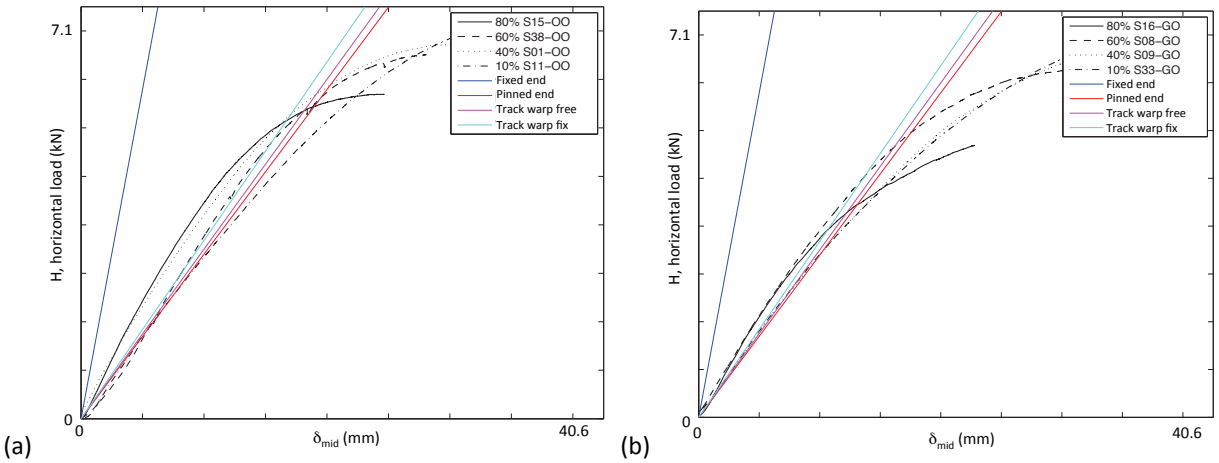

Figure 7 Horizontal force vs. mid-height horizontal displacement with comparison to fixed, pinned, and semi-rigid end conditions for the short segment of connected track for (a) OO and (b) GO sheathed specimens

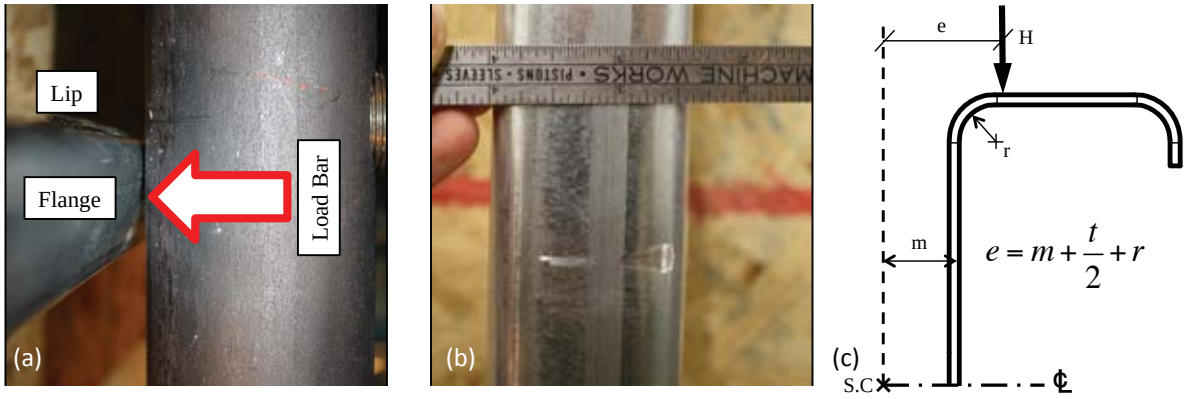

Figure 8 Location of laterally applied load (a) top view of load bar showing initial contact location, (b) etching of load bar on stud, showing load location moves to the termination of the flange flat, (c) assumed final location of lateral load for finite twist

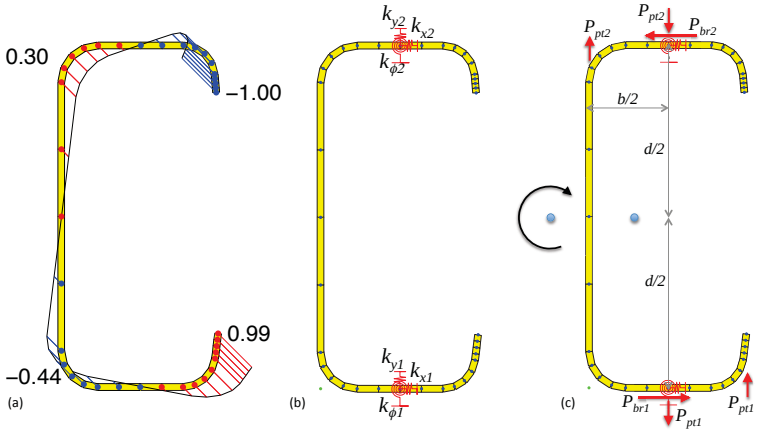

Figure 9 As-measured cross-section drawn to scale, with (a) longitudinal stress distribution due to warping alone, (b) rotational/pull-through (k_ϕ), lateral/bearing (k_x) and composite action/vertical (k_y) springs for the unloaded (1) and loaded (2) flanges, (c) torsional free-body diagram for resistance created by fasteners through bearing (P_{br}) and pull-through (P_{pt}).

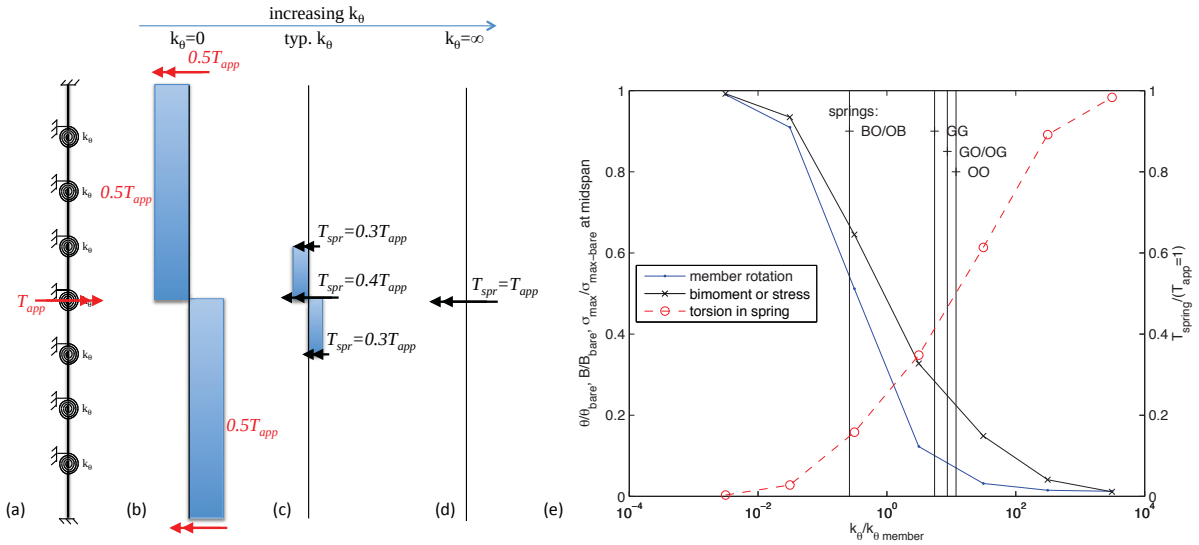

Figure 10 Torsional stiffness analysis model for a stud braced with rotational k_θ springs every 305 mm [12 in.] o.c over 2.4 m [96 in.] length and loaded by a point torque at midspan (a) basic model, (b) torsional moment diagram without springs, (c) torsional moment diagram and spring torsion for typical fastener-sheathing spring stiffness, (d) torsional moment diagram and spring torsion for infinitely stiff spring, (e) midpsan rotation, midpsan bimoment, and midspan torsion in the spring as a function of increasing k_θ (plot normalized to T_{app} = 113 N-m [1 kip-in.], θ_{bare} = 0.3124 rad, B_{bare} = 384 N-m^2 [11.57 kip-in^2], $\sigma_{max\text{-}bare}$ = 381 MPa [55.25 ksi])

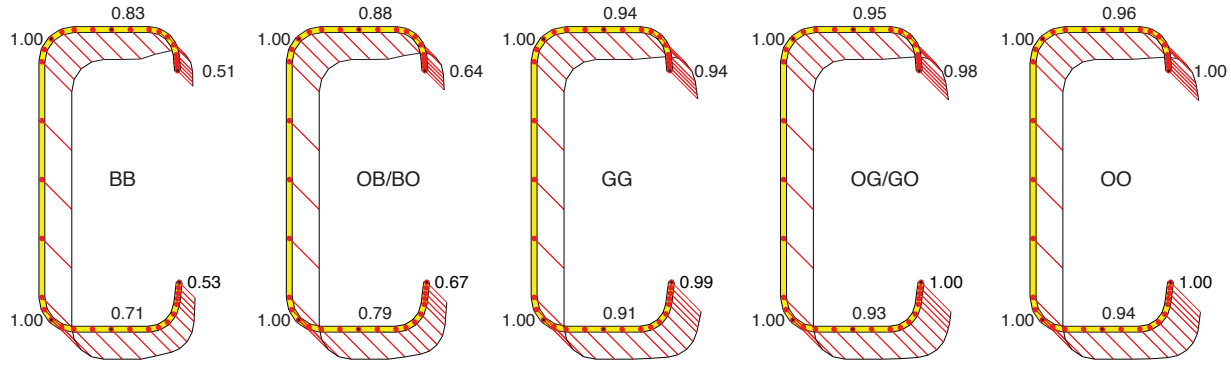

Figure 11 Distribution of bending strength reduction ratio R ($R = (\sigma_b)_{\max} / \left|\sigma_b + \sigma_w\right| \le 1.0$) for the five different sheathing configurations. Ratios less than 1 indicate the expected reduction in bending capacity due to the presence of longitudinal warping stresses.

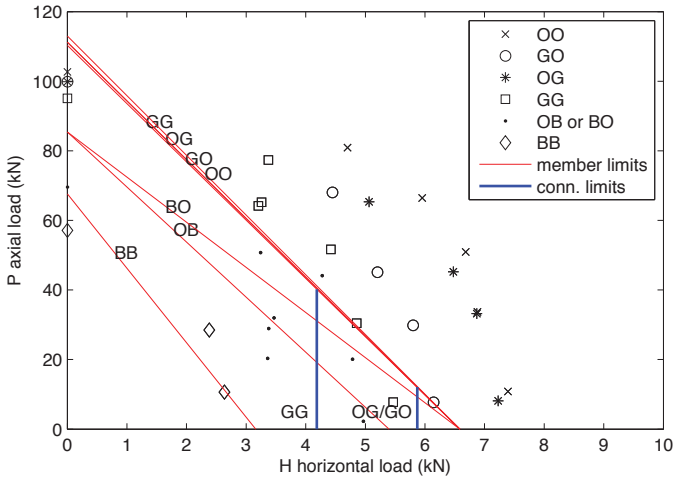

Figure 12 Comparison of observed axial and lateral failure loads of tested 362S162-68 studs with different sheathing configurations against predicted capacity for member limit states (Table 3) and connection limit state (Table 4)

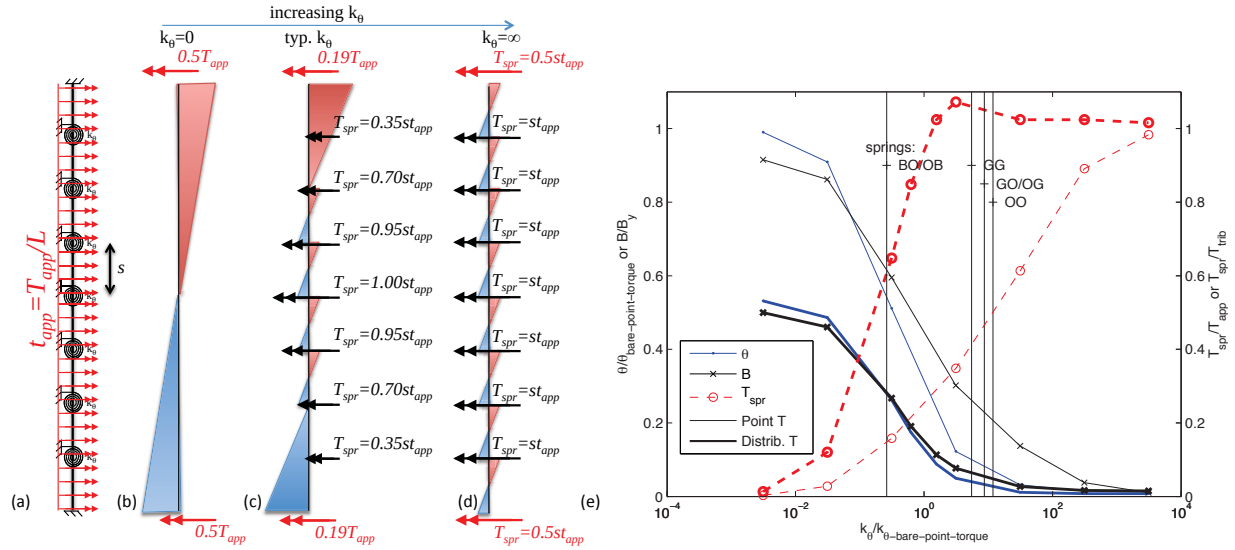

Figure 13 Extension of torsion stiffness analysis of Figure 10 from point torque (T_{app} = He) to distributed torque (t_{app}= (H/L)e = we), (a) basic model, (b) torsional moment diagram without springs, (c) torsional moment diagram and spring torsion for typical fastener-sheathing spring stiffness, (d) torsional moment diagram and spring torsion for infinitely stiff spring, (e) comparison of mid-height rotation, maximum bimoment, and mid-height torsion in the spring (fastener) as a function of increasing k_θ for point torque vs. distributed torque (plot normalized to T_{app} = 113 N-m [1 kip-in.], T_{trib} = 14 N-m [0.125 kip-in.], $\theta_{bare\text{-}point\text{-}torque}$ = 0.312 rad, B_y = 451 N-m^2 [12.54 kip-in^2], $\sigma_{max}(B_y)$ = F_y = 413 MPa [59.9 ksi])

American Iron and Steel Institute

25 Massachusetts Avenue, NW
Suite 800
Washington, DC 20001

www.steel.org

Steel Framing Alliance™
Steel. The Better Builder.

25 Massachusetts Avenue, NW
Suite 800
Washington, DC 20001

www.steelframing.org

Research Report RP-13-1

The New Steel